Fall 2018

Network Design for In-motion Wireless Charging of Electric Vehicles: Models and Algorithms

Mamdouh Mubarak
Southern Methodist University, mmubarak@smu.edu

NETWORK DESIGN FOR
IN-MOTION WIRELESS CHARGING OF ELECTRIC VEHICLES:
MODELS AND ALGORITHMS

Approved by:

Dr. Halit Üster
Professor of EMIS

Dr. Sila Çetinkaya
Department Chair and Professor of EMIS

Dr. Eli Olinick
Associate Professor of EMIS

Dr. Khaled Abdelghany
Associate Professor of CEE

Dr. Mohammad Khodayar
Assistant Professor of EE

NETWORK DESIGN FOR IN-MOTION WIRELESS CHARGING OF ELECTRIC VEHICLES: MODELS AND ALGORITHMS

A Dissertation Presented to the Graduate Faculty of the

Bobby B. Lyle School of Engineering

Southern Methodist University

in

Partial Fulfillment of the Requirements

for the degree of

Doctor of Philosophy

with a

Major in Operations Research

by

Mamdouh Mubarak

B.Sc., Mechanical Engineering, Damascus University, Syria
M.Sc., Engineering Management, Southern Methodist University

December 15, 2018

ACKNOWLEDGMENTS

I first would like to express my sincere gratitude to my advisor, Dr. Halit Üster for his continuous support and guidance. I am beyond grateful for having the opportunity to work under his supervision and could not have asked for a better mentor. He taught me the fundamentals of conducting scientific research and continually challenged me to perform to the best of my abilities.

I am extremely thankful to Dr. Khaled Abdelghany and Dr. Mohammad Khodayar for their invaluable contribution to my dissertation work and their continuous support.

I also would like to thank Dr. Sila Çetinkaya and Dr. Eli Olinick for serving on my supervisory committee and for their insightful comments and suggestions.

My sincere thanks to Ala Alnawaiseh and Hossein Hashemi for their kind help during the initial stage of my project.

My thanks also to my graduate student colleagues: Nadereh Mansouri, Farnaz Nourbakhsh, Amin Ziaeifar, Nahal Sakhavand, Angelika Leskovskaya, Zahra Gharibi, Pete Furseth, and Siavash Tabrizian, whom I had the pleasure of working, studying, and spending time with during my Ph.D. journey.

I am genuinely grateful to my wonderful friends that I was lucky to share my journey in Dallas with. My deepest appreciation goes to Obada Alhaj, Adel Ben Othman, Edoardo Rubino, Jumana Alhaj Abed, Ricardo Araújo, Andres Ruzo, Faris Tamimi, Mahdi Heidarizad, Sameen Wajid, Juman Haddad, Rafal Czajkowski, Essa Haddad, Lama Muwanas, Mo Sharafeddine, Fahed Alhaj, Mahmoud Badi, Areej Bashir, Paula Walvoord, Shahzodahon Hatamova, María Elena Villamil, Leo Pei Yu, Elise Sherron, Olga Boudali, Suzzane Horani, Rawan Shishakly, Rouba Shishakly, and Nora Abdullah for the countless wonderful memories we have together and for making my journey in Dallas truly remarkable.

Last but not least, I would like to thank my parents, my grandparents, my sister, and

my extended family, for their constant love and support throughout my time at SMU and life in general. Without them, this achievement would never have been possible.

There are so many wonderful people, that I could not mention here, that supported me throughout this journey. I am indebted for every one of them.

NOMENCLATURE

B&C	Branch and Cut
BD	Benders Decomposition
BRP	Bureau of Public Roads
CV	Conventional Vehicle
DRPS	Dual of Relaxed Subproblem
DSP	Dual of Subproblem
EV	Electric Vehicle
EVPR	Electric Vehicle Penetration Rate
IPT	Inductive Power Transfer
MIP	Mixed Integer Program
MP	Master Problem
SO	System Optimal
SOC	State Of Charge
SP	Subproblem
UBH	Upper Bound Heuristic
UE	User Equilibrium
V2I	Vehicle to Infrastructure
WCS	Wireless Charging Station

Mubarak, Mamdouh B.Sc., Mechanical Engineering, Damascus University, Syria
M.Sc., Engineering Management, Southern Methodist University

Network Design for
In-motion Wireless Charging of Electric Vehicles:
Models and Algorithms

Advisor: Dr. Halit Üster
Doctor of Philosophy degree conferred December 15, 2018
Dissertation completed August, 27, 2018

The aim of this research is to study the optimal deployment of wireless charging stations (WCS) in urban transportation networks. It is widely acknowledged that the relatively short driving range of EV and the long battery charging times collectively lead to a phenomenon known as "range anxiety" of EV drivers. This phenomenon remains to be the major factor that hampers EV adoption. Thus, in this dissertation, we study a cost-effective deployment plan of WCSs that facilitates EV adoption by alleviating the two major causes of the "range anxiety" phenomenon.

In the first part of this dissertation, we propose a deployment plan that, for societal benefits, satisfies the charging demands of all EVs in the traffic network at the minimum investment cost. For this purpose, we formulate a new mathematical model to strategically deploy WCSs in the traffic network in such a way that EVs can reach their destination without running out of energy. To solve the proposed model, we devise a combined combinatorial-classical Benders Decomposition approach and enhance its efficiency further via employing surrogate constraints and an upper bound heuristic. The model and algorithm are tested on a real network with data from Chicago, IL for a sensitivity analysis and a deeper understanding of different design components of the wireless charging system.

In the second part, we illustrate that the WCS deployment plan can be greatly influenced by the frequently-changing traffic pattern in the road network under study. We demonstrate how a WCS network design, that is obtained based on input data of a single traffic period,

might not be able to satisfy the charging demands during other traffic periods. We further show that even a WCS network design that is based on the peak traffic period might fail to satisfy the demands during less congested periods. That is, the peak traffic period is not the sole determinant of the optimal design. To that end, we study a robust deployment plan that is feasible and cost-effective across different realizations of traffic data. We build on the first part of this dissertation to propose a robust model where we consider the dynamic nature of the daily traffic patterns when we optimize the network design of the wireless charging infrastructure. We devise a customized Benders Decomposition approach to solve the proposed robust model, and we test the model and the algorithm on a real network data from Dallas, TX.

Finally, in the third part, we propose a new framework to plan the deployment of WCSs with the objective of influencing the routing behavior of EV drivers in an effort to improve the traffic assignment in the road network and alleviate congestion. For this purpose, we propose a new optimization model and test the applicability of the suggested approach on the famous Braess network and on Nguyen-Dupuis network. We illustrate, via the two examples, how an optimal WCS deployment can reform the traffic assignment and shift it from the (selfish-optimal) user equilibrium (UE) to the system (socially) optimal (SO) assignment. We further conduct sensitivity analyses to form a deeper understanding of the effectiveness of the suggested approach. The sensitivity analyses provide insights into the dependency of the traffic assignment on the EV population in the network, and on the attractiveness of the deployed WCSs for EVs

TABLE OF CONTENTS

LIST OF FIGURES

LIST OF TABLES

I dedicate this work to my family.

Chapter 1

INTRODUCTION

1.1. Background

Extraordinary investments poured from both public and private sector into the electric vehicle (EV) industry to achieve the ambitious goal of putting one million electric vehicles on the road by the end of 2015 [59]. However, EV adoption has been dramatically lagging behind anticipation; it was not until 2018 that the U.S. fleet of EVs reached 800,000 [2]. The relatively short driving range of EVs, mainly due to low energy-density of the batteries, and the long battery charging times remain to be the major factors that are keeping many consumers away from buying into the EV technology, despite the availability of EV conventional charging facilities.

To overcome these drawbacks, dynamic charging (also referred to as in-motion charging or on-line charging) was proposed, and successfully demonstrated in Onar et al. [49] and Jang et al. [30], as a promising convenient and safe solution. This innovative technology enables EVs to draw power wirelessly from roadbed transmitters while the vehicle is moving. This technology helps to reduce the range anxiety of EV owners, paving the way for an extensive market penetration for EV. Further, it allows automakers to produce EVs with smaller batteries which are highly desirable to facilitate market adoption by reducing the cost of the vehicle [39]. Another key advantage of dynamic wireless charging is that it paves the way for the realization of full autonomy of EV; eliminating the need for charging stops allows for an almost indefinite movement of autonomous EVs.

Enabling dynamic charging requires EVs with wireless charging abilities and roads with inductive power capabilities. The wireless charging technology has already been tested on numerous EV platforms, including Tesla, Renault, Nissan, BMW and Honda [23]. Other

automakers such as Mercedes-Benz and General Motors have declared their plans to introduce EVs with wireless charging capabilities to the market [23, 65]. On the other hand, experiments on roads with inductive power capabilities are being conducted in England and France to support the growth of the technology [13, 28]. Figure 1.1 features photos of testing Qualcomm dynamic wireless charging system on an EV by Renault in France. These attempts indicate that the future of dynamic charging looks very encouraging. We envision that with the advancement of driverless vehicles the interest and need for wireless in-motion charging will only increase at a higher rate. The technology pioneers such as Qualcomm and Momentum Dynamics has already announced their visions for "limitless EV range" and high-power charging infrastructure [12, 23].

Figure 1.1: Qualcomm and Renault testing dynamic wireless charging in France. Adopted from [28, 50]

.

1.2. Motivation

Despite the technological advancements in electric vehicles charging mechanisms, the shortage of EV charging facilities remains to be the "fundamental challenge" facing the growth of EV markets [24]. While many potential consumers are shying away from switching to EVs because of this particular limitation, both public and private sectors seem reluctant when it comes to investing in charging infrastructure. The reason behind this hesitation is the insufficient number of EVs on the road. The solution to this (chicken-and-egg) dilemma depends profoundly on a strategic deployment of charging stations that optimizes both locations and scales of these stations in urban areas [56].

This problem is addressed in **the first study of this dissertation** via an analytical approach in which the deployment of the new wireless charging technology is optimized to minimize the investment cost while capturing the existing traffic pattern on the road network represented by the user equilibrium (UE) traffic assignment [63]. In doing so, our approach encourages EV adoption by alleviating the two major anti-adoption factors, namely the long charging times and short ranges, without disturbing the existing traffic pattern.

More specifically, we examine the infrastructure deployment in a way that puts no extra burden on EV drivers to identify new routes for themselves and change their travel behaviors.

We approach the problem from the perspective of a city as the decision maker whose aim, for societal benefits, is to satisfy the charging demands of all EVs in its urban network at the minimum investment cost which, for our purposes, include both the installation cost (paid by tax-payers) and the travelers' usage costs. For this purpose, we suggest a new mathematical model to strategically deploy wireless charging stations (WCS) in the network in such a way that no EV runs out of energy before reaching its destination. We envision that, ultimately, the optimal locations of the WCSs at their corresponding capacities are constructed and operated by private entities as contractors.

To solve the proposed model, we develop a Benders Decomposition (BD) based algorithm as a solution methodology. In particular, we devise a combined combinatorial-classical BD approach and enhance its efficiency further for the specific problem at hand via devising surrogate constraints and an upper bound heuristic. We illustrate the applicability of our model and the solution algorithm via a case study with urban network data from Chicago, IL.

Another motivation for this research is to investigate the effect of varying wireless charging parameters and product design characteristics on the network design and the implementation cost of the infrastructure. This investigation is crucial at this early stage of the technology maturity to support the product design and offer insights, for the technology developers, on the effect of technical parameters on the system implementation cost. To that end, we conduct a sensitivity analysis on key system parameters to examine trade-offs between design and implementation costs inherent in WCS networks.

We observe that the network design of the wireless charging infrastructure is heavily dependent on the frequently-changing traffic condition in the road network. That is, an optimal WCS network design proposed to serve charging demands at a certain traffic period is not necessarily optimal (or feasible) during a different traffic period. Driven by this observation, **in the second study of the dissertation**, we investigate the dependency of the optimal WCS network design on the dynamic traffic patten. Specifically, we use the widely referenced Nguyen-Dupuis network, as an example, to show that a WCS network design, that is obtained based on input data of a single traffic period, might not be able to satisfy the charging demands during other traffic periods. We further illustrate that even the peak-period WCS network design might fail to satisfy the charging demands during less congested traffic periods. Therefore, we conclude that the peak traffic period cannot be considered as worst-case scenario when optimizing the WCS network design. We then, building on the first study, approach the network design problem at hand while considering multiple traffic periods, rather than a single traffic period. Our goal is to generate a robust optimal

solution that is feasible, and cost-effective, across all realizations of traffic conditions. For this purpose, we build on the model proposed in the first study to formulate a new robust network design model for the deployment of WCSs in urban traffic networks. We further devise a BD based solution algorithms tailored to solve the proposed model. The algorithm is strengthened via multiple sets of problem-specific surrogate constraints and a new upper bound heuristic for improved efficiency. The robust model and the proposed algorithm are tested on real network data from Dallas, TX.

Finally, **the third study in this dissertation** is motivated by a long-sought goal in the field of transportation: alleviating congestion in urban traffic networks by improving the efficiency of the network utilization. We recognize that unless the WCS network is designed to serve and maintain the existing traffic assignment in the road network, as in the approach of the first two studies, it can potentially disturb and change the traffic assignment. The reason is that as a response to the network design, EV drivers will have to change their route selection strategy to account for the availability of WCSs on their routes. Therefore, motivated by the potential impact of WCS network design on the traffic assignment, we introduce the idea of employing WCS network as a traffic management tool to influence the traffic assignment in a way that minimizes congestion in the road network. Specifically, we propose a new mathematical model with the objective of generating WCS network designs that can shift the traffic assignment from the selfish-optimal UE toward the system (socially) optimal (SO) traffic assignment, which corresponds to the optimal utilization of the road network. We further examine the validity of this concept by illustrating the proposed model on the well known Braess network and on the Nguyen-Dupuis network, and we conduct sensitivity analyses to measure the potential impact of the proposed approach on alleviating congestion.

1.3. Brief System Description

Dynamic charging utilizes the innovative technology of Inductive Power Transfer (IPT) to transmit energy from the power grid to the EV wirelessly while the EV is in motion. Figure 1.2 provides an illustration of the dynamic charging system. The stationary components of the system consist of source coils embedded in roadbed power transmitters and connected to power charging units. From the vehicle side, the receiver system includes at least one pick up coil installed beneath the vehicle. Further, the system is supplemented by a vehicle to infrastructure (V2I) communication system to facilitate the communication between the EV and the charging facilities.

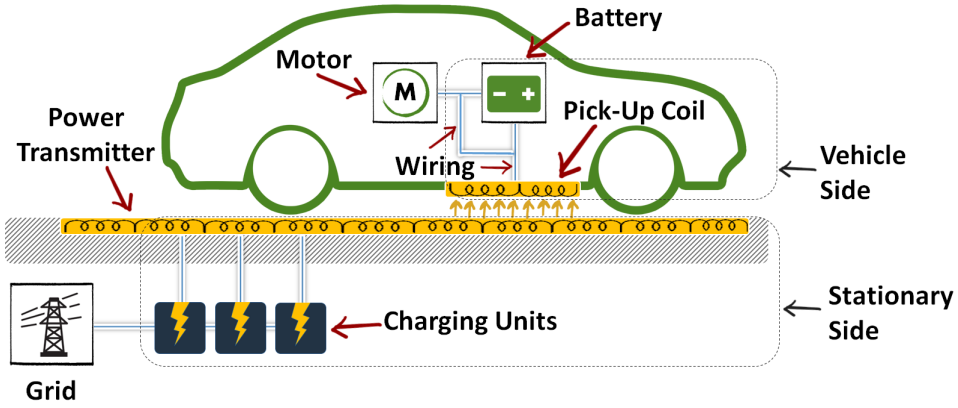

Figure 1.2: An illustration of the dynamic charging mechanism

When an EV places a charging request, the source coils in the power transmitter will be activated. While the EV travels over the power transmitter, the source coils deliver energy, via electrical pulses, to the pick-up coil in the vehicle. If the battery is fully charged, the energy drawn from the transmitters can be directly used to energize the electric motor of the vehicle [30]. An in-depth description of the technology and related hardware can be found in Onar et al. [49].

The charging scheme of the battery is dependent on its state of charge (SOC). Once the voltage of the battery is below the nominal voltage, the constant charging current would result in the increase of the battery voltage to its nominal value. After this point, the

battery will be charged using a constant voltage scheme and the current is regulated. In both charging schemes, the injected power can be regulated by controlling the voltage or the current. As the state of charge increases beyond 90%, the charging power decreases slightly; however, the charging power remains constant once the SOC of the battery is below 90% [60]. In this context, it is unlikely that an EV will wirelessly recharge above 90%. Therefore, considering fixed charging power for the battery is a valid assumption. In fact, technically the charging power can be regulated by changing the injected current and voltage as stated before. Several studies address similar concept including Khodayar et al. [33]. Fixed charging power for EV battery is considered in other related studies such as Chen et al. [9]. Specifically, consideration (IV) in page 346 which reads: "the amount of electricity charged is equal to a constant charging rate multiplying the charging time."

In this dissertation, we use the term Wireless Charging Station (WCS) to refer to the stationary side of the dynamic charging system installed on a segment of the road, i.e., the WCS consists of a number of charging units and roadbed power transmitters installed. The station's power capacity refers to the total power capacity of all charging units in a WCS.

In our modeling approach, we consider long loop configuration for a WCS where the power transmitter is installed along a whole road segment. Thus, an EV is assumed to be exposed to the power transmitter as long as it is traveling on the road segment with a WCS. Nevertheless, our models can be generalized to other design configurations such as sectional wired loop and spaced loop (see Yilmaz et al. [66] for various configurations) by adjusting the effective charging time in the models.

Finally, it's worth mentioning that the dynamic charging system has low efficiency compared to conventional static charging. Thus, the dynamic charging system, at least at this stage of its technical development, is meant to only increase the EV driving range but not to replace the need for conventional stationary charging. The latter has been accounted for in our modeling approach by considering initial state-of-charge for EVs.

1.4. Summary of Contributions

The contributions of this dissertation can be summarized as follows. The **first study of this dissertation** tackles the WCS network design problem with the goal of optimizing the deployment of the wireless charging infrastructure in traffic networks in an effort to support EV adoption. The study is motivated by the notion that, given the high cost associated with the cutting-edge wireless charging technology, delivering the substantial benefits of this technology can only be achieved via an optimized deployment of the infrastructure. The problem is approached via an analytical scheme and molded as a mixed integer program. The model decides on the WCS locations and the corresponding power capacity allocations. The goal is to minimize the infrastructure deployment cost from a system perspective, and the usage cost for the users. The model is structured to generate WCS network designs that can serve the EV charging demands in the traffic network without disturbing the existing traffic condition represented by the UE traffic assignment. From an algorithmic perspective, the first study offers a BD framework to solve the proposed optimization model. The proposed framework adopts features from classical BD and combinatorial BD. This solution framework has the potential to be generalized for other network design applications. The solution framework is strengthened via an upper bound heuristic and surrogate constraints for improved convergence. The model and the solution methodology are put to work on a case study using real network with data from Chicago, IL. In an effort to support the product design of the maturing wireless charging technology, the case study includes a sensitivity analysis that captures the interaction between key technical parameters of the wireless charging system and the infrastructure deployment cost. The study also paves the way for similar investigations of the interactions between product design and technology implementation cost.

The **second study of this dissertation** offers a robust framework to tackle the WCS network design problem. Specifically, the second study considers the interactions between the WCS network design and the dynamic traffic condition in the road networks. We provide examples to illustrate that, due to the strong dependency between the WCS network design

and the traffic conditions, WCS networks should be designed while considering the variability of the daily traffic pattern. That is, multiple traffic periods should be considered when planning the deployment of the wireless charging infrastructure. Our findings indicate that when it comes to WCS network design, even the peak traffic period cannot be singled out as a worst-case scenario, although it does correspond to the highest demands. We provide a detailed explanation of this phenomenon. To that end, the second study introduces an absolute robust WCS network design model. The model captures the interaction between WCS network design and the frequently-changing traffic pattern by considering multiple traffic periods rather than a single period. The model generates WCS network designs that are robust against the changes in the traffic conditions. From the methodological side, the study provides a BD solution algorithm tailored to solve the robust model. The algorithm is strengthened via several techniques including problem-specific surrogate constraints, a new upper bound heuristic, and cut strengthening. The robust model and the solution algorithm are then tested via a case study with real data from Dallas, TX. The results of the case study confirm the necessity of a robust solution to the problem at hand. We further provide a detailed cost breakdown analysis to investigate how different cost components differ between the robust solution and the individual single period solutions.

Finlay, the **third study of this dissertation** contributes to the field of traffic management with the new concept of employing the WCSs in the road network as a traffic management tool. Particularly, we propose the idea of taking advantage of the attractiveness of the deployed WCSs for EV drivers to influence their travel behaviors in an effort to improve the traffic assignment in the network. This study is motivated by the notion that the UE traffic assignment, which offers a realistic representation of traffic flows in a steady-state, does not correspond to the optimal utilization for the traffic system. To that end, we propose a mathematical model to locate WCSs in the network so that as a response to the WCS deployment, the traffic will re-regulate itself in a new equilibrium state which is closer to SO than the original UE. The validity of the proposed idea is tested on two widely referenced networks in the field of transportation including Braess network and Nguyen-

Dupuis network. Our findings confirm the validity of the proposed concept. Specifically, we conclude that the optimal WCS deployment plan, generated by our model, is able to improve the road network utilization by shifting the traffic assignment from original UE toward SO, which corresponds to the optimal utilization of the road network. We also find the shift from UE toward SO, as resulted by the WCS deployment, is dependent on the EV population in the network under study, and on the attractiveness of WCS as viewed by EV drivers. To that end, we conduct sensitivity analyses to investigate these dependencies. We conclude that shifting the traffic assignment from UE *completely* toward SO is only possible if the EV population in the network and the attractiveness of WCS for EV drivers, each crosses a certain threshold.

1.5. Dissertation Organization

The rest of this dissertation is organized as follows: A review of the related literature is provided in Chapter 2. The network design for in-motion wireless charging of electric vehicles is studied in Chapter 3. In Chapter 4 we introduce the robust version of the network design problem at hand. In Chapter 5 we provide a study on the concept of utilizing wireless charging of EVs to improve traffic assignments in congested traffic networks. Finally, we highlight the results and findings of this dissertation and discuss potential future research directions in Chapter 6.

Chapter 2

RELATED LITERATURE

Problems dealing with the optimal location of refueling/plug-in-recharging facilities has been well covered in the literature. Hodgson [25] developed a flow capturing location model (FCLM) with the goal of maximizing the covered demands between the network's origins and destinations by locating a fixed number of refueling facilities in the network. Kuby and Lim [36] proposed flow refueling location model (FRLM) to determine the locations of refueling stations for alternative fuel vehicles with limited driving range. Kuby and Lim [37] then enhanced the model with three methods to add candidate sites on arcs. Upchurch et al. [58] proposed a capacitated FRLM which forces a limit on the number of vehicles that can be charged at a certain facility. Wang and Lin [61] utilized a set covering approach to optimize the location of vehicle refueling stations. Later, MirHassani and Ebrazi [45] proposed a flexible reformulation of Wang and Lin [61] model. Wang and Lin [62] also developed a mixed integer programming model to locate multiple-types of recharging stations for EVs, and showed that an optimal deployment in planning areas can be achieved through the employment of multiple types of charging stations. More recently, Zheng et al. [67] studied the EV user equilibrium traffic assignment and the optimal locations of conventional charging facilities, subject to the range limitation.

In terms of dynamic wireless charging, most of the existing literature targets the technical side of the maturing technology. Yilmaz et al. [66] discuss the general design requirements of the dynamic wireless charging system. Their study includes an evaluation of the effect of different configurations of the roadbed power transmitter on the overall system efficiency. Covic and Boys [17] describe the different components of the wireless charging system in technical details. Onar et al. [49] demonstrate the concept of EV dynamic wireless charging on a laboratory prototype. They further investigate the effect of different road surfacing

materials, that cover the wireless power transmitter, on the transparency of the wireless power transfer magnetic field exposure. Lukic and Pantic [41] present a review of the basics of the state of the art IPT technology as used in dynamic wireless charging. Miller et al. [44] present an analysis for the power flow in wireless power transfer systems. Their analysis is based on experimental data from Oak Ridge National Laboratory.

When it comes to the operation and system studies of dynamic wireless charging, a recent survey paper by Jang [29] provides a thorough review of the literature in this area. The author reviews the related studies according to their focus area from five different perspectives including: charging infrastructure allocation; driving range extension; cost and benefit analyses; supporting systems; and miscellaneous perspectives. The study also discusses the recent developments and commercialization activities in the field.

Studies on driving range extension investigates the possible extension of the EV range using dynamic wireless charging. Examples of these studies are Chopra and Bauer [11] and García-Vázquez et al. [22]. Studies providing cost benefits analyses can be found in Ko and Jang [34], Jang et al. [31], and Fuller [21].

Studies that are most related to the research in this dissertation are the ones focusing on charging infrastructure allocation.

Ko and Jang [34] present a mathematical formulation to optimize the design of the dynamic-charging-based mass transportation system On-Line Electric Vehicle (OLEV) developed by Korea Advanced Institute of Science and Technology (KAIST). Their formulation considers the route of the bus as a continuous spatial decision space to determine the the starting and end points of each wireless charging lane. Their model also addresses the trade-off between the number of deployed power transmitters and the size of the batteries on buses.

Jang et al. [31] adopts the same setting of Ko and Jang [34] (i.e., OLEV transportation system). However, in this study, the authors consider a discretized decision space as they divide the route of the bus into multiple segments. Therefore, the continuous problem introduced in Ko and Jang [34] is turned into a discrete optimization problem in Jang et al.

[31].

Hwang et al. [27] also build on the same setting of Ko and Jang [34]. Specifically, the anthers generalize the single-route problem in Ko and Jang [34] to cinder multiple routes in the mass transportation system.

Liu and Song [40] also consider a multiple-route transportation system setting in an optimization problem with the goal of optimizing the locations of wireless charging facilities and the battery size of the electric buses. This is done while addressing the uncertainty of energy consumption and travel time in a robust optimization approach.

Riemann et al. [52] propose a flow-capturing location model with stochastic user equilibrium under a fixed number of wireless charging facilities. The authors consider the maximization of captured EV flow by locating a fixed number of WCSs without cost and capacity considerations. They also assume that an EV's battery is charged fully when an EV travels on a road segment with a WCS regardless of the travel time, i.e, WCSs are assumed to have infinite power capacities and charging rates. The use of the model was demonstrated on a network with 13 nodes and 19 arcs using data in [48].

Chen et al. [9] study the optimal deployment of charging lanes under a limited budget and a fixed charging power of the charging lanes. Their model minimizes the total travel time in the network while selecting arcs as charging lanes. They also illustrate their model on the same small network used in [52].

In another related study on dynamic charging implementation, Fuller [21] considers investment cost minimization for a WCS infrastructure that allows EV travel between 39 key origin-destination pairs in California. Specifically, the study utilizes the set covering model developed by Wang and Lin [61] (which was proposed with the goal of locating stationary refueling facilities) to locate fixed capacity recharging stations on the shortest paths of origin-destination pairs of interest. The model is solved using Branch and Bound technique as implemented by CPLEX.

More recently, Chen et al. [10] study the competitiveness of dynamic charging against stationary charging. Their study includes a deployment model for both charging lanes rep-

resenting dynamic chargers and stationary charging stations. The authors state that their model adopts a "highly simplified" setting where one traffic corridor is considered. That is, the authors consider a single road segment rather than a general network, and all EVs take identical trips from the beginning of the corridor to the end of it. The deployment model decides on the length and charging power of charging lanes, however, as a "macroscopic model," it does not optimize the locations of these charging lanes. The authors also assume that all EVs have identical batteries and start there trips with a full charge. The model further assumes a constant speed across the traffic corridor. They conclude that the use of charging lanes is preferable over the stationary charging stations for improved efficiency in transportation operations.

The above mentioned charging infrastructure allocation studies are the closest to our first study in this dissertation. However, our approach to the problem is significantly different. To start with, rather than considering a mass transportation system operating in a closed environment (as in Ko and Jang [34], Jang et al. [31], Hwang et al. [27], and Liu and Song [40]), or one traffic corridor with identical trips (as in Chen et al. [10]), we consider a complete traffic network with EVs taking different trips, originating from, and ending at different locations.

To promote EV adoption without causing disturbance to the traffic pattern, we locate facilities and further determine their associated power capacities by exploiting the economies-of- scale to serve EV charging demands on all used routes, at the minimum cost. By serving demands on all used routes in current UE, EV drivers will have no incentive to change their original routes. Consequently, the UE traffic assignment will remain undisturbed. In this context, the number of installed wireless charging stations is decided by our cost minimization model to capture all the EV traffic flow (as apposed to assuming a fixed number of stations as in Riemann et al. [52], or a fixed budget as in Chen et al. [9]).

Furthermore, considering a realistic implementation, we take into account charging rates and levels on road segments with WCSs in a way that is explicitly determined by the travel time and charging power installed on the road segments (as opposed to assuming full battery

charge once an EV travels on any WCS as in Riemann et al. [52]). This will be further discussed in Chapter 3.

The novelty of our second study in this dissertation lies in that, to our best knowledge, it is the first to consider the variability in the traffic pattern while optimizing the deployment of the wireless charging infrastructure.

Finally, our third study is novel in that it integrates the charging infrastructure allocation problem with the system optimal traffic assignment problem.

Chapter 3

NETWORK DESIGN FOR IN-MOTION WIRELESS CHARGING OF ELECTRIC VEHICLES

3.1. Introduction

Mass adoption of electric vehicles (EV) leads economies away from the dependency on fossil fuels, and promises an extensive reduction in pollution levels. This, motivated governments around the world to invest billions of dollars and to introduce a lot of policies and programs in effort to promote EV adoption. However, potential EV consumers continue to be concerned about the range anxiety; a phenomenon caused by the two major drawbacks of EVs, namely, the short driving range and the long charging time.

To alleviate range anxiety, dynamic (in-motion) wireless charging was proposed as a promising solution that would allow EVs to recharge while traveling in the road network. The ability to charge while in-motion also allows for a significant reduction in the size of the EV battery which, in turn, significantly reduces the cost and weight of EVs [32]. Jeong et al. [32] also found that dynamic wireless charging is beneficial to the extension of the battery life. Another key advantage of dynamic wireless charging is that it paves the way for the realization of full autonomy of EV; eliminating the need for charging stops allows for an almost indefinite movement of autonomous EVs. However, due to high costs associated with the deployment of this new technology, delivering the benefits of wireless charging can only be achieved via a strategic optimized deployment of the wireless charging facilities.

In this study, we propose a mathematical approach to address the problem of optimizing the deployment of wireless charging stations (WCS) in urban traffic networks. The proposed approach aims to generate WCS deployment plans to serve the charging demands of EVs in traffic networks, in effort to encourage EV adoption, while minimizing the investment costs.

We intend to design the wireless charging infrastructure network in a way that serves EV drivers without putting an extra burden on them to change routes. To this end, we first identify the *usual* UE travel pattern of the travelers (i.e., the routes that they currently choose before the deployment of the wireless charging infrastructure) and seek to identify best wireless charging network design to serve this pattern. Therefore, travelers do not need to change their routes to seek wireless charging; traffic assignments are not affected. That is, we are solving our problem to capture all flow for a well-defined long-term representation of the traffic pattern without impacting it. Our approach ensures that we provide the charging capacity along the different routes in such a way that the EV drivers do not need to change their routes in order to recharge on their daily routes.

Our contributions in this study can be summarized under three headings as follows. On the modeling side, our study contributes to the recent, and rather limited, literature in network planning for EV dynamic charging with a new mathematical formulation for strategic deployment of WCSs in urban networks. Unlike the previous models, the aim of our model is to optimally decide both location and power capacity of WSCs in a transportation network, while minimizing the total investment and charging related costs on the user. Instead of considering one traffic corridor with identical trips (as in Chen et al. [10]), we consider the whole traffic network with EVs taking different trips, originating from, and ending at different locations. Further, instead of assuming a fixed charging power (as in Chen et al. [9], Fuller [21]) or infinite capacity (as in Riemann et al. [52]), our model allows for incremental expansion of the power capacity on arcs independently. This feature of the model, while useful in bringing the model closer to reality, makes our cost function more complex; specifically, instead of assuming a fixed number of WCSs (as in Riemann et al. [52]), or a fixed budget and a fixed installation cost for WCSs (as in Chen et al. [9]), we employ a cost function that includes three types of costs: a fixed and a variable cost associated with the installation of WCSs (including base capacity and expansion costs of both inverters and the charging pads) in addition to a charging cost. Further, to promote EV adoption without causing disturbance to the traffic pattern, our approach first determines the existing traffic

pattern based on user equilibrium (UE) traffic assignment (in an a priori step) and imposes in-motion charging requirements so that all traveling EVs are ensured not to be stranded on their routes. Given the UE traffic pattern, our model accounts for traffic volumes and travel times to capture the special characteristics of EV dynamic charging. Mainly, the model captures the four-way relationship between travel times, the amount of charge withdrawn by an EV, the traffic volume, and the power capacity of the WCSs to determine the WCS location and capacities based on the inputs including (i) EVs' current routes, (ii) initial and desired ending states-of-charge, and (iii) battery capacities.

On the methodology side, to be able to efficiently solve large instances of the problem of interest, this study offers a BD based algorithm on the proposed specific formulation and a corresponding decomposition scheme that includes integer variables in the subproblem. The proposed approach utilizes both combinatorial Benders cuts (generated by the integer subproblem) and classical Benders cuts (generated by the linear relaxation of the integer subproblem). While Rubin [53] also suggests the approach that relies on the use of classical Benders cuts generated by linear relaxation of the subproblem, no computational evidence on its applicability is provided. Our initial computational experiments showed that a direct implementation of this approach suffers an excessively slow convergence. Therefore, we strengthen the algorithm via problem-specific surrogate constraints that improve the lower bounds and devise a heuristic algorithm to quickly obtain high-quality upper bounds.

Finally, on the computational side, we report extensive numerical experiments on algorithmic performance, using 90 randomly-generated traffic networks of various sizes. The goal of the experiment is to evaluate the efficiency of the suggested solution methodology in comparison to the Branch & Cut approach and classical BD approach in CPLEX. A case study using Chicago, IL road network is also presented to demonstrate the use of the overall approach on a real traffic network, and provide a sensitivity analysis of different input parameters on the objective function value to examine trade-offs between design and implementation costs inherent in WCS networks.

The rest of the chapter is organized as follows: The problem is described and formulated in Section 3.2. In Section 3.3, we describe the solution algorithm proposed to solve the problem. And in Section 3.4, we present the computational experiment and numerical results of testing the efficiency of the proposed algorithm. A case study is presented in Section 3.5.

3.2. Problem Definition and Formulation

We consider two costs associated with installing a WCS: the first one is the fixed cost that represents initial set up cost with a base power capacity; and the second one is the variable cost associated with unit power capacity expansion over the base capacity. These costs mainly capture the capital cost of the inverter as well as the installation cost associated with it. Furthermore, the cost of the charging pad proportionally increases with the capacity of the installed inverter. Therefore, the fixed and variable installation costs assumed in this study can also include the cost associated with the charging pads.

To set the stage for our formulation, we start by explaining the electric vehicle dynamic recharging logic which also provides insights into the interactions between network design and operations. In designing the network for EV wireless charging, two interdependent decisions include the locations of WCSs and their power capacities.

The interaction between these two decisions can be illustrated on a small network depicted in Figure 3.1. In this example, we consider 6 nodes and 5 arcs where on each arc (length in miles, travel time in minutes) data is provided.

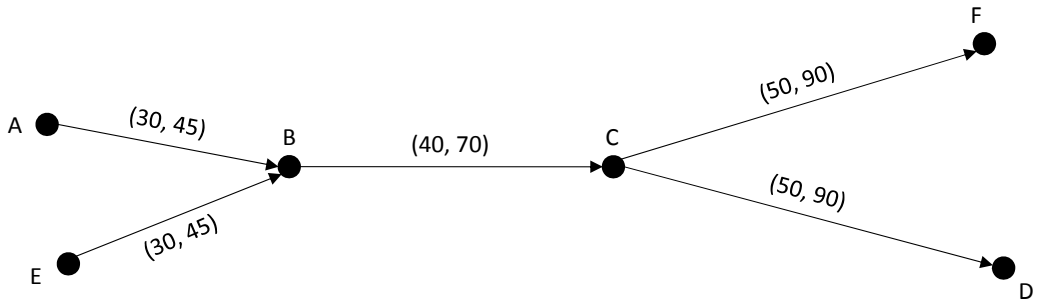

Figure 3.1: A small two-paths network example with OD pairs A-D and E-F

Assume that an EV1 with γ_1 kWh battery capacity, and a driving range of R_1 is traveling between OD-pair A-D on path A-B-C-D of length l_{AD}. We assume that EV1 starts the trip at node A with a $p_A\%$ state-of-charge and the driver wants to reach node D with at least $p_D\%$ state-of-charge ($p_D < p_A$). Let ξ_{AD} denote the energy consumed by the EV when traveling between OD-pair A-D. Due to energy conservation, the amount of charge that EV1 should receive on its path is $c_1 = \xi_{AD} + p_D\%\ \gamma_1 - p_A\%\ \gamma_1$. To receive the required c_1 kWh, at least one WCS is needed on the path between A and D. The location of the WCS should be selected in a way that EV1 does not run out of energy at any point of the path. In this example, we assume that all three arcs AB, BC, and CD are feasible candidates to install WCS on the path between A and D.

Note that electrical power P (kW) for a WCS is equal to $c/(\eta\, t)$ where C (kWh) is the energy that the WCS can deliver in one hour, η is the IPT system efficiency, and t is the effective charging hours (i.e., arc travel time). For example, if arc AB is selected to host the WCS, the installed capacity must be at least $P_{AB} = c_1/(\eta\, t_{AB})$ kW to deliver the required energy c_1 to EV1. Observing that $t_{AB} < t_{BC} < t_{CD}$ as given is Figure 3.1, we must have $P_{AB} > P_{BC} > P_{CD}$.

We consider a WCS installation cost (inverters and charging pads) function of the form $fc + vc\ Y$ where fc is the fixed cost of base power capacity installation, vc is the cost of unit capacity increment, and Y is the number of capacity units installed. Since there is a positive correlation between the cost and the capacity of a WCS (as implied by the term $vc\ Y$), we find that arc CD is the best (least costly) option to host the WCS on EV1's path.

Now consider another electric vehicle EV2 traveling between OD-pair E-F on path E-B-C-F. Under the same assumptions applied to EV1 above, we conclude that arc CF is the best candidate to host a WCS on the path E-B-C-F for EV2.

However, when examining the network as a whole, and by taking into account the economies-of-scale as implied by the fixed cost term fc, it can be argued that serving both EVs through one WCS (on arc BC) with a higher power level $P_{BC} = [(c_1 + c_2)/(\eta\, t_{BC})]$ kW capacity, instead of two separate WCSs on CD and CF, might be economically preferable.

This example provides an insight on favorable WCS locations and capacity levels in the case that the objective is to capture the current UE traffic pattern so as to promote EV adoption. In particular, it illustrates that it is preferable to choose WCS locations on the arcs with longer travel times (to reduce variable costs due to lower capacity installations) and/or on the arcs that are shared by multiple paths (to take advantage of economies-of-scale). Nonetheless, it is usually the case in traffic networks that the shared arcs are the most congested ones, and thus have longer travel times. This implies that more congested arcs are better candidates to host WCS(s), not only to take advantage of the economies-of-scale, but also because high travel volume on the arc increases the travel time, and therefore, decreases the required capacity (because the EV can charge for a longer duration) and associated cost of the installed WCS. We later use this insight in devising an upper bound heuristic employed to increase the efficiency of our solution algorithm.

3.2.1. Problem Setting and Definitions

We consider a directed graph $\mathcal{G}(\mathcal{N}, \mathcal{A})$ representing the traffic network where $\mathcal{N}$ is the set of nodes and $\mathcal{A}$ is the set of directed arcs. Each node represents an origin and/or a destination, as well as an intersection. Each arc represents a road segment and a candidate site for a WCS. Let $\mathcal{Q}$ be the set of all OD-pairs in the network, and $\mathcal{R}_q$ be the set of all routes between a certain OD-pair $q \in \mathcal{Q}$.

For operational purposes, electric vehicles traveling in the system can be divided into different classes based on (i) the initial state of charge of the EV, (ii) the desired ending state of charge[1], and (iii) the battery capacity. Let $\mathcal{K}$ be the set of all EV classes in the network. Note that related studies assumed that all EVs in the network start their trips fully charged and share the same battery size. We believe that our suggested classification of EVs, performed by the planning entity, brings the problem closer to reality. We define a cluster as a group of EVs of class $k \in \mathcal{K}$ traveling between a certain OD-pair $q \in \mathcal{Q}$ using a

[1]The dynamic charging system is meant to only increase the EV driving range, not to replace the conventional charging stations. Therefore, the ending state of charge of the EV battery (SOC) is typically expected to be less than the initial SOC for all practical purposes.

certain route $r \in \mathcal{R}_q$.

The traffic pattern in the network is assumed to follow a UE traffic assignment which offers a suitable system representation for long term planning purposes [43]. Specifically, the UE traffic assignment represents the steady-state of the traffic condition in traffic networks. Under this assignment, the traffic flows on each OD-pair follows Wardrop's first principle which reads:

> The journey times on all routes actually used are equal, and less than those which would be experienced by a single vehicle on any unused route [63].

Therefore, under UE, no driver can improve her travel time by switching route. It is important to note that this principle assumes that all travelers in the network have complete awareness of the current traffic condition.

We consider the UE of a peak traffic period as it corresponds to the highest traffic volume and therefore, the highest charging demands. The UE algorithm is executed prior to our network design optimization to generate part of the input to our model. Specifically, the algorithm's output includes the traffic flows on routes which, in turn, dictates the traffic volume and associated traffic density on each arc of the network, i.e., the parameters v_{ij} (vehicles/hour) and κ_{ij} (vehicles/mile) on each arc $(i,j) \in \mathcal{A}$ of the network under study. Using this data as well as the arc proportion[2] and the EV penetration rate for class k, denoted by $EVPR_k$, we calculate the average number of EVs of class k that are occupying arc (i,j) while traveling between OD-pair q along route r as

$$\rho_{ij}^{qrk} = \kappa_{ij}\ l_{ij} \left(\frac{\delta_{ij}^{qr}\ f^{qr}}{\sum\limits_{s \in \mathcal{Q}} \sum\limits_{t \in \mathcal{R}_q} (\delta_{ij}^{st}\ f^{st})} \right) EVPR_k \tag{3.1}$$

where

l_{ij} is the length of arc (i,j)

[2]For an arc (i,j) on a route r, arc proportion is the proportion of the flow on (i,j) that belongs to route r to the total flow on (i,j). It is expressed as the fraction on the right-hand side of (3.1).

δ_{ij}^{qr} is an indicator with value of 1 if arc (i, j) is part of route r, 0 otherwise

f^{qr} is the traffic volume on route r measured in vehicles/hour, obtained from UE.

The travel times on arcs are also determined by the UE algorithm using the Bureau of Public Roads (BRP) arc performance function [55] given as

$$t_{ij} = t_{ij}^{min}\left(1 + \alpha(\frac{v_{ij}}{tc_{ij}})^{\beta}\right) \tag{3.2}$$

where

t_{ij}^{min} is the free-flow travel time on arc (i, j)

tc_{ij} is the traffic capacity of arc (i, j) measured in vehicles/hour

α and β are deterministic permeates associated with the type of the road.

Next, we provide our model formulation to determine the optimal locations of WCSs, their capacity levels, and assignments of EV clusters to WCSs for recharging on their routes dictated by UE solution. We assume a planning horizon of a number of years during which the expected demand for wireless EV charging is steady, for example a desired target value, therefore, we assume that all costs are adjusted to reflect annual values.

3.2.2. Model Formulation

We first introduce the following notation used in our formulation.

Sets:

$\mathcal{N}$ set of nodes, $i, j \in \mathcal{N}$

$\mathcal{O}$ set of origins, $o \in \mathcal{O} \subset \mathcal{N}$

$\mathcal{D}$ set of destinations, $d \in \mathcal{D} \subset \mathcal{N}$

$\mathcal{A}$ set of arcs, $(i, j) \in \mathcal{A}$

$\mathcal{Q}$ set of all OD-pairs within the network, $q \in \mathcal{Q}$

$\mathcal{R}_q$ set of all used routes between a certain OD-pair q, $r \in \mathcal{R}_q$ where

o_r and d_r are the origin node and destination node of route r, respectively.

$\mathcal{N}_r$ set of nodes on a route $r \in \mathcal{R}_q,\ \mathcal{N}_r \subset \mathcal{N}$

$\mathcal{A}_r$ set of arcs on a route $r \in \mathcal{R}_q,\ \mathcal{A}_r \subset \mathcal{A}$

$\mathcal{K}$ set of EV classes, $k \in \mathcal{K}$

Parameters:

fc_{ij} fixed cost ($) associated with installing a WCS with basic capacity on arc (i, j)

vc variable cost ($) associated with adding one expansion charging unit to a WCS

cc charging cost ($/kWh)

tr average number of trips taken by an EV during one year period

b_{cap} basic power capacity (kW) of a WCS

e_{cap} power capacity (kW) associated with adding one expansion charging unit to a WCS

m_{cap} maximum power capacity (kW) that can be installed on one mile of a one-lane road segment

η efficiency coefficient of the wireless power transfer system

ξ_{ij} energy consumption (kWh) on arc (i, j)

ξ_r energy consumption (kWh) on route r

ϱ vehicle charging power (kW)

γ_k battery capacity (kWh) of an EV of class k

ρ_{ij}^{qrk} the average number of EVs of class k, that are occupying arc (i,j) while traveling between OD-pair q along route r, $q \in \mathcal{Q}$, $r \in \mathcal{R}_q$, $k \in \mathcal{K}$, $(i,j) \in \mathcal{A}_r$

l_{ij} length of arc (i,j) (mile)

n_{ij} number of lanes on arc (i,j)

t_{ij} travel time on arc (i,j) (hour)

δ_{ij}^{qr} an indicator with value of one if arc (i,j) is part of route r, 0 otherwise

ie_k initial energy level of an EV of class $k \in \mathcal{K}$

ee_k ending energy level of an EV of class $k \in \mathcal{K}$

Decision Variables:

x_{ij} 1 if a WCS is installed on candidate arc (i,j), 0 otherwise

y_{ij} number of power expansion charging units installed on arc (i,j)

e_i^{qrk} energy level at node i of an EV of class k, traveling between OD-pair q on route r, $q \in \mathcal{Q}$, $r \in \mathcal{R}_q$, $k \in \mathcal{K}$, $i \in \mathcal{N}_r$

c_{ij}^{qrk} amount of charge an EV of class k, traveling between OD-pair q on route r, receives from WCS on arc (i,j), $q \in \mathcal{Q}$, $r \in \mathcal{R}_q$, $k \in \mathcal{K}$, $(i,j) \in \mathcal{A}_r$

The wireless charging stations network design problem (**P**) can then be formulated as:

$$\text{Minimize} \quad \sum_{(i,j)\in\mathcal{A}} (fc_{ij}\, x_{ij} + vc\, y_{ij}) + \sum_{q\in\mathcal{Q}} \sum_{r\in\mathcal{R}_q} \sum_{k\in\mathcal{K}} \sum_{(i,j)\in r} (cc\ tr\ c_{ij}^{qrk}) \tag{3.3}$$

subject to

$$e_{o_r}^{qrk} + \sum_{(i,j)\in r} c_{ij}^{qrk} - e_{d_r}^{qrk} = \xi_r \qquad \forall\, q \in \mathcal{Q},\, r \in \mathcal{R}_q,\, k \in \mathcal{K} \tag{3.4}$$

$$e_i^{qrk} + c_{ij}^{qrk} - e_j^{qrk} = \xi_{ij} \qquad \forall\, q \in \mathcal{Q},\, r \in \mathcal{R}_q,\, k \in \mathcal{K},\, i, j, \in \mathcal{N}_r,\, (i,j) \in \mathcal{A}_r \quad (3.5)$$

$$e_i^{qrk} - \xi_{ij}\,(1 - x_{ij}) \geq 0 \qquad \forall\, q \in \mathcal{Q},\, r \in \mathcal{R}_q,\, k \in \mathcal{K},\, i \in \mathcal{N}_r,\, (i,j) \in \mathcal{A}_r \quad (3.6)$$

$$c_{ij}^{qrk} \leq \varrho\, t_{ij}\, x_{ij} \qquad \forall\, q \in \mathcal{Q},\, r \in \mathcal{R}_q,\, k \in \mathcal{K},\, (i,j) \in \mathcal{A}_r \quad (3.7)$$

$$\sum_{q \in \mathcal{Q}} \sum_{r \in \mathcal{R}_q} \sum_{k \in \mathcal{K}} (\delta_{ij}^{qr}\, \rho_{ij}^{qrk}\, c_{ij}^{qrk})$$

$$\leq \eta\,(b_{cap}\, x_{ij} + e_{cap}\, y_{ij})\, t_{ij} \qquad \forall\, (i,j) \in \mathcal{A} \quad (3.8)$$

$$b_{cap}\, x_{ij} + e_{cap}\, y_{ij} \leq m_{cap}\, n_{ij}\, l_{ij} \qquad \forall\, (i,j) \in \mathcal{A} \quad (3.9)$$

$$e_i^{qrk} + c_{ij}^{qrk} \leq \gamma_k + \xi_{ij} \qquad \forall\, q \in \mathcal{Q},\, r \in \mathcal{R}_q,\, k \in \mathcal{K},\, i \in \mathcal{N}_r,\, (i,j) \in \mathcal{A}_r \quad (3.10)$$

$$e_{o_r}^{qrk} = ie_k \qquad \forall\, q \in \mathcal{Q},\, r \in \mathcal{R}_q,\, k \in \mathcal{K} \quad (3.11)$$

$$e_{d_r}^{qrk} \geq ee_k \qquad \forall\, q \in \mathcal{Q},\, r \in \mathcal{R}_q,\, k \in \mathcal{K} \quad (3.12)$$

$$e_i^{qrk},\ c_{ij}^{qrk} \geq 0,\ x_{ij} \in \{0,1\}, y_{ij} \in Z^+ \qquad \forall\, q \in \mathcal{Q},\, r \in \mathcal{R}_q,\, k \in \mathcal{K},\, i \in \mathcal{N}, (i,j) \in \mathcal{A} \quad (3.13)$$

The first term in the objective function (3.3) represents the total cost of deploying all WCSs in the network. This includes the fixed installment cost of both inverters and charging pads to support a base power capacity as well as their variable costs associated with capacity expansions. As a part of the overall cost, the second term sums the charging cost (electricity cost) that an EV of cluster qrk consumes during one year period. A further motivation for this term is to reduce the number of possible optimal solutions by minimizing the amount of charge that each EV draws from the network. Specifically, for a traveler, there may be alternative locations to charge on the given route without violating remaining energy requirements, thus, this term on charging costs helps to differentiate between them and provides methodological benefit in solving the model.

Constraints (3.4) and (3.5) are the energy conservation constraints over paths and over arcs, respectively. Note that constraint (3.4) is redundant once constraint (3.5) is satisfied. However, our initial computational experiments showed that constraint (3.4) is helpful when solving the MIP. Constraints (3.6) ensure that at each node, each EV has enough energy to go to the next node on its route, if there is no WCS installed before the next node is

reached. Constraints (3.7) are linking constraints that serve two purposes. Each of these constraints ensures that a WCS is installed on arc (i, j) when EVs of a certain cluster is to recharge on the arc (as assigned by the model). A constraint of this type also enforces the maximum amount of energy that an EV can intake on a certain arc as an upper bound on the continuous variables c_{ij}^{qrk}. Constraints (3.8) ensure that a WCS installed on an arc has enough power capacity to satisfy all the charging demands on that arc. Constraints (3.9) bound the installed power capacity of WCSs. Constraints (3.10) bound the energy level of each EV by its battery capacity. Constraints (3.11) and (3.12) assign the values of initial and desired ending energy level for each cluster in the system to the corresponding variables. Finally, constraints (3.13) provides the structural requirements of the model.

Note that although the UE problem is solved on the overall underlying network $(\mathcal{N}, \mathcal{A})$ the network can be reduced in the above optimization problem by setting $\mathcal{N}$ and $\mathcal{A}$ to $\mathcal{N} = \bigcup_{q \in \mathcal{Q},\ r \in \mathcal{R}_q} \mathcal{N}_r$ and $\mathcal{A} = \bigcup_{q \in \mathcal{Q},\ r \in \mathcal{R}_q} \mathcal{A}_r$, respectively.

3.3. Solution Methodology

Based on our initial computational experiments on solving the smallest of our test instances (10 by 10 grid network), we observed that the Branch&Cut algorithm as implemented in CPLEX was not efficient especially due to excessive run times to generate good bounds. Therefore, in this section we devise an exact solution algorithm based on a framework that combines combinatorial BD with classical BD.

Classical BD [6] involves splitting a mixed integer program (MIP) into two problems: (i) Master Problem (MP) which includes all the integer variables from the original program, and (ii) Subproblem (SP) which includes only the continuous variables. In addition to the integer variables, MP includes a continuous auxiliary variable that facilitates the communication between the two problems. In general, the overall approach involves solving MP, which is a relaxation of the original problem and thus it provides a lower bound on the original MIP (in case of a minimization problem). The solution generated by MP is then used by fixing the values of the integer variables and utilizing them as inputs to solve the Dual

Subproblem (DSP) as a pure linear program. If DSP is feasible and bounded, its optimal objective function value and the integer part of MP's objective provide an upper bound on the original MIP. If a stopping criterion (solution quality or time) is not met the solution of DSP is used to generate a Benders optimality cut which is added to MP in the next iteration. On the other hand, if DSP is unbounded, we use its extreme rays to generate a Benders feasibility cut and add it to MP. This iterative process is continued until at least one stopping criterion is met.

More recently, combinatorial BD which employs Benders combinatorial cuts was suggested as an alternative to classical BD [14]. Similar to classical BD, the integer solution of the master problem is passed, iteratively, to the linear subproblem. Nonetheless, combinatorial BD deviates from classical BD by the types of cuts utilized and the process of reaching optimality. Specifically, in combinatorial BD, if MP's solution makes the subproblem infeasible, then a combinatorial Benders cut is appended to MP to force at least one of its binary variables to change its value from the previous iteration. Consequently, the new MP solution will generate a new SP. In case the objective function of the original problem does not contain any terms with continuous variables (that can serve to form the objective of SP), the iterative approach (and therefore generating combinatorial cuts) continues until reaching a feasible subproblem. This indicates that the most recent MP solution is also optimal for the original problem. On the other hand, if the objective function of the original problem contains only terms with continuous variables that also forms the SP objective function, a feasible MP solution is first obtained. If this solution produces a feasible SP, the incumbent solution is updated and the combinatorial cuts are added to MP to find a better feasible integer solution. This process is continued until MP is infeasible.

In this study, we combine features from classical and combinatorial BD after moving a set of integer variables from MP to SP to reduce the size (and consequently the difficulty) of MP at the cost of having to deal with a more complex integer SP. Only a handful of applications employed BD with integer subproblem. For example, in a study concerning integrated aircraft routing and crew scheduling problem [16], the decomposed model contained a binary

MP and a binary SP. The model is solved using a three-phase algorithm. The first phase includes a relaxation of all integrality constraints, and BD is used together with column generation to solve the LP relaxation of the integer model. The integrality constraints on MP are enforced in phase two and the integer MP is solved at each iteration of the BD algorithm. In the third phase, the integrality constraints on SP are re-enforced and SP is solved once for a fixed MP solution. In another study, Naoum-Sawaya and Elhedhli [47] devised a nested Benders approach with an integer SP to solve a telecommunication network planning problem. The authors used combinatorial BD to decompose the MIP model into a binary MP and an integer SP. In the solution approach, Benders combinatorial cuts are added to the binary MP after each iteration, while the integer SP is solved using classical BD. Our proposed BD approach works in a different fashion; a Benders combinatorial cut is generated whenever the integer SP is infeasible. On the other hand, if the integer SP is feasible, we generate a classical Benders optimality cut based on the solution of the linear relaxation of the integer SP. In what follows, we first present the components of the overall BD approach including combinatorial and classical Benders cuts, surrogate constraints, and an upper bound heuristic. Later, in Section 3.3.5 we present the overall BD algorithm for our problem.

3.3.1. Combinatorial Benders Decomposition

Our model can be expressed as a two-stage decision model. The first stage is to decide the locations of the WCSs in the network. The second-stage decision deals with the power capacities of the stations and the amount of electrical charge that each EV cluster should receive at each station. Accordingly, Benders subproblem can be obtained for a fixed set of locations of WCSs in the network, i.e., for given values of binary variables $\hat{x}_{ij}$, obtained from MP, SP(e_i^{qrk}, $c_{ij}^{qrk}, y_{ij} \mid \hat{x}_{ij}$) can be formulated as follows:

$$\text{Minimize} \quad \zeta = \sum_{(i,j)\in\mathcal{A}} (vc\, y_{ij}) + \sum_{q\in\mathcal{Q}} \sum_{r\in\mathcal{R}_q} \sum_{k\in\mathcal{K}} \sum_{(i,j)\in r} (cc\, tr\, c_{ij}^{qrk}) \tag{3.14}$$

subject to

(3.4), (3.5), (3.10), (3.11), (3.12),

$$e_i^{qrk} - \xi_{ij}\,(1 - \hat{x}_{ij}) \geq 0 \qquad \forall\, q \in \mathcal{Q},\, r \in \mathcal{R}_q,\, k \in \mathcal{K},\, i \in \mathcal{N}_r,\, (i,j) \in \mathcal{A}_r \tag{3.15}$$

$$c_{ij}^{qrk} \leq \varrho\, t_{ij}\, \hat{x}_{ij} \qquad \forall\, q \in \mathcal{Q},\, r \in \mathcal{R}_q,\, k \in \mathcal{K},\, (i,j) \in \mathcal{A}_r \tag{3.16}$$

$$\sum_{q\in\mathcal{Q}} \sum_{r\in\mathcal{R}_q} \sum_{k\in\mathcal{K}} (\delta_{ij}^{qr}\, \rho_{ij}^{qrk}\, c_{ij}^{qrk}) \leq \eta\,(b_{cap}\, \hat{x}_{ij} + e_{cap}\, y_{ij})\, t_{ij} \qquad \forall\, (i,j) \in \mathcal{A} \tag{3.17}$$

$$b_{cap}\, \hat{x}_{ij} + e_{cap}\, y_{ij} \leq m_{cap}\, n_{ij}\, l_{ij} \qquad \forall\, (i,j) \in \mathcal{A} \tag{3.18}$$

$$e_i^{qrk},\, c_{ij}^{qrk}, \geq 0,\, y_{ij} \in Z^+ \qquad \forall\, q \in \mathcal{Q},\, r \in \mathcal{R}_q,\, k \in \mathcal{K},\, i \in \mathcal{N}, (i,j) \in \mathcal{A} \tag{3.19}$$

and, thus, the master problem MP is given as

$$\text{Minimize} \quad \sum_{(i,j)\in\mathcal{A}} (fc_{ij}\, x_{ij}) + \zeta$$

$$\text{subject to} \quad x_{ij} \in \{0, 1\}$$

For given values of $\hat{\mathbf{X}}$, if SP is infeasible, then at least one of the x_{ij} variables in MP should be forced to change its value. Thus, a Benders combinatorial cut (i.e., no-good cut in [14]) of the form

$$\sum_{\{(i,j):\hat{x}_{ij}=0\}} x_{ij} + \sum_{\{(i,j):\hat{x}_{ij}=1\}} (1 - x_{ij}) \geq 1 \tag{3.20}$$

is added to the master problem. Let $\mathcal{V}^u$ denote the sets of all combinatorial cuts associated with infeasible subproblems in the first u iterations. Then, MP in iteration $u+1$ can be stated as

$$\text{Minimize} \quad \sum_{(i,j)\in\mathcal{A}} (fc_{ij}\, x_{ij}) + \zeta \tag{3.21}$$

subject to

$$\sum_{\{(i,j):x_{ij}^v=0\}} x_{ij} + \sum_{\{(i,j):x_{ij}^v=1\}} (1 - x_{ij}) \geq 1 \qquad \forall\, v \in \mathcal{V}^u \tag{3.22}$$

$$x_{ij} \in \{0,1\} \qquad \forall\, (i,j) \in \mathcal{A}. \tag{3.23}$$

Clearly, the MP formulation above is a relaxation of our original problem P, and thus, provides a lower bound when the subproblems are infeasible. Observe that the optimum value of ζ will always be zero in the solution. To avoid this situation and to improve the value of the lower bound provided by MP, we strengthen the MP formulation by utilizing classical Benders cuts as described next.

3.3.2. Benders Cuts based on Relaxed SP

To strengthen the lower bound provided by MP, in addition to combinatorial Benders cut, we consider adding classical Benders cuts obtained via a linear relaxation of SP, denoted by RSP. For this purpose, we relax the integrality requirements on the y_{ij} variables. First, ensuring that for a given MP solution $\hat{\mathbf{X}}$, SP is feasible, we use the dual of RSP to generate a classical Benders cut. Let $\psi_{qrk}^{ij}, \sigma_{qrk}^{ij}, \theta_{qrk}, \tau_{qrk}, \upsilon_{qrk}^{ij}, \nu_{qrk}^{ij}, \omega_{ij},$ and ϖ_{ij} be the dual variables associated with (3.5), (3.10), (3.11), (3.12), (3.15), (3.16), (3.17), and (3.18), respectively[3]. Further, define binary parameters λ_{qr}^i and ε_{qr}^i as one if $i \in \mathcal{O}$ and $i \in \mathcal{D}$, respectively, zero otherwise. Then, the dual of the RSP, denoted as DRSP$(\psi_{qrk}^{ij}, \sigma_{qrk}^{ij}, \theta_{qrk}, \tau_{qrk}, \upsilon_{qrk}^{ij}, \nu_{qrk}^{ij}, \omega_{ij}, \varpi_{ij} | \hat{x}_{ij})$

[3]Constraint (3.4), while helpful in solving integer SP, is redundant and, thus, omitted in constructing the dual of RSP.

is obtained as

$$\begin{aligned}\text{Maximize}\quad \zeta_R = & \sum_{q\in\mathcal{Q}}\sum_{r\in\mathcal{R}_q}\sum_{k\in\mathcal{K}}\sum_{(i,j)\in r}\Big(\xi_{ij}\,\psi^{ij}_{qrk} + \xi_{ij}\,(1-\hat{x}_{ij})\,\upsilon^{ij}_{qrk} \\ & + \varrho\,t_{ij}\,\hat{x}_{ij}\,\nu^{ij}_{qrk} + (\gamma_k+\xi_{ij})\,\sigma^{ij}_{qrk}\Big) \\ & + \sum_{(i,j)\in\mathcal{A}}\Big(\eta\,b_{cap}\,\hat{x}_{ij}\,t_{ij}\,\omega_{ij} + (m_{cap}\,n_{ij}\,l_{ij} - b_{cap}\,\hat{\mathbf{X}})\,\varpi_{ij}\Big) \\ & + \sum_{q\in\mathcal{Q}}\sum_{r\in\mathcal{R}_q}\sum_{k\in\mathcal{K}}(ie_k\,\theta_{qrk} + ee_k\,\tau_{qrk}) \end{aligned} \tag{3.24}$$

subject to

$$\begin{aligned}&\lambda^i_{qr}\,(\theta_{qrk}+\psi^{ij}_{qrk}+\upsilon^{ij}_{qrk}+\sigma^{ij}_{qrk})+ \\ &\quad \varepsilon^i_{qr}\,(\tau_{qrk}-\psi^{ij}_{qrk}) + (1-\lambda^i_{qr}-\varepsilon^i_{qr})\times \\ &\qquad (\psi^{ij}_{qrk} - \psi^{k\ i-1\ j-1}_{qr} + \upsilon^{ij}_{qrk}+\sigma^{ij}_{qrk}) \le 0 \qquad \forall\, q\in\mathcal{Q},\, r\in\mathcal{R}_q,\, k\in\mathcal{K},\, i\in N_r \end{aligned} \tag{3.25}$$

$$\psi^{ij}_{qrk} + \nu^{ij}_{qrk} + \rho^{qrk}_{ij}\,\omega_{ij} + \sigma^{ij}_{qrk} \le cc\;tr \qquad \forall\, q\in\mathcal{Q},\, r\in\mathcal{R}_q,\, k\in\mathcal{K},\, (i,j)\in\mathcal{A}_r \tag{3.26}$$

$$-\eta\,e_{cap}\,t_{ij}\,\omega + e_{cap}\,\varpi \le vc \qquad \forall\,(i,j)\in\mathcal{A} \tag{3.27}$$

$$\psi^{ij}_{qrk},\ \theta_{qrk} \quad URS; \tag{3.28}$$

$$\upsilon^{ij}_{qrk},\ \tau_{qrk}\ge 0,\ \nu^{ij}_{qrk},\ \omega_{ij},\ \varpi_{ij},\ \sigma^{ij}_{qrk}\le 0 \qquad \forall\, q\in\mathcal{Q},\, r\in\mathcal{R}_q,\, k\in\mathcal{K},(i,j)\in\mathcal{A} \tag{3.29}$$

Let $\mathcal{P}$ denote the set of all extreme points of DRSP polyhedron given by (3.25) - (3.29), and let $\psi^{ijp}_{qrk}, \sigma^{ijp}_{qrk}, \theta^p_{qrk}, \tau^p_{qrk}, \upsilon^{ijp}_{qrk}, \nu^{ijP}_{qrk}, \omega^p_{ij}, \varpi^p_{ij}$, and ζ^p_R denote the associated dual variables and the value of the objective function respectively. Further, let ζ^* denote the optimal value of DRSP. Since $\zeta^p_R \le \zeta^*,\ \forall p\in\mathcal{P}$, DRSP can be restated as $\min_{\zeta\ge 0}\{\zeta : \zeta^p \le \zeta,\ \ \forall p\in\mathcal{P}\}$, where

$$
\begin{aligned}
\zeta_R^p = \quad & \sum_{q\in\mathcal{Q}} \sum_{r\in\mathcal{R}_q} \sum_{k\in\mathcal{K}} \sum_{(i,j)\in r} \Big(\xi_{ij}\, \psi_{qrk}^{ijp} + \xi_{ij}\, (1-\hat{x}_{ij})\, \upsilon_{qrk}^{ijp} \\
& + \ \varrho\, t_{ij}\, \hat{x}_{ij}\, \nu_{qrk}^{ijp} + (\gamma_k + \xi_{ij}\, \sigma_{qrk}^{ijp}) \Big) \\
& + \sum_{ij\in\mathcal{A}} \Big(\eta\, b_{cap}\, \hat{x}_{ij}\, t_{ij}\, \omega_{ij} + (m_{cap}\, n_{ij}\, l_{ij} - b_{cap}\, \hat{\mathbf{X}})\, \varpi_{ij} \Big) \\
& + \sum_{q\in\mathcal{Q}} \sum_{r\in\mathcal{R}_q} \sum_{k\in\mathcal{K}} (ie_k\, \theta_{qrk}^p + ee_k\, \tau_{qrk}^p)
\end{aligned}
$$

The above representation of DRSP gives:

$$
\zeta \geq \zeta_R^p \qquad\qquad \forall\, p \in \mathcal{P} \tag{3.30}
$$

which represents a classical Benders optimality cut that can be generated for each feasible SP and then added to MP. Further, if SP and its linear relaxation are both infeasible problems, then a classical Benders feasibility cut may be generated based on the extreme rays of the unbounded DRSP polyhedron. In the course of the iterative procedure, classical Benders cuts are added to MP whenever the integer SP is feasible in an iteration.

3.3.3. Problem-Specific Surrogate Constraints for MP

To further improve the solution quality of MP, we propose three sets of surrogate constraints that are valid while redundant for the original problem P. We also define new auxiliary non-negative variables $c_{ij}^{\prime qrk}$, and new auxiliary parameters $\hat{c}^{qrk}$. As a duplicate of variable c_{ij}^{qrk} in the original MIP, the auxiliary variable $c_{ij}^{\prime qrk}$ refers to the amount of charge an EV of a cluster qrk (i.e., an EV of class k traveling on route r between the OD pair q) will receive when charging at a WCS located on arc (i, j). Parameter $\hat{c}^{qrk}$ is calculated as the required amount of charge of an EV of a cluster qrk based on the given values of the initial and ending SOC levels. The first surrogate constraint is obtained from (3.4), and it ensures that each EV of a certain cluster will receive enough charge to finish its trip with

the required ending SOC:

$$\sum_{(i,j)\in\mathcal{A}_r} c'^{qrk}_{ij} \geq \hat{c}^{qrk} \qquad \forall\, q \in \mathcal{Q},\, r \in \mathcal{R}_q,\, k \in \mathcal{K}. \tag{3.31}$$

The second surrogate constraint is given as

$$c'^{qrk}_{ij} \leq \varrho\, t_{ij}\, x_{ij} \qquad \forall\, q \in \mathcal{Q},\, r \in \mathcal{R}_q,\, k \in \mathcal{K},\, (i,j) \in \mathcal{A}_r, \tag{3.32}$$

which is a copy of constraint (3.7) in the original problem. Finally, the third surrogate constraint is derived from (3.8) and (3.9) and is given as follows:

$$\sum_{q\in\mathcal{Q}} \sum_{r\in\mathcal{R}_q} \sum_{k\in\mathcal{K}} (\delta^{qr}_{ij}\, \rho^{qrk}_{ij}\, c'^{qrk}_{ij}) \leq \eta\, (m_{cap}\, n_{ij}\, l_{ij})\, t_{ij} \qquad \forall\, (i,j) \in \mathcal{A}. \tag{3.33}$$

3.3.4. Upper Bound Heuristic

In our preliminary computational experiment, MP always produced solutions that led to infeasible subproblems and, consequently, the generation of too many combinatorial cuts. A feasible subproblem (and therefore an upper bound solution) was never attainable in an acceptable amount of time. Therefore, to guarantee feasibility in SP, and thus, to generate good upper bounds and Benders optimality cuts, we devise a heuristic approach.

The idea of this approach is to determine WCSs locations and their capacities by considering subsets of OD pairs and sequentially solving smaller problems until all OD pairs are handled. Observe that, since the routes are known for OD pairs, a given subset of OD pairs in a step s of the process, $\mathcal{Q}^s$, dictates a subnetwork $(\mathcal{N}^s,\ \mathcal{A}^s)$ of the traffic network at hand. Therefore, our approach essentially relies on splitting the traffic network into several smaller subnetworks sequentially and solving a modified version (P^s) of the original MIP P for each such subnetwork. In doing so, while solving for a subnetwork, we assume the existence of a set $\mathcal{S}$ which represents the arcs with installed WCS with known capacities up until that point.

The new mixed integer program (P^s), where the superscript s refers to a subnetwork, has the same objective function and constraints as P, but it is solved for only a subnetwork defined by $\mathcal{Q}^s \subset \mathcal{Q}$, $\mathcal{N}^s \subset \mathcal{N}$, and $\mathcal{A}^s \subset \mathcal{A}$, and it has the following two additional constraints:

$$x_{ij} = 1 \qquad \forall\,(i,j) \in \mathcal{S} \cap \mathcal{A}^s \tag{3.34}$$

$$\sum_{q \in \mathcal{Q}} \sum_{r \in \mathcal{R}_q} \sum_{k \in \mathcal{K}} (\delta_{ij}^{qr}\, \rho_{ij}^{qrk}\, c_{ij}^{qrk}) \leq \eta\,(e_{cap}\, y_{ij})\, t_{ij} \qquad \forall\,(i,j) \in \mathcal{S} \cap \mathcal{A}^s. \tag{3.35}$$

Constraint (3.34) ensures that all WCSs resulted by solving for previous subnetworks do exist (are installed) when solving for the next subnetwork. Constraint (3.35) is derived from constraint (3.8) in the original problem P and it ensures that, for WCSs that have been already installed (when solving for previous subnetworks), the added power capacity (the right hand side of 3.35) corresponds only to the expansion needed at that step. Further, to avoid arcs over-capacitating (in terms of electric power) that might result from the integrality constraints on variables y_{ij}, in problem P^s, we relax these constraints, i.e., $y_{ij} \in \mathbb{R}^+$. Moreover, constraint (3.9) is adjusted to account for the capacities that have already been installed when solving previous subproblems:

$$b_{cap}\, x_{ij} + e_{cap}\, y_{ij} \leq m_{cap}\, n_{ij}\, l_{ij} - e_{cap}\, \hat{y}_{ij} \qquad \forall\,(i,j) \in \mathcal{A}^s \tag{3.36}$$

where $\hat{y}_{ij}$ is a parameter representing the existing power capacities installed on arc (i,j) for which the already installed base capacity is accounted for by constraints (3.34). Because of the relaxation of the integrality constraint on variable y_{ij}, constraint (3.36) needs to be reformulated in order to avoid solutions of P^s that might make P infeasible. Thus, we rewrite constraint (3.36) as follows

$$y_{ij} \leq \left\lfloor \frac{m_{cap}\, n_{ij}\, l_{ij} - e_{cap}\, \hat{y}_{ij} - b_{cap}}{e_{cap}} \right\rfloor x_{ij} \qquad \forall\,(i,j) \in \mathcal{A}^s \tag{3.37}$$

For example, with values of b_{cap} and e_{cap} equal to 30 and 15 respectively, for an arc with a total capacity ($m_{cap}\, n_{ij}\, l_{ij}$) of 100, y_{ij} can be at most four.

To decide on how to best construct the smaller subnetworks with each containing n OD pairs in sequence, we build on the insight provided in Section 3.2 which implies that the more congested arcs are better candidates to host WCSs. Therefore, at each step of our heuristic, we construct a subnetwork out of the n ODs with the highest traffic volume. The proposed upper bound heuristic (UBH) is displayed in Algorithm 1.

The inputs to UBH include a set of arcs $\mathcal{S}$, with existing WCSs as potential candidates for capacity expansion along with there existing capacity levels (given by y_{ij} values), and the parameter n to limit the size of subset $\mathcal{Q}^s$, where s represents the step number in the sequential algorithm.

We initiate the sequential algorithm (line 2) with a set $\mathcal{T}$ that initially contains all OD pairs in the network, and set $\mathcal{Q}^s$ as an empty set.

Algorithm 1 Upper Bound Heuristic (UBH)

1: **inputs** $\mathcal{S} = \{(i,j) \mid x_{ij} = 1\}$, $\hat{y}_{ij} \quad \forall (i,j) \in \mathcal{A}$, and n
2: **initialize** $\mathcal{Q}^s = \emptyset$, $\mathcal{T} = \mathcal{Q}$, $s = 0$
3: **while** $\mathcal{T} \neq \emptyset$ **do**
4: set $\mathcal{Q}^s = \emptyset$
5: choose min($|\mathcal{T}|$, n) OD pairs with the highest traffic volume from $\mathcal{T}$
6: move them from $\mathcal{T}$ to $\mathcal{Q}^s$, and also from set $\mathcal{A}^s$
7: solve $\mathbf{P}^s$ to obtain x_{ij}, y_{ij},
8: **for each** $(i,j) \in \mathcal{A}^s$ **do**
9: **if** $x_{ij} = 1$ **then**
10: $\mathcal{S} = \{(i,j)\} \cup \mathcal{S}$
11: $\hat{y}_{ij} = \hat{y}_{ij} + y_{ij}$
12: **end if**
13: **end for**
14: **end while**
15: solve $\hat{\mathbf{P}}$ with constraint $x_{ij} = 0$, $\forall\, (i,j) \in \mathcal{A} \setminus \mathcal{S}$, to obtain the objective value $Z_{\hat{\mathbf{P}}}$
16: return $Z_{\hat{\mathbf{P}}}$

At the beginning of each step we choose the n OD pairs with the highest traffic volume (demand) from set $\mathcal{T}$ and we move them to set $\mathcal{Q}^s$ (line 5 and 6). We solve P^s and we add the resulting WCSs to set $\mathcal{S}$ and update the potential capacities of these WCSs (lines 7 - 13). When the sequential procedure is over, as the last step, we solve a modified version of the original problem P, denoted by $\hat{\mathrm{P}}$ which considers only the locations contained in set $\mathcal{S}$ as candidates for WCS locations (line 15). This helps in obtaining a further improved upper bound in a short runtime because the number of potential locations, and therefore the number of binary variables in the problem P is reduced to $|\mathcal{S}|$, rather than $|\mathcal{A}|$.

3.3.5. BD Implementation

We provide our overall Benders approach that combines all the ingredients described above in Algorithm 2 in which the best upper and lower bounds are represented by UB and LB, respectively. Parameter ϵ represents the allowed optimality gap and parameter `optgap` denotes the optimality gap with the best current bounds (calculated as $(UB - LB)/UB$).

We start the iterations ($itr = 1$) by obtaining an initial solution, with Z_{UBH} and $\hat{x}_{ij}$, via our upper bound heuristic (UBH) (lines 2 - 4). The $\hat{x}_{ij}$ values obtained are passed to Benders (integer) subproblem SP which is guaranteed to provide a feasible solution with an objective value Z_{SP} (line 7). Then, a new upper bound is calculated as $\sum_{(i,j)}(fc_{ij}\ \hat{x}_{ij}) + Z_{SP}$ and the best UB is updated if necessary (lines 8 - 9). We next proceed to solve the dual problem of the LP relaxation of the integer subproblem $\mathrm{DRSP}(\psi^{ij}_{qrk}, \upsilon^{ij}_{qrk}, \nu^{ij}_{qrk}, \omega_{ij}, \varpi_{ij}, \sigma^{ij}_{qrk}, \theta_{qrk}, \tau_{qrk} \mid \hat{x}_{ij})$. Using the dual variables obtained, we generate a Benders classical optimality cut (3.30) and add it to MP (lines 12 - 13). Next, MP is solved to obtain a lower bound on the original problem P (lines 14 - 16). At this point, we check the stopping criteria, which include the runtime and optimality gap calculated based on the current best bounds values, and terminate the algorithm if at least one criterion is met (line 17). Otherwise, we continue by solving a new SP with the most recent $\hat{x}_{ij}$ values generated by MP (line 20). Note that the locations $\hat{x}_{ij}$ generated by MP are not guaranteed to render a feasible SP. Therefore, if SP is feasible, we update the upper bound (line 22), and we check the stopping criteria (line 24).

Algorithm 2 BD Implementation

1: **initialize** $itr = 1$, $\mathcal{S} = \emptyset$, $UB = \infty$, $LB = 0$, $\epsilon = 0.02$, `runtime`=0, `stoptime`=7200 seconds, and n
2: solve **UBH**$(e_i^{qrk},\ c_{ij}^{qrk}, y_{ij},\ x_{ij} \mid \mathcal{S},\ n)$ for $Z_{UBH} = Z_{\hat{\mathbf{P}}}$ and $\hat{x}_{ij}$
3: **if** $Z_{UBH} < UB$ **then** $UB = Z_{UBH}$
4: **end if**
5: **if** `optgap` $< \epsilon$ **or** `runtime` $\geq$ `stoptime` **then** break (return best UB solution)
6: **else**
7: solve **SP**$(e_i^{qrk},\ c_{ij}^{qrk}, y_{ij} \mid \hat{x}_{ij})$ for Z_{SP}
8: **if** $\sum_{(i,j)}(fc_{ij}\ \hat{x}_{ij}) + Z_{SP} < UB$ **then** $UB = \sum_{(i,j)}(fc_{ij}\ \hat{x}_{ij}) + Z_{SP}$
9: **end if**
10: **if** `optgap` $< \epsilon$ **or** `runtime` $\geq$ `stoptime` **then** break (return best UB solution)
11: **else**
12: solve **DRSP**$(\psi_{qrk}^{ij}, \upsilon_{qrk}^{ij}, \nu_{qrk}^{ij}, \omega_{ij}, \varpi_{ij}, \sigma_{qrk}^{ij}, \theta_{qrk}, \tau_{qrk} \mid \hat{x}_{ij})$
13: generate classical Benders optimality cut (3.30) and add it to **MP**
14: solve **MP** for Z_{MP} and $\hat{x}_{ij}$
15: **if** $Z_{MP} > LB$ **then** $LB = Z_{MP}$
16: **end if**
17: **if** `optgap` $< \epsilon$ **or** `runtime` $\geq$ `stoptime` **then** break (return best UB solution)
18: **else**
19: $itr++$
20: solve **SP**$(e_i^{qrk},\ c_{ij}^{qrk}, y_{ij} \mid \hat{x}_{ij})$
21: **if SP** is feasible **then**
22: **if** $Z_{SP} + Z_{MP} - \zeta < UB$ **then** $UB = Z_{SP} + Z_{MP} - \zeta$
23: **end if**
24: **if** `optgap` $< \epsilon$ **or** `runtime` $\geq$ `stoptime` **then** break (return best UB solution)
25: **else**
26: go to step 12
27: **end if**
28: **else**
29: **for each** $(i,j) \in \mathcal{A}$ **do**
30: **if** $\hat{x}_{ij} = 1$ **then** $\mathcal{S} = \{(i,j)\} \cup \mathcal{S}$
31: **end if**
32: **end for**
33: generate combinatorial Benders cut (3.22) and add it to **MP**
34: $n = n\ itr$
35: **end if**
36: **end if**
37: **end if**
38: **end if**
39: go to step 2

If the corresponding objective value (new UB) still does not produce an acceptable optimality gap, we proceed with solving the dual of the LP relaxation of SP (line 26). On the other hand, if SP is not feasible, we update the set of candidate locations $\mathcal{S}$ based on the current MP solution (line 30), and we generate a combinatorial Benders cut to be added to MP (3.22). We also update the value of parameter n (line 34) before we invoke a new UBH (39) with input including the updated set $\mathcal{S}$ and parameter n. As described in Algorithm 1, parameter n refers to the size of the OD subsets in each step and varying its value in successive UBH runs helps to improve the solution quality. The iterative procedure continues in this fashion until a stopping criterion is met in line 17 or 24.

3.4. Computational Study on Algorithmic Performance

The effectiveness of the proposed solution methodology is assessed based on comparisons to (i) Branch & Cut (B&C) approach implemented by CPLEX, and (ii) standard Benders Decomposition implemented by CPLEX. Random data sets are generated to represent different transportation networks in the state of traffic UE. Experiments are conducted using Java environment with CPLEX and Concert Technology (IBM, Inc.) on a machine with Intel Core i7 3.60 GHz processor and 32.0 GB RAM running 64-bit OS.

3.4.1. Data Generation

To test the performance of the proposed algorithm, we employ 3 data sets, each with three different data classes. Test classes are obtained by considering three different sizes of grid networks including 10×10, 20×20, and 30×30 grids and each data class consist of 10 randomly generated network instances. The input network data is summarized in Table 3.1 where, for a network class, $|\mathcal{N}|$, $|\bar{\mathcal{A}}|$, and $|\mathcal{Q}|$ represent the number of nodes, the average number of arcs over the 10 instances, and the number of OD pairs, respectively.

Each grid network (test instance) is constructed on a square geographical area of size 40 units. Links are randomly generated in a way that ensures a connected graph and a density in the range 58%-62%. After selecting a $|\mathcal{Q}|$ number of OD pairs randomly in each data set,

Table 3.1: Data classes and their sizes

Data set	S1			S2			S3		
Data class	C1	C2	C3	C4	C5	C6	C7	C8	C9
$\lvert\mathcal{N}\rvert$	100	400	900	100	400	900	100	400	900
$\lvert\bar{\mathcal{A}}\rvert$	349	1462	3332	349	1462	3332	349	1462	3332
$\lvert\mathcal{Q}\rvert$	5000	5000	5000	6536	6536	6536	8000	8000	8000

their traffic demands are generated in a way that the average speed in the networks under UE is in the range of 22 to 25 miles/hour. This has been achieved through some experimentation in the initial stage of the computational study. Specifically, on each generated test instance, the UE traffic assignment is first performed using the Method of Successive Averages[4]; and then, traffic volume and density values are calculated accordingly for each arc to be used as input to our model from the UE results obtained.

We consider 3 classes of EVs ($|\mathcal{K}| = 3$), where the parameters associated with each class are given in Table 3.2. We assume that the classes A, B, and C constitute 35%, 35%, and 30% of the EVs in the network, respectively. The values of the rest of the model parameters, and the test instances can be found online at http://lyle.smu.edu/INETS/TestInstances/EV-wireless-charging-network-data1.htm.

Table 3.2: Parameter of EV classes

	γ	ie	ee
EV class A	30	U[15,20] (medium SOC)	U[0,5] (low SOC)
EV class B	30	U[25,30] (high SOC)	U[10,15] (medium SOC)
EV class C	40	U[27,40] (high SOC)	U[0,13] (low SOC)

[4]The Method of Successive Averages is presented in Appendix A

3.4.2. Numerical Results

The results on runtimes and optimality gaps obtained by the B&C and our customized BD approaches are presented in Table 3.3. Similarly, the results on runtimes and optimality gaps obtained by the standard BD as implemented by CPLEX compared to our customized BD approach are presented in Table 3.4. Our initial approach to evaluate the effectiveness of our customized BD algorithm was to solve the test instances using B&C, and using BD, to the same optimality gap and compare the runtimes of the two methods. However, the initial runs using B&C as implemented by CPLEX indicated that for most of the instances, the solver could not obtain acceptable gaps even when left running for long times. For many instances, CPLEX could not reach acceptable gaps even after 48 hours of runtime. Therefore, and due to the excessive solution times with the B&C method, for a fair comparison, we solve each instance first by using the proposed BD approach with an optimality gap of 2.0% and record the runtime. The BD runtime is employed as a stopping criterion when solving the same instance using the B&C approach and the optimality gap upon termination is recorded.

The results show superior performance for the proposed methodology in comparison to the B&C approach. For all tested data classes, under the same runtimes, our suggested BD approach was able to solve the model to optimality gaps significantly less than 2%. On the other hand, B&C produced low-quality solutions, specifically with poor upper bound values and, most of the time, without lower bounds which are the cases noted as N.B. in Table 3.3.

Comparing our customized BD algorithm to the standard BD as implemented by CPLEX 12.8 provides further evidence in favor of the quality of our algorithm (Table 3.4). Under the same runtimes, our customized BD was able to solve all test instances to optimality gaps significantly less than 2%, while the standard BD implementation provided low-quality solutions with very high gaps. These results prove our finding in 3.3.4 that a direct implementation of BD algorithm was found unsatisfactory to solve the problem at hand. The results confirm the essentiality of the roles played by the upper bound heuristic as well as the surrogate constraints in the algorithmic performance of the customized BD.

Table 3.3: Numerical results (N.B. : no bound obtained)

	B&C results						Customized BD results					
Class	Runtime (secs)			Opt.Gap (%)			Runtime (secs)			Opt.Gap (%)		
No.	Avg.	Max	Min	Avg.	Max	Min	Avg.	Max	Min	Avg.	Max	Min
C1	650	1596	94	98.73	N.B.	98.16	628	1584	83	0.35	1.29	0.07
C2	445	675	237	N.B.	N.B.	N.B.	346	541	187	0.45	1.01	0.17
C3	821	997	458	N.B.	N.B.	N.B.	614	783	330	0.68	1.33	0.23
C4	694	2414	224	99.32	N.B.	98.85	618	2391	154	0.29	0.81	0.10
C5	617	1376	229	N.B.	N.B.	N.B.	505	1254	175	0.52	0.93	0.13
C6	1298	3087	801	N.B.	N.B.	N.B.	1031	2689	508	0.89	1.80	0.31
C7	654	1340	213	99.57	N.B.	97.60	615	1276	205	0.25	0.67	0.02
C8	720	1426	319	N.B.	N.B.	N.B.	636	1276	226	0.54	1.13	0.11
C9	1371	3218	549	N.B.	N.B.	N.B.	1167	2856	462	0.97	1.67	0.54

Table 3.4: Numerical results (N.B. : no bound obtained)

	CPLEX BD results						Customized BD results					
Class	Runtime (secs)			Opt.Gap (%)			Runtime (secs)			Opt.Gap (%)		
No.	Avg.	Max	Min	Avg.	Max	Min	Avg.	Max	Min	Avg.	Max	Min
C1	646	1586	109	96.10	98.15	95.08	628	1584	83	0.35	1.29	0.07
C2	452	600	240	96.22	96.67	95.88	346	541	187	0.45	1.01	0.17
C3	778	941	454	96.30	97.07	95.54	614	783	330	0.68	1.33	0.23
C4	671	2429	190	95.99	N.B.	94.87	618	2391	154	0.29	0.81	0.10
C5	686	1380	236	96.23	99.40	95.78	505	1254	175	0.52	0.93	0.13
C6	1396	3098	630	95.69	96.55	92.99	1031	2689	508	0.89	1.80	0.31
C7	678	1311	270	95.13	99.00	93.94	615	1276	205	0.25	0.67	0.02
C8	771	1287	314	95.58.	96.13	95.24	636	1276	226	0.54	1.13	0.11
C9	1350	3236	514	96.88	N.B.	93.40	1167	2856	462	0.97	1.67	0.54

3.5. A Case Study: Chicago Sketch Network

Chicago sketch network is an aggregated traffic network that provides a reasonably realistic representation of Chicago area for which the data is available online [4]. The network consists of 933 nodes, 2,950 arcs, and 378 zones. Our goal in this case study is to demonstrate the applicability of our model and the proposed algorithm on real traffic network and provide a sensitivity analyses on some of the system parameters that affect the system cost. We assume that all of the 1,260,907 vehicles traveling in the network are EVs with wireless charging capabilities. We also assume that these EVs are classified as follows: 35% of the EVs are of class D, 35% are of class E, and 30% are of class F. The parameters associated with each EV class are provided in Table 3.5. For the model parameters, we use the nominal values provided online at http://lyle.smu.edu/INETS/TestInstances/EV-wireless-charging-network-data1.htm. However, to be able to observe changes in system cost values more thoroughly, for parameters ϱ, m_{cap}, and η, we assume the nominal values of 100, 1000, and 70%, respectively.

Table 3.5: EV classes parameters

	γ	ie	ee
EV class D	30	(medium SOC)	(low SOC)
EV class E	30	(high SOC)	(medium SOC)
EV class F	30	(high SOC)	(low SOC)

Next, we present an analysis on the effects of varying values of system and product design characteristics – including vehicle charging power (ϱ), system efficiency (η), and the battery capacity (γ) – on the total system implementation cost.

3.5.1. Vehicle Charging Power (ϱ) vs. Total Cost

Vehicle charging power (i.e., car charger) is the maximum charging power of the EV. The value of this parameter ranges from 1 to 200 kW [19]. To evaluate the effect of this parameter on the total system cost, we solve our optimization model for charging power values of 20

kW up to 200 kW. Moreover, to detect any interactions between vehicle charging power (ϱ) and system efficiency (η), we run the model for each value of parameter ϱ while considering three different values for η, including 0.5, 0.7, and 0.9. Likewise, to detect any interactions between ϱ and battery capacity (γ) we run the model for each value of ϱ with γ values of 20, 30, and 40 kWh.

The results of this experiment are summarized in Figures 3.2a and 3.2b. The blue curve in each figure represents the behavior of the cost function under the nominal values for η (=0.7) and γ (=30). The curve indicates that an increase in the vehicle charging power from 20 kW to 60 kW results in 14% decrease in the total annual system cost ($31.6 million to $ 27.3 million). It also shows that a further increase of the vehicle charging power will have a lesser impact on the total cost. The cost function almost flattens as the vehicle charging power exceeds 140 kW. The figures also show large shifts in the cost curve under different values of system efficiency and battery capacity (Note that when parameters γ and ϱ are both equal to 20 (red curve), the charging demands could not be met, i.e., the problem is infeasible).

We observe that our model captures the interaction between the parameters systems efficiency, charging power, and battery capacity as they relate to the total system cost. Specifically, trade-offs in our case study can be summarized as follows. A reduction in the system efficiency by 0.2 increased the total cost by 32% on average, while increasing it by 0.2 decreased the total cost by 18%. Similarly, decreasing battery capacity by 10 units increases the system cost by 61% on average, while increasing it by 10 units decreases the cost by 42% on average.

Figure 3.3 shows two different network designs for Chicago region based on two different values of vehicle charging power. The total annual costs of the designs with $\varrho = 200$ kW and $\varrho = 20$ kW are $26.8 million (with 121 WCSs) and $ 31.6 million (with 312 WCSs), respectively. Increasing the vehicle charging power means that more energy can be passed from a WCS to an EV. Therefore, design with $\varrho = 200$ kW employs a smaller number of WCSs but with larger power capacity per WCS to satisfy the recharging demands. On the

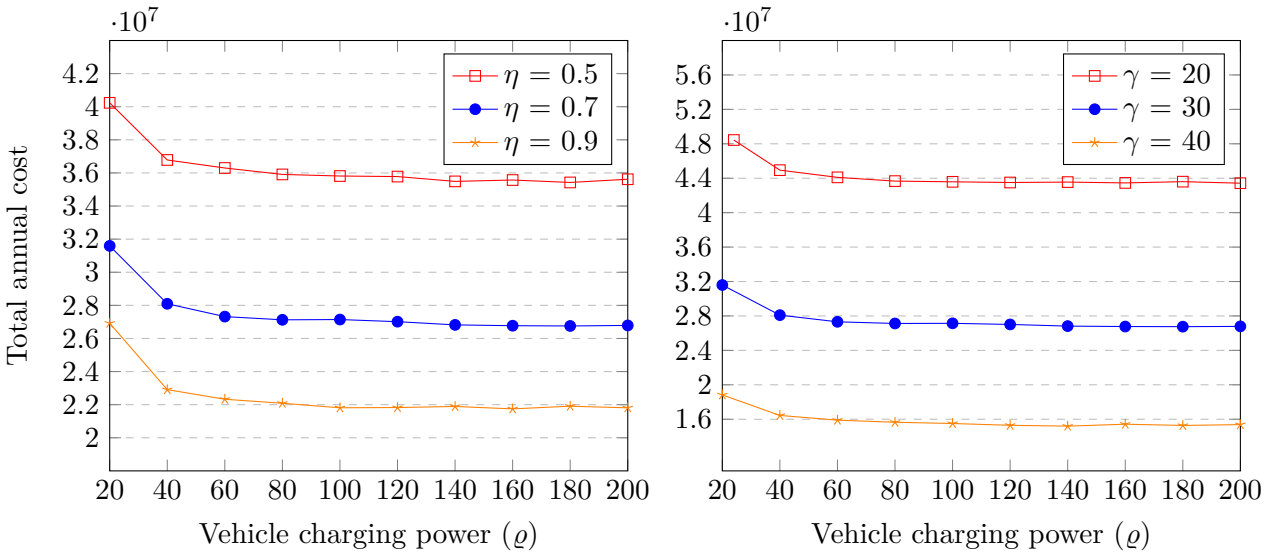

(a) $\gamma = 30$ (b) $\eta = 0.7$

Figure 3.2: Vehicle charging power vs. total cost

other hand the design with $\varrho = 20$ kW includes a larger number of WCSs that are, on average, with a smaller capacity than those resulted in the $\varrho = 200$ kW case.

3.5.2. System Efficiency (η) vs. Total Cost

System (charging) efficiency is defined as the ratio of the amount of charge transmitted to an EV to the total amount of electricity supplied by the charger [1]. As a system parameter, it is an important criterion affecting the system cost in wireless charging while it is not as critical in conventional charging in which the efficiency is close to 100%. To examine its effect on the total system cost, we consider varying values of η including 50%, 60%, 70%, 80%, and 90%.

In Figure 3.4a, we present the results for four different values of vehicle charging power as the nominal values of parameter γ. We observe that while an increase in η from 50% to 60% decreases the total cost by 13%, a similar increase from 80% to 90% reduces the total cost by 6% (although significant, this indicates a diminishing rate of return). In line with the pattern of any curve in Figure 3.2a, we also observe that increasing the value of ϱ from 20 kW to 60 kW reduces the total cost significantly while the further increments in ϱ have

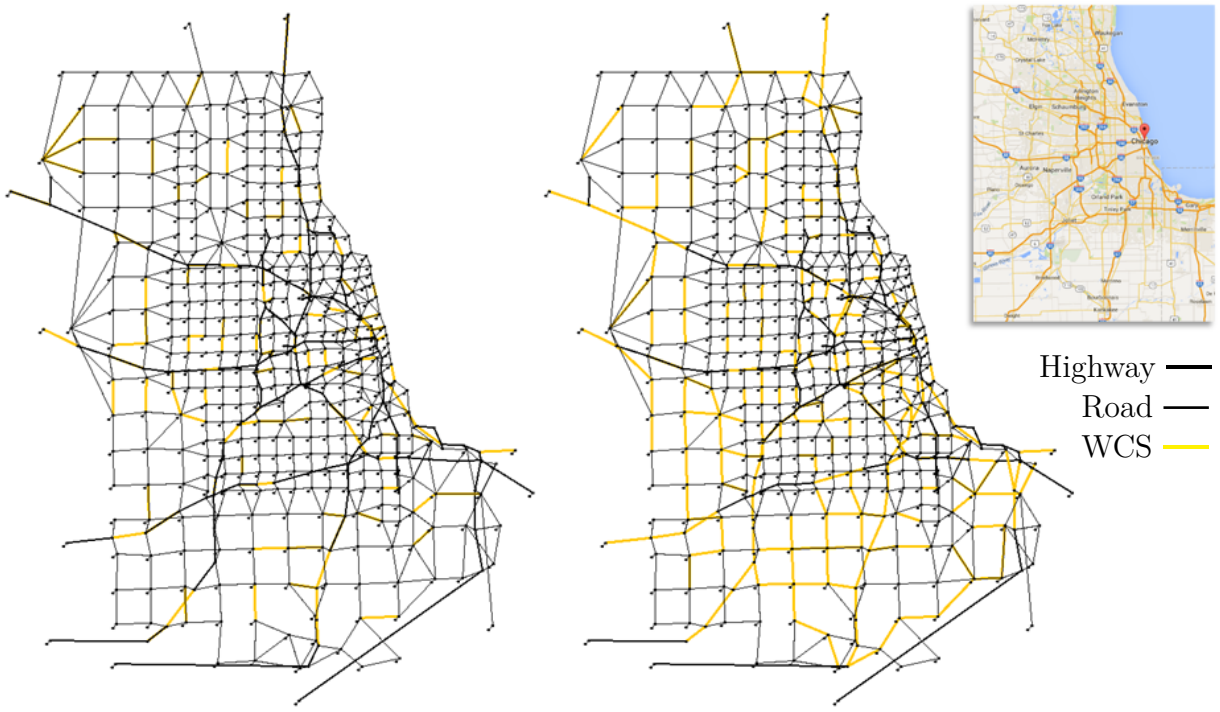

(a) $\varrho = 200$ kW (b) $\varrho = 20$ kW

Figure 3.3: Chicago sketch network

little impact on the total cost.

Further, Figure 3.4b presents the results for the nominal values of parameter ϱ and three different values of parameter γ including 20, 30, and 40 kWh. The three curves in Figure 3.4b show that the system cost decreases with increased battery capacity shifts. It is also important to observe that the rate of change in cost decrease with increasing efficiency is more significant if the battery capacity is low. It gradually becomes less significant with increasing battery capacity. In a way, efficiency and battery capacity act as surrogates to each other.

3.5.3. Battery Capacity vs. Total Cost

Battery capacity determines the EV range which has always been considered the bottleneck in EV design. As we mentioned in Chapter 1, one of the benefits of implementing dynamic charging technology is to allow EV manufacturers to design EVs with smaller bat-

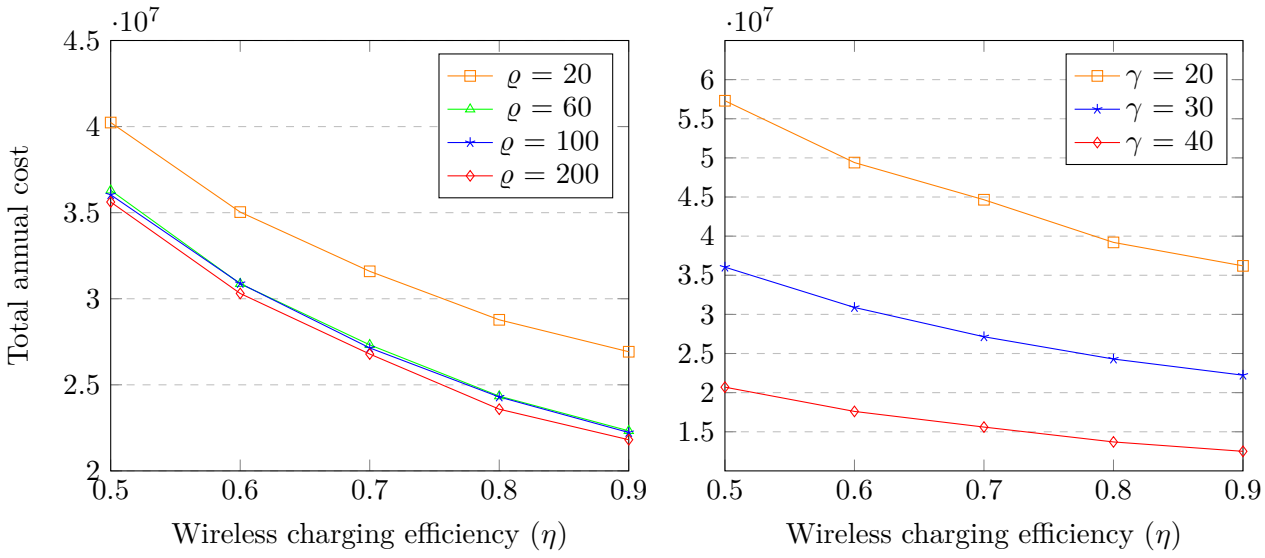

(a) $\gamma = 30$ (b) $\varrho = 100$

Figure 3.4: Charging efficiency vs. total cost

teries and therefore reduce the vehicle cost. However, this comes at the expense of increased cost. Hence, the inherent trade-off is illustrated in Figure 3.5. Clearly, an EV with a larger battery can be less dependent on dynamic charging since it can enter the transportation network with a higher state of charge, and thus, require less energy from the dynamic charging system to reach its destination. In this case, the network has fewer WCS locations and lower total cost. As depicted in Figures 3.5a and 3.5b for the Chicago network under varying values of ϱ and η, our model captures the increase in total system cost that results from smaller battery capacities. Furthermore, although the charging power has less impact above a threshold value, a combination of increased efficiency provides a lower rate of increase in the total cost when the batter capacity is reduced.

3.6. Concluding Remarks

This study introduces a new mathematical formulation to address the network design problem to support EV dynamic wireless charging. With the aim of promoting EV adoption and alleviating the range anxiety common for EV drivers, our model decides on the locations and power capacities of WCSs in an urban traffic network. In doing so, it explicitly takes

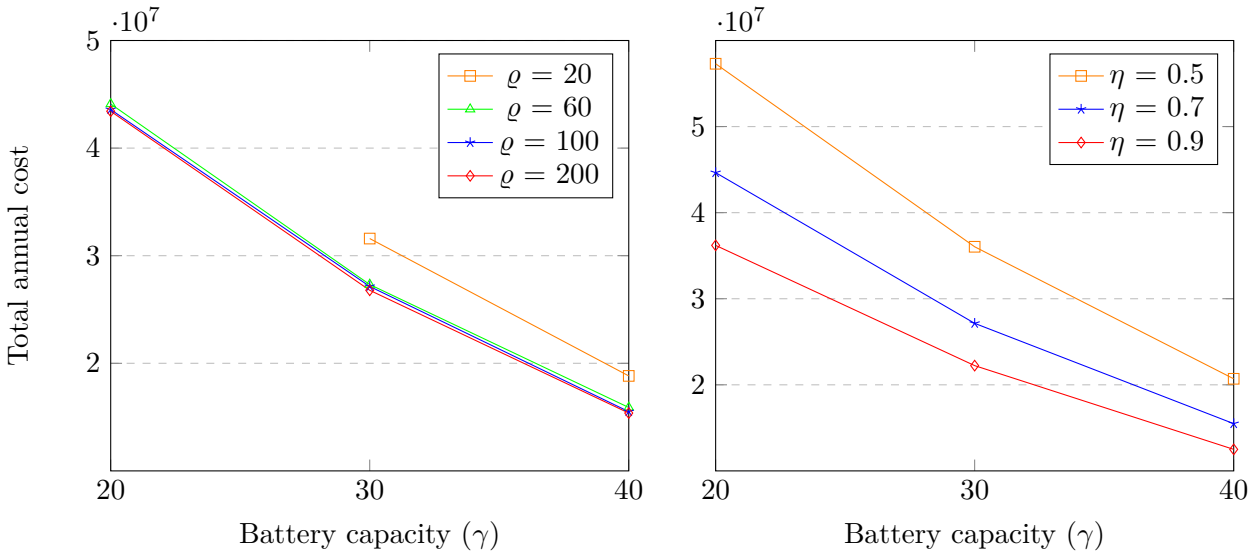

(a) $\eta = 0.7$ (b) $\varrho = 100$

Figure 3.5: Battery capacity vs. total cost

into account the user equilibrium traffic assignment as an input to facilitate easy adoption as well as the electrical parameters of the wireless charging system to ensure practical relevance.

A combined combinatorial-classical BD algorithm is devised and tested to solve relatively large-scale instances of the proposed model. The algorithm decomposes the problem into integer master and integer subproblems (as opposed to classical linear subproblem) and integrates both classical and combinatorial Benders cuts for improved lower bounds. Further enhancements was achieved via an effective upper bound heuristic that utilizes inherent characteristics of good solutions to the problem as well as additional valid inequalities employed as surrogate constraints in the master problem. The algorithmic performance is tested on a set of randomly generated networks and is found superior to the B&C approach in terms of solution quality and runtime.

Finally, a case study on Chicago sketch network is conducted, illustrating the applicability of the model on real networks. The case study also contains an evaluation of the effect of different system parameters on the network design and the cost of implementing dynamic charging technology on the road network and sets the stage for similar evaluations on different traffic networks. The results indicate that the model captures key dynamics among

input parameters including battery capacity, charging power, and system efficiency and thus provide the means of analyzing trade-offs involved in different real networks.

Chapter 4

ROBUST NETWORK DESIGN FOR IN-MOTION WIRELESS CHARGING OF ELECTRIC VEHICLES

4.1. Introduction

Wireless charging of electric vehicles (EV) has made strides in the past few years within the domain of automotive research and has recently made multiple appearances at several prestigious motor shows around the globe [64] [20] [57]. This cutting-edge technology has been under development as an EV power management solution to overcome the range anxiety of EV drivers, and therefore accelerate EV adoption. The concept lies on transmitting energy wirelessly from a roadbed inductive power line via electromagnetic pulses, to a power receiver embedded in the EV. In the case of in-motion wireless charging, the power transmission can take place dynamically as EVs travel on the electrified road segments.

Deploying in-motion wireless charging technology in the road network has many potential benefits including alleviating the range anxiety and reducing the battery size and the cost of EVs. It is also a step forward toward the realization of EV full automation. But this deployment also comes with the challenge of finding the most economic wireless charging infrastructure network design to serve the charging demands for EVs, at the minimum investment cost, while causing no disturbance to the traffic on the road network.

The network design of the wireless charging infrastructure is associated with two main decisions including (i) the multiple locations of wireless charging stations(WCS), and (ii) the power capacities associated with each station. These two decisions are heavily dependent on the traffic parameters of the road network including speeds, travel times, and EV flows on each road segment. In turn, these traffic parameters are dictated by the user equilibrium (UE) traffic assignment, which provides an adequate description of the traffic condition for

long term planning purposes [43]. Furthermore, the UE assignment depends on the traffic density which fluctuates dramatically within 24 hours of a typical day, shifting between different peak and off-peak traffic periods (Figure 4.1), resulting in varying UE assignments.

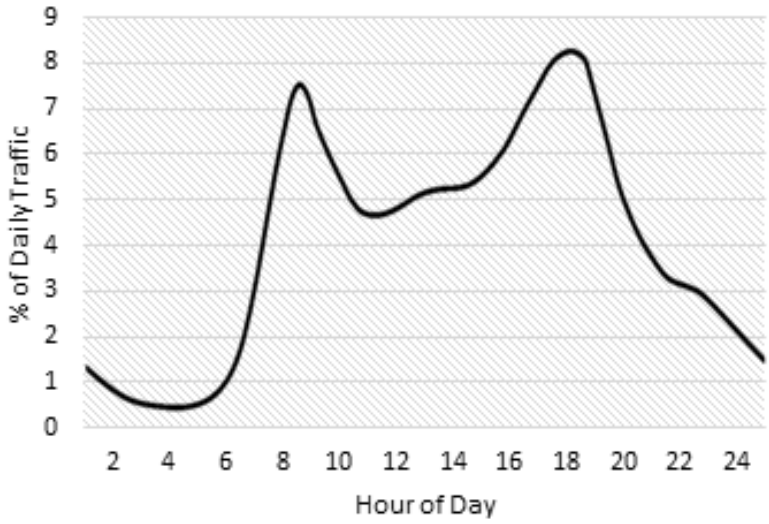

Figure 4.1: An example of typical variation of traffic density throughout the day.
Source: Federal Highway Administration [18]

Accordingly, the decisions of the WCS network design are dependent on traffic periods and UE assignments associated with these traffic periods. Therefore, an optimal solution obtained for a certain traffic period may not necessarily be optimal, or even feasible, during another traffic period. We illustrate this point via two examples in Section 4.4. Specifically, we demonstrate that even when an optimal WCS network design solution is obtained to serve the charging demands of the peak traffic period, the solution can still be infeasible during other less congested traffic periods. That is, even the peak-period cannot be singled out as a worst-case scenario for the network design problem of interest. For this particular reason, the fluctuation of traffic-related parameters must be taken into consideration in this optimization. That is, instead of considering a single traffic period, as in Chapter 3, different traffic periods must be considered to obtain a *robust* optimal solution that is feasible, and cost-effective, across all possible realizations of traffic data.

Driven by this motivation, we propose a robust optimization model to plan the deployment of WCSs in urban traffic networks. Through this model, we consider the dynamic nature of daily traffic patterns as we optimize the WCS network design including the locations and power capacities of WCSs. We build on the study in Chapter 3 as we adopt a perspective of a city, as a planning entity, in an effort to minimize the deployment cost of the wireless charging infrastructure and the charging cost for users. Furthermore, in order not to overburden EV drivers with any changes in route selection or driving behavior, we intend to generate optimal designs that maintain the UE traffic assignment in each traffic period. This is achieved by capturing the entire flow of the EV fleet on each used route of the network.

Considering multiple traffic periods, instead of a single-period, increases the complexity of the WCS network design problem. Specifically, the number of continuous variables and the number of constraints are multiplied by the number of considered traffic periods. Therefore, to solve the robust model, we devise a customized Benders Decomposition based algorithm. The algorithm builds on the solution framework presented in Chapter 3. However, to deal with the increase in the problem complexity, we apply a slight tweak to the formulation for algorithmic purposes. We then devise multiple new sets of problem-specific surrogate constraints as well as a new upper bound heuristic for improved efficiency. In addition, we employ a cut strengthening technique for faster convergence. We provide computational evidence to demonstrate the effectiveness of the proposed algorithm. We lastly apply the proposed approach in a case study and we compare the robust optimal solution to different individual single-period solutions obtained under different traffic periods.

The rest of this chapter is organized as follows: In Section 4.2 we explain the robust optimization approach selected to tackle the problem at hand. In section 4.3 we provide the definition and the formulation for the problem at hand. In Section 4.4 we illustrate the need for a robust solution via two examples representing two different traffic networks. The proposed BD solution algorithm is parented in Section 4.5. An extensive computational experiment on the performance of the proposed algorithm is presented in Section 4.6. Finally,

a case study is presented in Section 4.7.

4.2. Robust Optimization

Robust Optimization (RO) is a decision making tool that deals with decision making under uncertainty. Instead of optimizing a certain problem based on a specific data scenario, RO offers decision makers the opportunity to obtain a *Robust Decision*, that is feasible and performs well across all scenarios of input data.

While we are not dealing with uncertainty in this study, a robust optimization approach can be useful to tackle the problem of interest. Specifically, by viewing each traffic period as an input data "scenario", a robust optimization model can generate a WCS network design that is feasible, and cost-effective, across all daily traffic periods.

Kouvelis and Yu [35] lists three different robustness criteria including Absolute Robustness, Robust Deviation, and Relative Robustness.

The Absolute Robustness criterion is the most conservative robustness criterion. The approach minimizes the maximum cost taken across all possible scenarios.

The Robust Deviation criterion minimizes the maximum regret across all scenarios. Here, regret is defined, for each scenario, as the difference between the cost of the robust solution, and the cost of the optimal solution under the input data for that scenario. That is, robust deviation corresponds to the best worst-case deviation from optimality under all input scenarios.

Finally, the Relative Robustness criterion also minimizes the maximum regret across all scenarios. However, regret here is defined as the ratio of regret, as defined in the Robust Deviation case, to the cost of the optimal solution of each scenario. That is, this criterion corresponds to the worst-best-case percentage deviation from optimality under all input scenarios.

Both robust deviation and relative robustness criteria are less conservative than the absolute robustness criterion since they both account for the "missed opportunity" of a robust decision by comparing it to the optimal decisions under the different scenarios.

We now present the mathematical formulation associated with each of the three robustness criteria.

Given an LP defined for a specific input data scenario s as

$$
\begin{aligned}
z^s = \ & \min c^s x \\
& \text{subject to} \\
& A^s x = b^s \\
& x \geq = 0,
\end{aligned}
$$

let $\mathcal{S}$ be the set of all possible scenarios. Then the absolute robust linear programming problem is given as

$$
\begin{aligned}
z^A = \ & \min [\max_{s \in \mathcal{S}} \ c^s x \,] \\
& \text{subject to} \\
& A^s x = b^s \qquad \forall\, s \in \mathcal{S} \\
& x \geq = 0.
\end{aligned}
$$

Further, the robust deviation linear programming problem is given as

$$
\begin{aligned}
z^D = & \min [\max_{s \in \mathcal{S}} \ c^s x - z^s \,] \\
& \text{subject to} \\
& A^s x = b^s \qquad \forall\, s \in \mathcal{S} \\
& x \geq = 0.
\end{aligned}
$$

Finally, the relative robust linear programming problem is given as

$$
\begin{aligned}
z^R = & \min \left[\max_{s \in \mathcal{S}} \ \frac{c^s x - z^s}{z^s} \right] \\
& \text{subject to}
\end{aligned}
$$

$$A^s x = b^s \qquad \forall\, s \in \mathcal{S}$$

$$x \geq = 0.$$

In this study, we adopt an absolute robustness approach in an effort to generate network designs that are feasible and cost-effective across all scenarios (traffic periods). Another key advantage of the absolute robustness approach is that it is computationally easier when compared to the other two criteria. This is because, unlike the other two criteria, the absolute robustness does not require computing the optimal solutions for each input scenario individually.

Next, building on the definition of the absolute robustness, we define and formulate the robust WCS network design problem.

4.3. Problem Definition

We define the problem on a traffic network represented by a directed graph $\mathcal{G}(\mathcal{N}, \mathcal{A})$ where $\mathcal{N}$ represents a set of nodes and $\mathcal{A}$ represents a set of arcs. We consider a set of traffic periods $\mathcal{S}$. Each traffic period $s \in \mathcal{S}$ is associated with a traffic pattern defined by a state of user equilibrium UE_s which provides a proper characterization of a traffic system for long term planning purposes [43] . Each traffic period is also associated with a set of origin-destination (OD) pairs $\mathcal{Q}_s$, and each OD pair $q \in \mathcal{Q}_s$ is connected with a set of routes $\mathcal{R}_q$ containing at least one route $r \in \mathcal{R}_q$. The used routes at each traffic period s are defined by the associated UE traffic pattern UE_s.

We further consider a set $\mathcal{K}$ representing different classes of EVs, where each class $k \in \mathcal{K}$ is characterized by the initial and desired ending states of charge as well as the capacity of the battery. Based on the above-mentioned definitions, we define a commodity ($sqrk$) as a fleet of EVs belonging to a class $k \in \mathcal{K}$ traveling in the network during traffic period $s \in \mathcal{S}$ between an OD-pair $q \in \mathcal{Q}_s$ using route r.

Finally, we assume that installing a WCS on a road segment is associated with two costs; the first is a per-mile construction cost associated with building one mile of WCS. The second

cost is a power installation cost associated with installing one charging unit at a WCS. While we considered, in Chapter 3, a "base power capacity" associated with installing a WCS, here, we relax this assumption for algorithmic purposes. This "tweak" allows us to devise the new surrogate constraint 4.49.

We next present the model formulation of the robust network design for in-motion wireless charging of electric vehicles.

4.3.1. Model Formulation

We first introduce an expanded notation used in our robust formulation.

Sets:

$\mathcal{N}$ set of nodes, $i, j \in \mathcal{N}$

$\mathcal{O}$ set of origins, $o \in \mathcal{O} \subset \mathcal{N}$

$\mathcal{D}$ set of destinations, $d \in \mathcal{D} \subset \mathcal{N}$

$\mathcal{A}$ set of arcs, $(i, j) \in \mathcal{A}$

$\mathcal{S}$ set of traffic periods, $s \in \mathcal{S}$

$\mathcal{Q}_s$ set of all OD-pairs within the network during traffic period s, $q \in \mathcal{Q}_s$

$\mathcal{R}_q$ set of all used routes between a certain OD-pair q, $r \in \mathcal{R}_q$ where

o_r and d_r are the origin node and destination node of route r, respectively.

$\mathcal{N}_r$ set of nodes on a route $r \in \mathcal{R}_q$, $\mathcal{N}_r \subset \mathcal{N}$

$\mathcal{A}_r$ set of arcs on a route $r \in \mathcal{R}_q$, $\mathcal{A}_r \subset \mathcal{A}$

$\mathcal{K}$ set of EV classes, $k \in \mathcal{K}$

Parameters:

fc	construction cost ($) associated with constructing one mile of a WCS
vc	power installation cost ($) associated with installing one charging unit at a WCS
cc	charging cost ($/kWh)
tr	average number of trips taken by an EV during project lifetime
p_{cap}	power capacity (kW) associated with installing one charging unit at a WCS
m_{cap}	maximum power capacity (kW) that can be installed on one mile of a one-lane road segment
η	efficiency coefficient of the wireless power transfer system
ξ_{ij}	energy consumption (kWh) on arc (i, j)
ξ_r	energy consumption (kWh) on route r
ϱ	vehicle charging power (kW)
γ_k	battery capacity (kWh) of an EV of class k
v^{sqrk}	traffic volume of EV fleet of class k on route r that are traveling between OD-pair q during traffic period s
ρ_{ij}^{sqrk}	the expected number of EVs of class k, that are occupying arc (i, j) under traffic pattern of period s while traveling between OD-pair q along route r, $s \in \mathcal{S}$, $q \in \mathcal{Q}_s$, $r \in \mathcal{R}_q$, $k \in \mathcal{K}$, $(i, j) \in \mathcal{A}_r$
l_{ij}	length of arc (i, j) (mile)
n_{ij}	number of lanes on arc (i, j)
t_{ij}^s	travel time (hour) on arc (i, j) during traffic period s
δ_{ij}^{sqr}	an indicator with value of one if arc (i, j) is part of route r, 0 otherwise, $s \in \mathcal{S}$, $q \in \mathcal{Q}_s$, $r \in \mathcal{R}_q$, $k \in \mathcal{K}$, $(i, j) \in \mathcal{A}_r$

ie_k initial energy level of an EV of class $k \in \mathcal{K}$

ee_k ending energy level of an EV of class $k \in \mathcal{K}$

Decision Variables:

x_{ij} 1 if a WCS is installed on candidate arc (i,j), 0 otherwise

y_{ij} number of power charging units installed on arc (i,j)

e_i^{sqrk} energy level at node i of an EV of class k, traveling between OD-pair q on route r under traffic pattern of period $s \in \mathcal{S}$, $q \in \mathcal{Q}_s$, $r \in \mathcal{R}_q$, $k \in \mathcal{K}$, $i \in \mathcal{N}_r$

c_{ij}^{sqrk} amount of charge an EV of class k, traveling between OD-pair q on route r under traffic pattern of period s, receives from charging station at arc (i,j), $s \in \mathcal{S}$, $q \in \mathcal{Q}_s$, $r \in \mathcal{R}_q$, $k \in \mathcal{K}$, $(i,j) \in \mathcal{A}_r$

The wireless charging stations robust network design problem (**R**) can then be formulated as follows:

$$\min \quad \Big[\sum_{(i,j)\in\mathcal{A}} (fc\; l_{ij}\, n_{ij}\; x_{ij} + vc\; y_{ij}) \; + \max_{s\in\mathcal{S}} \sum_{q\in\mathcal{Q}_s} \sum_{r\in\mathcal{R}_q} \sum_{k\in\mathcal{K}} \sum_{(i,j)\in\mathcal{A}_r} (cc\; tr\; v^{sqrk} c_{ij}^{sqrk}) \Big] \tag{4.1}$$

subject to

$$e_{o_r}^{sqrk} + \sum_{(i,j)\in\mathcal{A}_r} c_{ij}^{sqrk} - e_{d_r}^{sqrk} = \xi_r \quad \forall\, s \in \mathcal{S},\, q \in \mathcal{Q}_s,\, r \in \mathcal{R}_q,\, k \in \mathcal{K} \tag{4.2}$$

$$e_i^{sqrk} + c_{ij}^{sqrk} - e_j^{sqrk} = \xi_{ij} \quad \forall\, s \in \mathcal{S},\, q \in \mathcal{Q}_s,\, r \in \mathcal{R}_q,\, k \in \mathcal{K},\, (i,j) \in \mathcal{A}_r \tag{4.3}$$

$$e_i^{sqrk} - \xi_{ij}\,(1 - x_{ij}) \geq 0 \quad \forall\, s \in \mathcal{S},\, q \in \mathcal{Q}_s,\, r \in \mathcal{R}_q,\, k \in \mathcal{K},\, i \in \mathcal{N}_r,\, (i,j) \in \mathcal{A}_r \tag{4.4}$$

$$c_{ij}^{sqrk} \leq \varrho\, t_{ij}^s\, x_{ij} \quad \forall\, s \in \mathcal{S},\, q \in \mathcal{Q}_s,\, r \in \mathcal{R}_q,\, k \in \mathcal{K},\, (i,j) \in \mathcal{A}_r \tag{4.5}$$

$$\sum_{q\in\mathcal{Q}_s} \sum_{r\in\mathcal{R}_q} \sum_{k\in\mathcal{K}} (\delta_{ij}^{sqr}\; \rho_{ij}^{sqrk}\; c_{ij}^{sqrk}) \leq \eta\,(p_{cap}\, y_{ij})\, t_{ij}^s \quad \forall\, s \in \mathcal{S},\, (i,j) \in \mathcal{A} \tag{4.6}$$

$$p_{cap}\, y_{ij} \leq m_{cap}\, n_{ij}\, l_{ij} \qquad \forall\, (i,j) \in \mathcal{A} \tag{4.7}$$

$$e_i^{sqrk} + c_{ij}^{sqrk} \leq \gamma_k + \xi_{ij} \qquad \forall\, s \in \mathcal{S},\, q \in \mathcal{Q}_s,\, r \in \mathcal{R}_q,\, k \in \mathcal{K},\, i \in \mathcal{N}_r,\, (i,j) \in \mathcal{A}_r \tag{4.8}$$

$$e_{o_r}^{sqrk} = ie_k \qquad \forall\, s \in \mathcal{S},\, q \in \mathcal{Q}_s,\, r \in \mathcal{R}_q,\, k \in \mathcal{K} \tag{4.9}$$

$$e_{d_r}^{sqrk} \geq ee_k \qquad \forall\, s \in \mathcal{S},\, q \in \mathcal{Q}_s,\, r \in \mathcal{R}_q,\, k \in \mathcal{K} \tag{4.10}$$

$$e_i^{sqrk},\ c_{ij}^{sqrk} \geq 0,$$

$$x_{ij}\ \in \{0,1\},\ y_{ij} \in Z^+ \qquad \forall\, s \in \mathcal{S},\, q \in \mathcal{Q}_s,\, r \in \mathcal{R}_q,\, k \in \mathcal{K},\, i \in \mathcal{N}, (i,j) \in \mathcal{A} \tag{4.11}$$

The objective function (4.1) minimizes the infrastructure deployment cost and the maximum charging cost across all considered traffic periods. The infrastructure deployment cost incorporates two types of costs. The first is the construction cost of WCS. The second is a variable cost, representing the cost of the power capacity units installed on WCS. Constraints (4.2) and (4.3) represent the energy conservation constraints over paths and over arcs, respectively. Constraints (4.4) ensure that the energy level at each node is sufficient to energize the EV until reaching the next WCS. Constraint (4.5) is a dual-purpose constraint. It ensures that charging on an arc is only possible if the arc is electrified (has a WCS on it). It also links the amount of charge that an EV can receive on a certain arc to the exposure time between the EV and the WCS.

Constraints (4.6) ensure that the power installation on each WCS is sufficient to serve the charging demands on the WCS. Note that in the single-period model presented in Chapter 3, the power installation constraint includes a base power installation in the right hand side on the constraint. For algorithmic purposes, we are not considering a base power installation in this formulation. Still, any deployed WCS will contain at least one charging unit. This is because the binary variable x_{ij}, in constraint (4.5), and the integer variable y_{ij}, in constraint (4.6), are both triggered by the continuous variable c_{ij}^{sqrk}. That is, when c_{ij}^{sqrk} is positive, it triggers both x_{ij} and y_{ij}. Therefore, we will not run into a situation where the model deploys a WCS on a certain arc (i.e., $x_{ij} = 1$), with no power installation on the arc (i.e., $y_{ij} = 0$).

Constraints (4.7) enforce a limit on the power installation on each WCS. Constraints (4.8) limit the amount of charge of an EV by the capacity of its battery (EV range). Constraints (4.9) and (4.10) bound the initial and ending energy levels of EVs. Lastly, constraints (4.11) define nonnegativity and integrality requirements of the decision variables.

4.4. Illustrating the Need for a Robust Solution

Unlike many other strategic infrastructure planning problems, designing the network of WCS when considering only the peak traffic period (as a bottleneck associated with the highest traffic demands) might lead to solutions that are infeasible for other off-peak traffic periods. That is, an optimal solution for the problem that is obtained for a single traffic period is not necessarily feasible for another traffic period with less traffic demands. We illustrate this point in what follows through a single-OD network example first, and then on a multi-OD network.

4.4.1. Single-OD Network Example

Consider three different routes (r_1, r_2, r_3) connecting an OD pair. For the sake of simplicity and without loss of generality, assume that each route is represented by one arc only. The lengths, speed limits, free-flow travel times, and the traffic capacities of the three routes (arcs) are given in Table 4.1.

Table 4.1: Routes data

	r1	r2	r3
Length	40	40	40
Speed limit	60	75	50
Free-flow travel time ft_r (min)	40	32	48
Traffic capacity	2,000	2,000	2,000

Assume that during the peak traffic period s_1, the traffic demands between the OD pair is 4000. We use the Method of Successive Averages[1] to obtain the UE assignment which is described by the volumes and travel times given in Table 4.2, where v_r and t_r represent traffic volume and travel time (minutes), respectively.

Table 4.2: UE data of peak period s_1

	r1	r2	r3
v_r (vehicle/hr)	1,365	1,795	840
t_r (min)	52	52	52

Now consider solving a single period WCS network design problem considering these three routes and the peak traffic period s_1. Assume that each EV needs to be recharged with 8 kWh to complete its trip along each route. Using an EV charging power of $\varrho = 10$ kW and the travel times associated with s_1 (provided in Table 4.2), we find that electrifying the three routes can provide each EV with $c = \varrho * t_r = 10 * \frac{52}{60} = 8.67$ kWh of energy along each route.

Finally, consider an off-peak traffic period s_2 where only r_2 is being used (as it is the fastest path between the OD pair) and the traffic is moving with the free flow speed of 75 mile/hr. Accordingly, electrifying this route can provide, during traffic period s_2, each EV with $c = \varrho * ft_{r2} = 10 * \frac{32}{60} = 5.33$ kWh of energy. Therefore, the charging demands of 8 kWh per EV cannot be met during s_2.

This example illustrates that given two traffic periods s_1 and s_2, if the traffic demands during s_1 are higher than those during s_2, a solution for the WCS network design problem obtained only considering the traffic pattern of s_1 is not necessarily feasible for s_2.

[1]The Method of Successive Averages is presented in Appendix A

4.4.2. Nguyen-Dupuis Network

Consider the Nguyen-Dupuis network, presented in Figure 4.2, with a set of four OD pairs: $\mathcal{Q} = \{(1-2), (1-3), (4-2), (4-3)\}$.

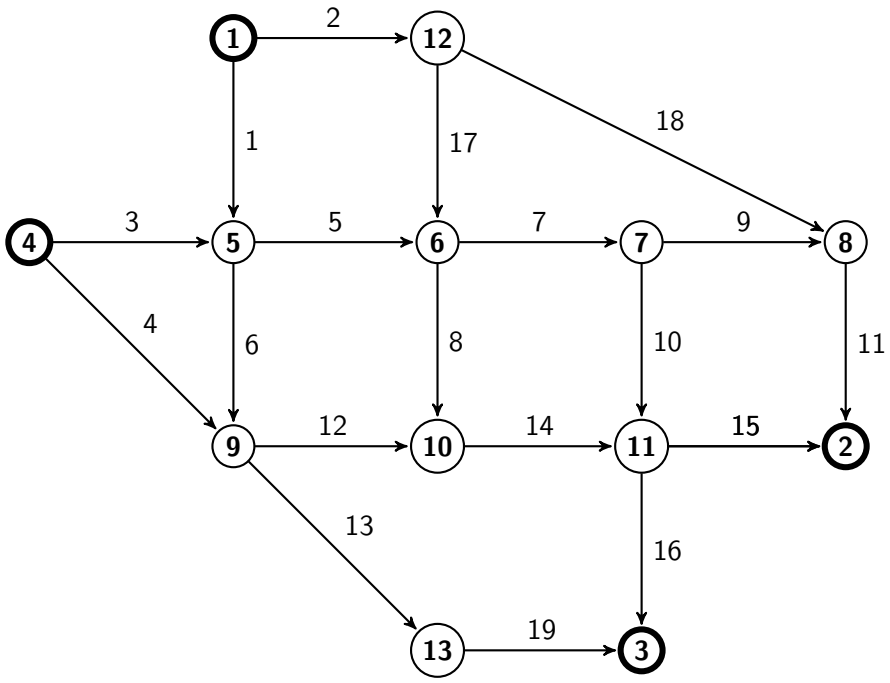

Figure 4.2: Nguyen-Dupuis network

We assume that the travel times on links are dictated by Bureau of Public Roads (BRP) arc performance function [55] given as

$$t_{ij} = t_{ij}^{min}\left(1 + \alpha(\frac{v_{ij}}{tc_{ij}})^{\beta}\right) \tag{4.12}$$

where

t_{ij}^{min} is the free-flow travel time on arc (i, j)

v_{ij} is the traffic volume on arc (i, j)

tc_{ij} is the traffic capacity of arc (i, j) measured in vehicles/hour

α and β are deterministic permeates associated with the type of the road.

We consider the values of 0.88 and 9.8 for α and β, respectively [26]. We further assume a link capacity of 300 vehicle/hr, and a free flow speed of 65 mile/hr on each link. Further, consider an EV wireless charging system with the parameters given in Table 4.3.

Table 4.3: Wireless charging system parameters

Parameter	fc	vc	cc	tr	p_{cap}	ϱ	m_{cap}	ξ	η	γ_k
Value	\$800,000	\$11,000	\$0.15	7,200	20	20	1,000	0.33	80%	20

Now consider three different traffic periods s_1, s_2, and s_3 with the demand matrices provided in Table 4.4.

Table 4.4: Demand matrices

	s1		s2		s3	
	2	3	2	3	2	3
1	300	600	200	400	133	267
4	450	150	300	100	200	67

As shown in Table 4.4, the number of travelers between each OD pair decreases by a rate of $\frac{1}{3}$ between traffic period s_1 and traffic period s_2. Similarly, the number of travelers between each OD pair decreases by the same rate going from traffic period s_2 into traffic period s_3. Assume that the initial state of charge (SOC) for all EVs is 20 kWh, and the required ending SOC at the destinations is at least 10 kWh.

The UE solution associated with the first (peak) traffic period s_1, obtained using the Method of Successive Averages, contains 17 routes connecting the two origins with the two destinations. The average arcs speed, as resulted by solving the UE, is 27 mile/hr. The UE parameters associated with the routes and with the arcs are given in Tables 4.5 and 4.6, respectively.

Table 4.5: Routes parameters associated with the UE of traffic period s1

Route	Origin	Destination	Volume	Travel time
1-12-8-2	1	2	300.00	2.6
1-5-9-13-3	1	3	295.61	2.9
1-12-6-7-11-3	1	3	104.84	2.9
1-5-6-10-11-3	1	3	54.16	2.9
1-12-6-10-11-3	1	3	57.48	2.9
1-5-6-7-11-3	1	3	63.12	2.9
1-5-9-10-11-3	1	3	24.78	2.9
4-9-10-11-2	4	2	227.33	2.0
4-5-6-7-8-2	4	2	87.36	2.0
4-5-9-10-11-2	4	2	4.23	2.0
4-5-6-7-11-2	4	2	120.82	2.0
4-5-6-10-11-2	4	2	10.25	2.0
4-9-13-3	4	3	82.42	2.0
4-5-6-7-11-3	4	3	20.74	2.0
4-9-10-11-3	4	3	32.74	2.0
4-5-9-13-3	4	3	11.00	2.0
4-5-6-10-11-3	4	3	3.10	2.0

Table 4.6: Arcs parameters associated with the UE of traffic period s1

Arc	Origin	Destination	v_{ij}	Speed	t_{ij}
1	1	5	414.09	10	0.8
2	1	12	362.64	17	0.5
3	4	5	360.97	17	0.5
4	4	9	162.32	63	0.1
5	5	6	300.00	32	0.6
6	5	9	389.03	13	0.6
7	6	7	462.32	6	1.4
8	6	10	437.68	7	1.1
9	7	8	257.50	45	0.2
10	7	11	342.50	21	0.5
11	8	2	359.56	18	0.5
12	9	10	335.62	23	0.3
13	9	13	125.00	64	0.1
14	10	11	396.88	12	0.7
15	11	2	309.53	30	0.3
16	11	3	87.36	65	0.1
17	12	6	387.36	13	0.6
18	12	8	289.09	36	0.2
19	13	3	389.03	13	0.9

Given the UE solution for s_1 and the parameters in Table 4.3, the optimal solution for the single-period network design problem at hand features four WCSs with 63 charging units as depicted in Figure 4.3. The associated construction and power installation cost is \$26.29M.

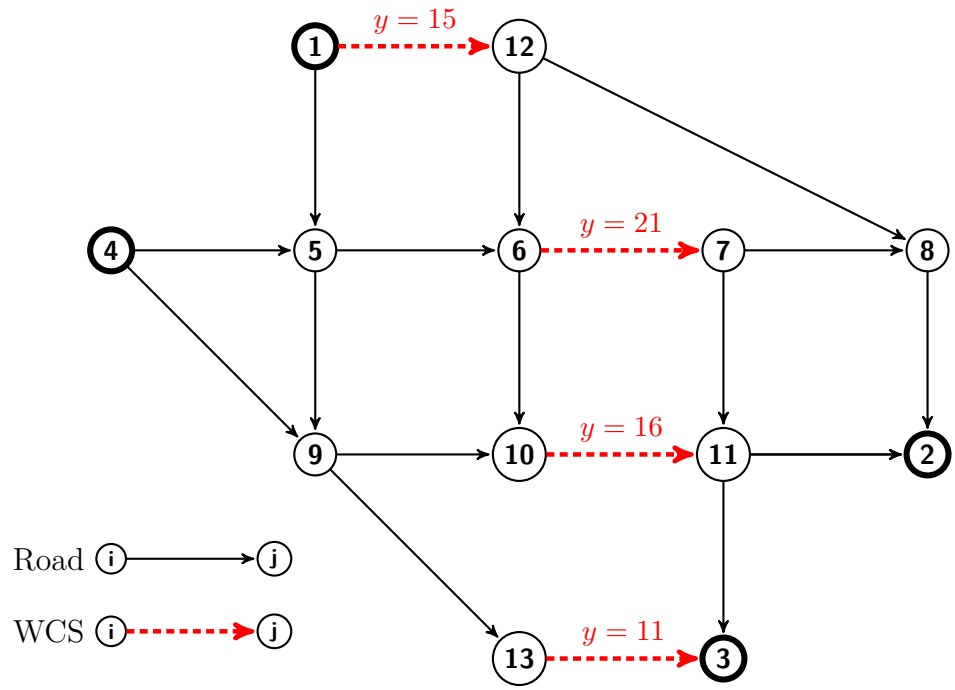

Figure 4.3: Single-period optimal WCS network design for traffic period s_1

Now consider traffic period s_2 were the travel demands decrease by a rate of $\frac{1}{3}$. The UE solution associated with this period contains 14 routes connecting the two origins with the two destinations. Moreover, as a result of the decrease in the traffic volume, the average arc speed, as resulted by UE solution, goes up to 51 mile/hr. Tables 4.7 and 4.8 provide the new UE parameters associated with the routes and with the arcs, respectively.

Given the new UE and the system parameters in Table 4.3, the optimal solution for the single-period network design problem is illustrated in Figure 4.4. The solution also features four WCSs, but with only 41 charging units. The associated construction and power installation cost is \$26.05M - only slightly lower than the cost associated with s_1.

Table 4.7: Routes parameters associated with the UE of traffic period s2

Route	Origin	Destination	Volume	Travel time
1-12-8-2	1	2	200.00	0.7
1-5-9-13-3	1	3	200.38	0.8
1-12-6-7-11-3	1	3	73.58	0.8
1-12-6-10-11-3	1	3	32.43	0.8
1-5-6-7-11-3	1	3	52.43	0.8
1-5-6-10-11-3	1	3	39.48	0.8
1-5-9-10-11-3	1	3	1.71	0.8
4-9-10-11-2	4	2	174.93	0.8
4-5-6-7-8-2	4	2	57.10	0.8
4-5-6-7-11-2	4	2	65.97	0.8
4-5-6-10-11-2	4	2	2.00	0.8
4-9-13-3	4	3	72.34	0.7
4-5-6-7-11-3	4	3	8.73	0.7
4-9-10-11-3	4	3	18.92	0.7

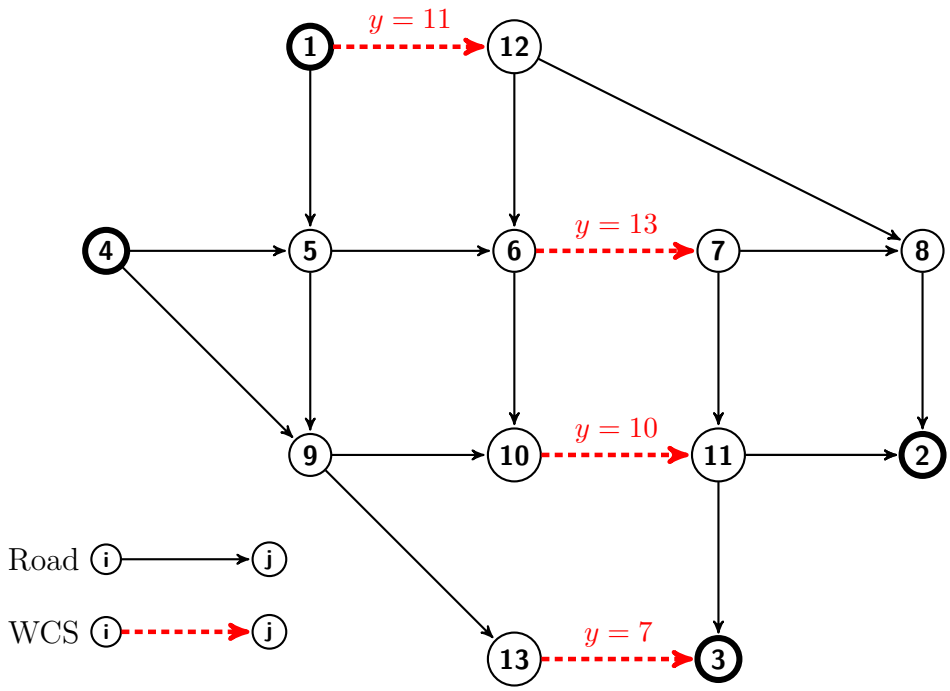

Figure 4.4: Single-period optimal solution for traffic period s_2

Table 4.8: Arcs parameters associated with the UE of traffic period s2

Arc	Origin	Destination	v_{ij}	Speed	t_{ij}
1	1	5	269.48	42	0.2
2	1	12	242.90	49	0.2
3	4	5	227.28	53	0.2
4	4	9	106.01	65	0.1
5	5	6	200.00	58	0.3
6	5	9	272.72	41	0.2
7	6	7	306.01	31	0.3
8	6	10	293.99	34	0.2
9	7	8	133.80	64	0.1
10	7	11	266.20	43	0.3
11	8	2	225.70	53	0.1
12	9	10	202.09	58	0.1
13	9	13	73.91	65	0.1
14	10	11	257.80	45	0.2
15	11	2	200.71	58	0.1
16	11	3	57.10	65	0.1
17	12	6	257.10	45	0.2
18	12	8	195.57	59	0.1
19	13	3	272.72	41	0.3

By comparing the two individual optimal solutions obtained for the two traffic periods s_1 and s_2 we observe that the decrease in travel demands caused a decrease in the optimal installation cost (Table 4.11). Moreover, we observe that the optimal network design for the peak traffic period s_1 is a feasible solution for the problem under traffic period s_2, as expected.

Now consider traffic period s_3 were travel demands further decrease by the rate of $\frac{1}{3}$ (as in Table 4.4). The UE solution associated with this traffic period features only 7 routes connecting the two origins with the two destinations. Furthermore, because of the low travel demands, the average speed in the network increases to 61 mile/hr. Tables 4.9 and 4.10 provide the new UE parameters associated with the routes and with the arcs, respectively.

Given the new UE solution and the system parameters in Table 4.3, the optimal solution for the single-period network design problem features five WCSs with a total 24 charging units as illustrated in Figure 4.5. Here, the associated construction and power installation cost is \$32.26M - considerably higher than the installation costs associated with s_1 and s_2.

Table 4.9: Routes parameters associated with the UE of traffic period s3

Route	Origin	Destination	Volume	Travel time
1-12-8-2	1	2	133.00	0.5
1-5-9-13-3	1	3	162.39	0.6
1-12-6-7-11-3	1	3	66.97	0.6
1-5-6-7-11-3	1	3	37.64	0.6
4-9-10-11-2	4	2	176.29	0.6
4-5-6-7-8-2	4	2	23.71	0.6
4-9-13-3	4	3	67.00	0.6

Table 4.10: Arcs parameters associated with the UE of traffic period s3

Arc	Origin	Destination	v_{ij}	Speed	t_{ij}
1	1	5	176.29	62	0.1
2	1	12	176.29	62	0.1
3	4	5	104.61	65	0.1
4	4	9	66.97	65	0.1
5	5	6	133.00	64	0.3
6	5	9	229.39	53	0.2
7	6	7	199.97	58	0.1
8	6	10	200.03	58	0.1
9	7	8	23.71	65	0.1
10	7	11	243.29	49	0.2
11	8	2	61.35	65	0.1
12	9	10	162.39	63	0.1
13	9	13	0.00	65	0.1
14	10	11	128.32	64	0.1
15	11	2	104.61	65	0.1
16	11	3	23.71	65	0.1
17	12	6	156.71	63	0.1
18	12	8	176.29	62	0.1
19	13	3	229.39	53	0.2

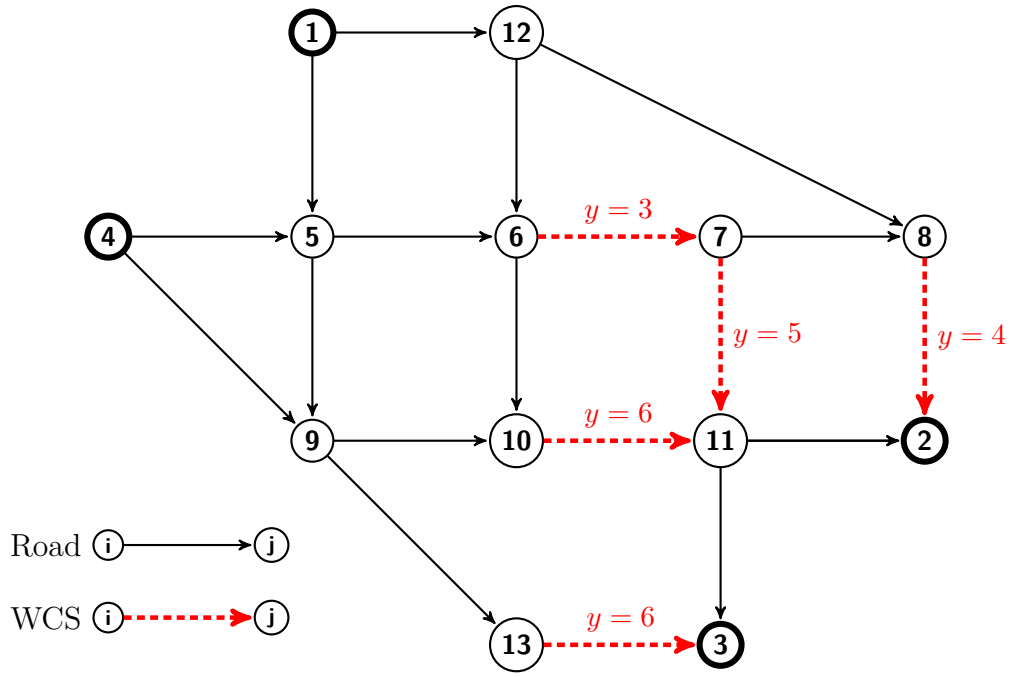

Figure 4.5: Single-period optimal solution for traffic period s_3

By comparing the three individual optimal solutions obtained for the traffic periods s_1, s_2 and s_3 we observe that the decrease in the travel demands caused, *unexpectedly*, an increase in the optimal construction and power installation costs (Table 4.11). The reason behind this increase is that the optimal solution for period s_3 requires the opening of five WCSs instead of four, in spite of the fact that there are fewer routes to cover in period s_3. This is because under the specified parameters and the high speed on the network, an EV going on the route $(1-12-6-7-11-3)$ cannot pick up all the required energy to reach its destination, with the required ending SOC, from one WCS. The case is similar for EVs going on the route $(1-5-6-7-11-3)$. This makes the two optimal solutions obtained for the two traffic periods s_1 and s_2 infeasible when considering traffic period s_3. On the other hand, the optimal solution obtained for traffic period s_3 does not feature enough power capacity to serve the higher volumes of EVs in periods s_1 or s_2. Therefore, the optimal solution obtained for s_3 is also infeasible when considering periods s_1 or s_2.

Once again, this example confirms that the individual single-period solution obtained considering the peak traffic period is not necessarily feasible for the other less-congested

Table 4.11: Optimal solutions under different scenarios

Traffic period	Traffic volume	Number of routes	Avg. speed	Number of WCSs	Construction & Power installation cost ($M)
s1	1500	17	27	4	26.29
s2	1000	14	51	4	26.05
s3	667	7	61	5	32.26

traffic periods. Therefore a robust solution is needed to guarantee that all charging demands are met during all traffic periods.

4.5. Solution Methodology

To solve the large instances of the problem at hand, we devise a customized Benders decomposition (BD) framework and employ problem-specific surrogate constraints for improved efficiency. In the classic BD framework, large-scaled MIPs are decomposed into a master problem (MP) and a subproblem (SP). MP includes the integer variables from the original MIP, while SP includes the continuous ones. The algorithm iterates between the two problems, passing forward integer solutions of MP to SP and passing back Benders cuts from SP to MP. The algorithm terminates once the gap between the upper bound (determined after solving SP) and the lower bound (given by MP) is less than a preferred threshold.[6].

Our decomposition scheme in this study is different than the classical BD. Specifically, we build on the solution framework devised in Chapter 3 as we decompose the problem in a way where both MP and SP are integer programs. This decomposition scheme dramatically reduces the complexity of MP as one set of integer variables is moved from MP to SP. Furthermore, the binary structure of MP allows the generation of combinatorial Benders cuts whenever an MP solution leads to an infeasible SP. To tackle the increase in the problem size and complexity associated with considering multiple traffic periods rather than a single period, we introduce five new sets of surrogate constraints to be added to MP. We further strengthen the proposed algorithm with a new upper bound heuristic, and we employ a cut

strengthening technique for improved efficiency. In what follows, we present the details of our BD framework.

4.5.1. Benders Subproblem and Dual Subproblem

For a fixed binary vector $\hat{X}$ representing the set of opened locations of WCSs, we obtain subproblem SP($e_i^{sqrk},\ c_{ij}^{sqrk}, y_{ij} \mid \hat{X}$) as:

$$\min \quad \Big[\sum_{(i,j)\in\mathcal{A}} (vc\ y_{ij}) \ + \max_{s\in\mathcal{S}} \sum_{q\in\mathcal{Q}_s} \sum_{r\in\mathcal{R}_q} \sum_{k\in\mathcal{K}} \sum_{(i,j)\in\mathcal{A}_r} (cc\ tr\ v^{sqrk} c_{ij}^{sqrk}) \Big] \tag{4.13}$$

subject to

(4.2), (4.3), (4.6), (4.7), (4.8), (4.9), (4.10), and

$$e_i^{sqrk} - \xi_{ij}\,(1-\hat{x}_{ij}) \geq 0 \qquad \forall\, s\in\mathcal{S},\ q\in\mathcal{Q}_s,\ r\in\mathcal{R}_q,\ k\in\mathcal{K},\ i\in\mathcal{N}_r,\ (i,j)\in\mathcal{A}_r \tag{4.14}$$

$$c_{ij}^{sqrk} \leq\ \varrho\, t_{ij}^{s}\, \hat{x}_{ij} \qquad \forall\, s\in\mathcal{S},\ q\in\mathcal{Q}_s,\ r\in\mathcal{R}_q,\ k\in\mathcal{K},\ (i,j)\in\mathcal{A}_r \tag{4.15}$$

$$e_i^{sqrk},\ c_{ij}^{sqrk} \geq 0,\ y_{ij}\in Z^{+} \qquad \forall\, s\in\mathcal{S},\ q\in\mathcal{Q}_s,\ r\in\mathcal{R}_q,\ k\in\mathcal{K},\ i\in\mathcal{N},(i,j)\in\mathcal{A} \tag{4.16}$$

By introducing the non-negative auxiliary variable u, SP can be rewritten as:

$$\min\ u \tag{4.17}$$

subject to

(4.2), (4.3), (4.6), (4.7), (4.8), (4.9), (4.10), (4.14), (4.15), (4.16),

$$\sum_{q\in\mathcal{Q}_s} \sum_{r\in\mathcal{R}_q} \sum_{k\in\mathcal{K}} \sum_{(i,j)\in\mathcal{A}_r} (cc\ tr\ v^{sqrk} c_{ij}^{sqrk}) \ + \sum_{(i,j)\in\mathcal{A}} (vc\ y_{ij}) \leq u \qquad \forall\, s\in\mathcal{S} \tag{4.18}$$

$$u \geq 0 \tag{4.19}$$

Let $\psi_{sqrk}^{ij}, \upsilon_{sqrk}^{ij}, \nu_{qrk}^{ij}, \omega_{ij}^{s}, \varphi_{ij}, \sigma_{sqrk}^{ij}, \theta_{sqrk}, \tau_{sqrk}$, and ϖ_s be the dual variables associated with the linear relaxation of constraints (4.3), (4.14), (4.15), (4.6), (4.7), (4.8), (4.9), (4.10), and

(4.18) respectively. Moreover, define binary parameters λ^{i}_{sqr} and ε^{i}_{sqr} as one if $i \in \mathcal{O}$ and $i \in \mathcal{D}$, respectively, zero otherwise. Then, the dual of the linear relaxation of SP, denoted as DRSP$(\psi^{ij}_{sqrk}, \upsilon^{ij}_{sqrk}, \nu^{ij}_{sqrk}, \omega^{s}_{ij}, \varphi_{ij}, \sigma^{ij}_{sqrk}, \theta_{sqrk}, \tau_{sqrk}, \varpi_{s} \mid \hat{X})$ is obtained as

$$\begin{aligned}\text{Maximize} \quad \zeta_R = & \sum_{s\in\mathcal{S}} \sum_{q\in\mathcal{Q}_s} \sum_{r\in\mathcal{R}_q} \sum_{k\in\mathcal{K}} \sum_{(i,j)\in\mathcal{A}_r} \Big(\xi_{ij}\, \psi^{ij}_{sqrk} + \xi_{ij}\,(1-\hat{x}_{ij})\, \upsilon^{ij}_{sqrk} + \\ & \varrho\, t^{s}_{ij}\, \hat{x}_{ij}\, \nu^{ij}_{sqrk} + (\gamma_k + \xi_{ij})\, \sigma^{ij}_{sqrk} \Big) + \sum_{(i,j)\in\mathcal{A}_r} (m_{cap}\, n_{ij}\, l_{ij})\, \varphi_{ij} + \\ & \sum_{s\in\mathcal{S}} \sum_{q\in\mathcal{Q}_s} \sum_{r\in\mathcal{R}_q} \sum_{k\in\mathcal{K}} (ie_k\, \theta_{sqrk} + ee_k\, \tau_{sqrk}) \end{aligned} \tag{4.20}$$

subject to

$$\begin{aligned} & \lambda^{i}_{sqr}\,(\theta_{sqrk} + \psi^{ij}_{sqrk} + \upsilon^{ij}_{sqrk} + \sigma^{ij}_{sqrk}) + \\ & \quad \varepsilon^{i}_{sqr}\,(\tau_{sqrk} - \psi^{ij}_{sqrk})(1 - \lambda^{i}_{sqr} - \varepsilon^{i}_{sqr}) \;\times\; + \\ & \qquad (\psi^{ij}_{sqrk} - \psi^{i-1\;\,j-1}_{sqrk} + \upsilon^{ij}_{sqrk} + \sigma^{ij}_{sqrk}) \le 0 \qquad \forall\, s \in \mathcal{S},\, q \in \mathcal{Q}_s,\, r \in \mathcal{R}_q, \\ & \qquad\qquad\qquad\qquad\qquad\qquad\qquad\qquad\qquad\qquad k \in \mathcal{K},\, i \in N_r \end{aligned} \tag{4.21}$$

$$\begin{aligned} & \psi^{ij}_{sqrk} + \nu^{ij}_{sqrk} + \rho^{sqrk}_{ij}\, \omega^{s}_{ij} + \sigma^{ij}_{sqrk} + cc\; tr\; v^{sqrk} \le 0 \qquad \forall\, s \in \mathcal{S},\, q \in \mathcal{Q}_s,\, r \in \mathcal{R}_q, \\ & \qquad\qquad\qquad\qquad\qquad\qquad\qquad\qquad\qquad\qquad k \in \mathcal{K},\; (i,j) \in \mathcal{A}_r \end{aligned} \tag{4.22}$$

$$-\,\varpi_s \le 1 \qquad\qquad \forall\, s \in \mathcal{S} \tag{4.23}$$

$$\begin{aligned} & \psi^{ij}_{sqrk},\; \theta_{sqrk}\; URS; \\ & \quad \upsilon^{ij}_{sqrk},\; \tau_{sqrk} \ge 0,\; \nu^{ij}_{sqrk},\; \omega_{ij},\; \varpi_{ij},\; \sigma^{ij}_{sqrk} \le 0 \qquad \forall\, s \in \mathcal{S},\, q \in \mathcal{Q}_s,\, r \in \mathcal{R}_q, \\ & \qquad\qquad\qquad\qquad\qquad\qquad\qquad\qquad\qquad\qquad k \in \mathcal{K}, (i,j) \in \mathcal{A} \end{aligned} \tag{4.24}$$

Let $\mathcal{P}$ denote the set of all extreme points of DRSP polyhedron given by (4.21) - (4.24), and let $\psi^{ijp}_{sqrk}, \upsilon^{ijp}_{sqrk}, \nu^{ijp}_{qrk}, \omega^{s}_{ijp}, \varphi_{ijp}, \sigma^{ijp}_{sqrk}, \theta^{p}_{sqrk}, \tau^{p}_{sqrk}, \varpi^{p}_{s}$ and ζ^{p}_{R} denote the associated dual variables and the value of the objective function respectively. Further, let ζ^{*} de-

note the optimal value of DRSP. Since $\zeta_R^p \leq \zeta^*$, $\forall p \in \mathcal{P}$, DRSP can be restated as $\min_{\zeta \geq 0}\{\zeta : \zeta^p \leq \zeta, \ \forall p \in \mathcal{P}\}$, where

$$\zeta_R^p = \sum_{s\in\mathcal{S}} \sum_{q\in\mathcal{Q}} \sum_{r\in\mathcal{R}_q} \sum_{k\in\mathcal{K}} \sum_{(i,j)\in\mathcal{A}_r} \Big(\xi_{ij}\, \psi_{sqrk}^{ijp} + \xi_{ij}\,(1 - x_{ij})\, \upsilon_{sqrk}^{ijp} + \varrho\, t_{ij}^s\, x_{ij}\, \nu_{sqrk}^{ijp} + (\gamma_k + \xi_{ij})\, \sigma_{sqrk}^{ijp} \Big) + \sum_{(i,j)\in r} (m_{cap}\, n_{ij}\, l_{ij})\, \varphi_{ijp} + \sum_{s\in\mathcal{S}} \sum_{q\in\mathcal{Q}} \sum_{r\in\mathcal{R}_q} \sum_{k\in\mathcal{K}} (ie_k\, \theta_{sqrk}^p + ee_k\, \tau_{sqrk}^p) \tag{4.25}$$

The above representation of DRSP gives:

$$\zeta \geq \zeta_R^p \qquad\qquad \forall\, p \in \mathcal{P} \tag{4.26}$$

which represents a classical Benders optimality cut that can be generated for each feasible SP and then added to MP.

4.5.2. Benders Master Problem

Given the above representation of DRSP, a lower bound on the overall problem can be obtained as:

$$\min \sum_{(i,j)\in\mathcal{A}} (fc\, l_{ij}\, n_{ij}\, x_{ij}) \ + \ \zeta \tag{4.27}$$

$$\text{subject to (4.26)}$$

But due to the large number of constraints (4.26), and because not all of them will be binding at optimality, in the BD framework, we solve a relaxed version of the above program where Benders cuts (4.26) are added in a delayed fashion, one at each iteration. Therefore, the relaxed version of the lower bound problem, called Benders master problem (MP), contains only a subset of constraints (4.26) and its optimal solution provides

a valid lower bound on the overall problem. To generate Benders cuts, at each iteration, DRSP($\psi^{ij}_{sqrk}, \upsilon^{ij}_{sqrk}, \nu^{ij}_{sqrk}, \omega^{s}_{ij}, \varphi_{ij}, \sigma^{ij}_{sqrk}, \theta_{sqrk}, \tau_{sqrk}, \varpi_s \mid \hat{X}$) is solved and the optimal values of the dual variables are used to construct a Benders cut (4.26).

In the case where MP solution (represented by the binary locations vector $\hat{X}$) causes DRSP to be unbounded (SP is infeasible), the binary structure of MP allows the generation of Benders combinatorial cut of the form:

$$\sum_{\{(i,j):\hat{x}_{ij}=0\}} x_{ij} + \sum_{\{(i,j):\hat{x}_{ij}=1\}} (1 - x_{ij}) \geq 1 \tag{4.28}$$

where $\hat{x}_{ij} \in \hat{X}$. This cut forces MP to exclude the combination of binary variables that led to the unboundedness of DRSP. [14]

4.5.3. Surrogate Constraints for MP

To improve the quality of MP solution and to reduce the possibility of generating MP solutions that will lead to the infeasibility of SP, we introduce five sets of surrogate constraints. While these constraints are valid, they are also redundant in the original formulation.

4.5.3.1. Constraint on Exposure Time over Route

Let $\hat{c}^{sqrk}$ denote the minimum amount of charge required by an EV of commodity $(sqrk)$, i.e.,

$$\sum_{(i,j)\in\mathcal{A}_r} c^{sqrk}_{ij} \geq \hat{c}^{sqrk} \qquad \forall\, s \in \mathcal{S},\ q \in \mathcal{Q}_s,\ r \in \mathcal{R}_q,\ k \in \mathcal{K}$$

Using the bounds on the initial and ending levels of energy for each commodity (ie_k and ee_k, respectively), $\hat{c}^{sqrk}$ can be pre-calculated as:

$$\hat{c}^{sqrk} = \xi_r + ee_k - ie_k \qquad \forall\, s \in \mathcal{S},\ q \in \mathcal{Q}_s,\ r \in \mathcal{R}_q,\ k \in \mathcal{K}$$

Then, an aggregated version of the dual-purpose constraint (4.5) can be given as:

$$\sum_{(i,j)\in\mathcal{A}_r} \varrho\, t_{ij}^{s}\, x_{ij} \geq \hat{c}^{sqrk} \qquad \forall\, s \in \mathcal{S},\, q \in \mathcal{Q}_s,\, r \in \mathcal{R}_q,\, k \in \mathcal{K} \tag{4.29}$$

A constraint of this type ensures that enough number of WCSs are selected by MP to provide enough exposure time for EVs to receive the minimum amount of charge required on their routes.

4.5.3.2. Constraint on Charging Availability over the Initial Part of the Trip

Let $e_{o_r}^{sqrk} = ie_k$ be the energy of EVs of commodity $(sqrk)$ at the origin of route r (node o_r). Further, let $\hat{\mathcal{A}}_r \subset \mathcal{A}_r$ be the subset of connected arcs of route r that EVs of this commodity can travel starting from o_r until running out of charge (including the arc at which the EVs will run out of charge). That is, $\hat{\mathcal{A}}_r$ represents the initial part of the commodity's trip. Then, to ensure that EVs will not run out of charge on the initial part of the trip, the following constraint can be added to MP:

$$\sum_{(i,j)\in\hat{\mathcal{A}}_r} x_{ij} \geq 1 \qquad \forall\, s \in \mathcal{S},\, q \in \mathcal{Q}_s,\, r \in \mathcal{R}_q,\, k \in \mathcal{K} \tag{4.30}$$

This constraint ensures that, for each commodity, at least one WCS is installed on the commodity's route between the commodity's origin and the point where EVs will run out of charge.

By taking into consideration the exposure time between WCSs and EVs, a tighter version of constraint (4.30) can be given as:

$$\sum_{(i,j)\in\hat{\mathcal{A}}_r} \varrho\, t_{ij}^{s}\, x_{ij} \geq \xi_{\hat{r}} - ie_k \qquad \forall\, s \in \mathcal{S},\, q \in \mathcal{Q}_s,\, r \in \mathcal{R}_q,\, k \in \mathcal{K} \tag{4.31}$$

where $\xi_{\hat{r}}$ is the energy consumption over $\hat{\mathcal{A}}_r$. Not only this form of the constraint ensures the opening of at least one WCS on the initial part of the route before EVs runs out of energy, but it also guarantees that the opened station(s) can provide enough exposure times

for the EVs to receive enough charge to travel the initial part of the trip.

4.5.3.3. Constraint on Charging Availability over the Last Part of the Trip

Let $e_{d_r}^{sqrk} = ee_k$ be the minimum required energy of EVs of commodity $(sqrk)$ at the destination of route r (node d_r). Further, let $\tilde{\mathcal{A}}_r \subset \mathcal{A}_r$ be the largest subset of connected arcs at the end of route r such that if an EV of type k enters the first arc of $\tilde{\mathcal{A}}_r$ with a full range, then it can reach the end of route r with a level of energy $e_{d_r}^{sqrk} \geq ee_k$. Let $\check{\mathcal{A}}_r = \tilde{\mathcal{A}}_r \cup (a)$ where (a) is the arc of $\mathcal{A}_r$ that directly precede $\tilde{\mathcal{A}}_r$. Accordingly, if none of the arcs of $\check{\mathcal{A}}_r$ has a WCS, EVs cannot reach the destination with the required amount of energy. Therefore, we can construct the following constraint for each commodity:

$$\sum_{(i,j)\in\check{\mathcal{A}}_r} x_{ij} \geq 1 \qquad \forall\, s \in \mathcal{S},\, q \in \mathcal{Q}_s,\, r \in \mathcal{R}_q,\, k \in \mathcal{K} \tag{4.32}$$

These constraints ensure that, for each commodity, at least one WCS is installed on the last part of the commodity's route to serve the charging demands at that part of the route.

By taking into consideration the exposure time between WCSs and EVs, a tighter version of this constraint can be given as:

$$\sum_{(i,j)\in\check{\mathcal{A}}_r} \varrho\, t_{ij}^{s}\, x_{ij} \geq \xi_{\check{\mathcal{A}}_r} + \gamma_k - ee_k \qquad \forall\, s \in \mathcal{S},\, q \in \mathcal{Q}^s,\, r \in \mathcal{R}_q,\, k \in \mathcal{K} \tag{4.33}$$

where $\xi_{\check{\mathcal{A}}_r}$ represents the energy consumption on $\check{\mathcal{A}}_r$. Similar to constraint (4.31), this form of this surrogate constraint ensures that the selected WCS at the last part of the route can provide enough exposure time to satisfy the charging demands on that part of the route.

4.5.3.4. Constraint on Maximum Power Capacity

While the first three surrogate constraints (4.29), (4.31), and (4.33) deal with the exposure time between the EVs and the selected WCSs, the fourth constraint deals with the length of these stations. Specifically, to assist getting a feasible SP, the WCSs featured in the MP

solution should provide enough millage to host the power capacity required to serve the minimum charging demands. That is, MP solution should provide enough electrified millage in order for constant (4.7) in SP to hold. By substituting constraint (4.7) from the original problem in (4.6) we obtain

$$\sum_{q\in\mathcal{Q}_s}\sum_{r\in\mathcal{R}_q}\sum_{k\in\mathcal{K}}(\delta_{ij}^{sqr}\,\rho_{ij}^{sqrk}\,c_{ij}^{sqrk}) \le \eta\,(m_{cap}\,n_{ij}\,l_{ij})\,t_{ij}^{s} \qquad \forall\, s\in\mathcal{S},\ (i,j)\in\mathcal{A}. \quad (4.34)$$

If no WCS is installed on arc (i,j), i.e., $x_{ij}=0$, then the left hand side of (4.34) must be equal to zero. Therefore, it is valid to write

$$\sum_{q\in\mathcal{Q}_s}\sum_{r\in\mathcal{R}_q}\sum_{k\in\mathcal{K}}(\delta_{ij}^{sqr}\,\rho_{ij}^{sqrk}\,c_{ij}^{sqrk}) \le \eta\,(m_{cap}\,n_{ij}\,l_{ij})\,t_{ij}^{s}\,x_{ij} \qquad \forall\, s\in\mathcal{S},\ (i,j)\in\mathcal{A}. \quad (4.35)$$

Let $\mathcal{G}_{ij}^{s}$ be defined as the set of all routes that pass through arc (i,j) during traffic period s. For each route $g\in\mathcal{G}_{ij}^{s}$ let q_g denote the OD pair of route g. Accordingly, equation (4.35) can be rewritten as

$$\sum_{g\in\mathcal{G}_{ij}^{s}}\sum_{k\in\mathcal{K}}(\rho_{ij}^{sq_ggk}\,c_{ij}^{sq_ggk}) \le \eta\,(m_{cap}\,n_{ij}\,l_{ij})\,t_{ij}^{s}\,x_{ij} \qquad \forall\, s\in\mathcal{S},\ (i,j)\in\mathcal{A}. \quad (4.36)$$

Now let $\mathcal{A}_{\mathcal{G}_{ij}^{s}}$ be the set of arcs that form all routes in set $\mathcal{G}_{ij}^{s}$. Then, an aggregation of equation (4.36) over set $\mathcal{A}_{\mathcal{G}_{ij}^{s}}$ can be written as

$$\sum_{a\in\mathcal{A}_{\mathcal{G}_{ij}^{s}}}\sum_{g\in\mathcal{G}_a^{s}}\sum_{k\in\mathcal{K}}(\rho_{a}^{sq_ggk}\,c_{a}^{sq_ggk}) \le \sum_{a\in\mathcal{A}_{\mathcal{G}_{ij}^{s}}}\eta\,(m_{cap}\,n_a\,l_a)\,t_a^{s}\,x_a \qquad \forall\, s\in\mathcal{S},\ (i,j)\in\mathcal{A}. \quad (4.37)$$

Since $\mathcal{G}_{ij}^{s}\subseteq\bigcup_{a\in\mathcal{A}_{\mathcal{G}_{ij}^{s}}}\mathcal{G}_a^{s}$ for all $(i,j)\in\mathcal{A}$, it is valid to write

$$\sum_{a\in\mathcal{A}_{\mathcal{G}_{ij}^{s}}}\sum_{g\in\mathcal{G}_{ij}^{s}}\sum_{k\in\mathcal{K}}(\rho_{a}^{sq_ggk}\,c_{a}^{sq_ggk}) \le \sum_{a\in\mathcal{A}_{\mathcal{G}_{ij}^{s}}}\sum_{g\in\mathcal{G}_a^{s}}\sum_{k\in\mathcal{K}}(\rho_{a}^{sq_ggk}\,c_{a}^{sq_ggk}) \qquad \forall\, s\in\mathcal{S},\ (i,j)\in\mathcal{A} \quad (4.38)$$

therefore, by combining (4.37) and (4.38) we obtain

$$\sum_{a\in\mathcal{A}_{\mathcal{G}^s_{ij}}}\sum_{g\in\mathcal{G}^s_{ij}}\sum_{k\in\mathcal{K}}(\rho_a^{sq_ggk}\,c_a^{sq_ggk}) \le \sum_{a\in\mathcal{A}_{\mathcal{G}^s_{ij}}}\eta\,(m_{cap}\,n_a\,l_a)\,t_a^s\,x_a \qquad \forall\, s\in\mathcal{S},\,(i,j)\in\mathcal{A}. \quad (4.39)$$

Now let $\hat{c}^{sq_ggk}$ denote the minimum amount of charge required by an EV of commodity (sq_ggk), i.e.,

$$\sum_{a\in\mathcal{A}_g} c_a^{sq_ggk} \ge \hat{c}^{sq_ggk} \qquad \forall\, s\in\mathcal{S},\, g\in\mathcal{G}^s_{ij},\,(i,j)\in\mathcal{A},\,k\in\mathcal{K} \quad (4.40)$$

where $\mathcal{A}_g$ is the set of arcs that form route $g\in\mathcal{G}^s_{ij}$. Also, by letting $\rho^{sq_ggk}_{(min)} = \min_{a\in\mathcal{A}_g}\{\rho_a^{sq_ggk} : \forall\, s\in\mathcal{S},\, g\in\mathcal{G}^s_{ij},\,(i,j)\in\mathcal{A},\,k\in\mathcal{K}\}$, we obtain

$$\sum_{a\in\mathcal{A}_g}\rho_a^{sq_ggk}\,c_a^{sq_ggk} \ge \rho^{sq_ggk}_{(min)}\,\hat{c}^{sq_ggk} \qquad \forall\, s\in\mathcal{S},\, g\in\mathcal{G}^s_{ij},\,(i,j)\in\mathcal{A},\,k\in\mathcal{K}. \quad (4.41)$$

By aggregating (4.41) over sets $(\mathcal{G}^s_{ij})$ and $(\mathcal{K})$ we obtain

$$\sum_{a\in\mathcal{A}_g}\sum_{g\in\mathcal{G}^s_{ij}}\sum_{k\in\mathcal{K}}\rho_a^{sq_ggk}\,c_a^{sq_ggk} \ge \sum_{g\in\mathcal{G}^s_{ij}}\sum_{k\in\mathcal{K}}\rho^{sq_ggk}_{(min)}\,\hat{c}^{sq_ggk} \qquad \forall\, s\in\mathcal{S},\,(i,j)\in\mathcal{A}. \quad (4.42)$$

And since $\mathcal{A}_g\subseteq\mathcal{A}_{\mathcal{G}^s_{ij}}$ for all $g\in\mathcal{G}^s_{ij}$, then

$$\sum_{a\in\mathcal{A}_{\mathcal{G}^s_{ij}}}\sum_{g\in\mathcal{G}^s_{ij}}\sum_{k\in\mathcal{K}}\rho_a^{sq_ggk}\,c_a^{sq_ggk} \ge \sum_{a\in\mathcal{A}_g}\sum_{g\in\mathcal{G}^s_{ij}}\sum_{k\in\mathcal{K}}\rho_a^{sq_ggk}\,c_a^{sq_ggk} \qquad \forall\, s\in\mathcal{S},\,(i,j)\in\mathcal{A}. \quad (4.43)$$

Therefore, in view of equations (4.39), (4.42), and (4.43) we may write

$$\sum_{g\in\mathcal{G}^s_{ij}}\sum_{k\in\mathcal{K}}\rho^{sq_ggk}_{(min)}\,\hat{c}^{sq_ggk} \le \eta\,m_{cap}\sum_{a\in\mathcal{A}_g}(n_a\,l_a\,t_a^s\,x_a) \qquad \forall\, s\in\mathcal{S},\,(i,j)\in\mathcal{A} \quad (4.44)$$

which is a valid inequality that could be added to MP as a fourth set of surrogate constraints.

4.5.3.5. Lower Bound on the Auxiliary Variable

The fifth surrogate constraint to be added to MP provides a lower bound on the auxiliary variable ζ. This MP variable represents the value of SP objective. Therefore, by letting α denote a lower bound on any feasible SP, it is valid to write

$$\zeta \geq \alpha \tag{4.45}$$

We obtain α as follows. The objective (4.17) of SP is given as

$$\min \quad \Big[\sum_{(i,j)\in\mathcal{A}} (vc\ y_{ij}) \ + \max_{s\in\mathcal{S}} \sum_{q\in\mathcal{Q}_s} \sum_{r\in\mathcal{R}_q} \sum_{k\in\mathcal{K}} \sum_{(i,j)\in\mathcal{A}_r} (cc\ tr\ v^{sqrk} c_{ij}^{sqrk}) \Big].$$

Let y_{min} be the minimum amount of total power capacity installation required to satisfy the charging demands on the whole network, i.e., for any feasible solution of the original problem, we must have the following constraint to hold:

$$vc\ y_{min} \leq \sum_{(i,j)\in\mathcal{A}} (vc\ y_{ij}). \tag{4.46}$$

Therefore, the term $(vc\ y_{min})$ provides a lower bound on the first part of the SP objective function (4.17). We calculate y_{min} by solving a version of SP where all arcs are WCSs, i.e., SP$(e_i^{sqrk},\ c_{ij}^{sqrk}, y_{ij} \mid \hat{x}_{ij} = 1)$.

Further, let $\hat{c}^{sqrk}$ be the minimum amount of charge required by commodity $(sqrk)$ as defined in 4.5.3.1. Accordingly, any feasible solution of the problem needs to satisfy the following equation:

$$\sum_{q\in\mathcal{Q}_s} \sum_{r\in\mathcal{R}_q} \sum_{k\in\mathcal{K}} (cc\ tr\ v^{sqrk} \hat{c}^{sqrk}) \leq \sum_{q\in\mathcal{Q}_s} \sum_{r\in\mathcal{R}_q} \sum_{k\in\mathcal{K}} \sum_{(i,j)\in r} (cc\ tr\ v^{sqrk} c_{ij}^{sqrk}) \qquad \forall s \in \mathcal{S}.$$

Therefore, we have

$$\max_{s\in\mathcal{S}} \sum_{q\in\mathcal{Q}_s} \sum_{r\in\mathcal{R}_q} \sum_{k\in\mathcal{K}} (cc\ tr\ v^{sqrk}\hat{c}^{sqrk}) \leq \max_{s\in\mathcal{S}} \sum_{q\in\mathcal{Q}_s} \sum_{r\in\mathcal{R}_q} \sum_{k\in\mathcal{K}} \sum_{(i,j)\in\mathcal{A}_r} (cc\ tr\ v^{sqrk}c_{ij}^{sqrk}). \tag{4.47}$$

That is, the left hand side of (4.47) is a lower bound on the second part of SP objective (4.17). Thus, since the left hand side of (4.46), and the left hand side of (4.47) provide lower bounds on the first part and the second part of SP objective, respectively, it is valid to write

$$\alpha = vc\ y_{min} + \max_{s\in\mathcal{S}} \sum_{q\in\mathcal{Q}_s} \sum_{r\in\mathcal{R}_q} \sum_{k\in\mathcal{K}} (cc\ tr\ v^{sqrk}\hat{c}^{sqrk}) \tag{4.48}$$

where α is a lower bound on SP objective function, by definition. By substituting (4.48) in (4.45) we obtain

$$\zeta \geq vc\ y_{min} + \max_{s\in\mathcal{S}} \sum_{q\in\mathcal{Q}_s} \sum_{r\in\mathcal{R}_q} \sum_{k\in\mathcal{K}} (cc\ tr\ v^{sqrk}\hat{c}^{sqrk}) \tag{4.49}$$

which is the fifth surrogate constraint to be added to MP.

4.5.4. Benders Cut Strengthening

For a fixed binary vector $\hat{X}$ representing MP solution, subproblem SP(e_i^{sqrk}, c_{ij}^{sqrk}, $y_{ij} \mid \hat{X}$) may possess degeneracy. Therefore, the associated DRSP may have multiple optimal solutions, and a different Benders cut can be generated based on each solution. Thus, we seek to generate the strongest cut possible at each iteration. For an optimization problem $\min_{y\in\mathcal{Y},z\in\mathcal{R}}\{z : z \geq f(w) + yg(w), \forall w \in \mathcal{W}\}$, a cut $z \geq f(v) + yg(v)$ is stronger than another cut $z \geq f(w) + yg(w)$ if $f(v) + yg(v) \geq f(w) + yg(w), \forall y \in \mathcal{Y}$ and if $f(v)+yg(v) > f(w)+yg(w)$ for at least one $y \in \mathcal{Y}$ [42]. To obtain a stronger cut at a certain iteration (n), we start by solving DRSP($\psi_{sqrk}^{ij}, \upsilon_{sqrk}^{ij}, \nu_{sqrk}^{ij}, \omega_{ij}^{s}, \varphi_{ij}, \sigma_{sqrk}^{ij}, \theta_{sqrk}, \tau_{sqrk}, \varpi_s \mid \hat{X}$) for the associated dual vector $(\psi^n, \upsilon^n, \nu^n, \omega^n, \varphi^n, \sigma^n, \theta^n, \tau^n, \varpi^n)$. Then, we fix the dual variables that are associated with the nonzero coefficients in (4.20), and consider the remaining dual variables as decision variables as we solve a second problem:

$\text{DRSP}_2(\psi^{ij}_{sqrk}, \upsilon^{ij}_{sqrk}, \nu^{ij}_{sqrk}, \omega^{s}_{ij}, \varphi_{ij}, \sigma^{ij}_{sqrk}, \theta_{sqrk}, \tau_{sqrk}, \varpi_s \mid \psi^n, \upsilon^n, \nu^n, \omega^n, \varphi^n, \sigma^n, \theta^n, \tau^n, \varpi^n, \hat{X})$ which is given as:

$$\text{Maximize} \quad \sum_{s\in\mathcal{S}} \sum_{q\in\mathcal{Q}_s} \sum_{r\in\mathcal{R}_q} \sum_{k\in\mathcal{K}} \sum_{(i,j)\in\mathcal{A}_r} \left(\xi_{ij} \left(1 - \hat{x}_{ij}\right) \upsilon^{ij}_{sqrk} \; + \varrho \, t^{s}_{ij} \, \hat{x}_{ij} \, \nu^{ij}_{sqrk} \right) \tag{4.50}$$

$$\text{subject to (4.21) to (4.24)}$$

The idea here is to maximize the values of the dual variables that are associated with zero coefficients in the objective function of DRSP since these variables can hold any value without affecting the optimal value of the objective function. We use the new values of the dual variables obtained by solving DRSP_2 to generate a stronger Benders cut.

4.5.5. Upper Bound Heuristic (UBH)

While the surrogate constraints help improving the quality of MP solution, the addition of these constraints does not guarantee that the binary vector representing the MP solution will lead to a feasible SP. This might delay obtaining a feasible solution to the overall problem. Therefore, to guarantee obtaining a feasible solution to the problem at an early stage of the solution procedure, we devise an optimization-based greedy heuristic that is solved at the very beginning of the procedure.

The heuristic first reduces the size of the problem by selecting (in a greedy fashion) only a subset of arcs as candidates for WCSs. The candidates are selected based on their travel time. Specifically, the algorithm selects, on each route, a subset of arcs with the longest travel time to provide maximum exposure time between the EVs and WCSs while keeping the number of WCSs at minimum. After the subset of candidates is formed, it is passed to a modified version of the original problem which is solved only considering a subset of candidates, providing an upper bound on the original problem. The heuristic procedure is presented in Algorithm 3.

Algorithm 3 UBH

1: **initialize** set of candidate arcs $\mathcal{C} = \emptyset$

2: **for** each commodity $(sqrk)$ **do**

3: calculate the minimum amount of charge required by commodity, $\hat{c}^{sqrk}$

4: initialize set of candidate arcs to serve commodity $(sqrk)$, $\mathcal{L}_{sqrk} = \emptyset$

5: let $\grave{\mathcal{A}}_r$ be the set of links on route (r), sorted (in a non-increasing order) based on travel time

6: **for** link $(i,j) \in \grave{\mathcal{A}}_r$ **do**

7: $\mathcal{L}_{sqrk} = (i,j) \cup \mathcal{L}_{sqrk}$

8: **if** commodity can be served by $\mathcal{L}_{sqrk}$ **then**

9: $\mathcal{C} = \mathcal{L}_{sqrk} \cup \mathcal{C}$

10: break

11: **end if**

12: **end for**

13: **end for**

14: solve problem $\mathbf{P}(e_i^{sqrk},\ c_{ij}^{sqrk}, y_{ij},\ x_{ij} \mid\ x_{ij} = 0, \quad \forall\, (i,j) \in \mathcal{A} \setminus \mathcal{C})$ for an upper bound

4.5.6. BD Implementation

The overall implementation of our customized BD solution methodology is displayed in Algorithm 4. We denote the best upper bound, the best lower bound, and the optimality gap by UB, LB, and ϵ, respectively. After initializing the algorithmic parameters (line 1), The algorithm starts by solving problem $\mathbf{SP}(e_i^{sqrk},\ c_{ij}^{sqrk}, y_{ij} \mid x_{ij} = 1)$ in order to calculate the minimum required power capacity as $y_{min} = \sum_{(i,j)\in\mathcal{A}} y_{ij}$ to use it in the surrogate constraint (4.49). We then solve the upper bound heuristic (UBH) for an upper bound solution (lines 3 - 5). Then, we use the locations vector $\hat{X}$ as resulted by solving UBH to generate an initial Benders cut (lines 6 - 7). After obtaining an upper bound and an initial Benders cut we start the iterative procedure (line 8).

Algorithm 4 BD Implementation

initialize $\mathcal{C} = \emptyset$, $UB = \infty$, $LB = 0$, $\epsilon = 0.02$, `runtime`=0, and `stoptime`=1800 seconds

solve **SP**$(e_i^{sqrk},\ c_{ij}^{sqrk}, y_{ij} \mid x_{ij} = 1)$ to obtain $y_{min} = \sum_{(i,j)\in\mathcal{A}} y_{ij}$

solve **UBH**$(e_i^{sqrk},\ c_{ij}^{sqrk}, y_{ij},\ x_{ij} \mid \mathcal{C})$ for Z_{UBH} and $\hat{X}$

if $Z_{UBH} < UB$ **then** $UB = Z_{UBH}$

end if

solve **DRSP**$(\psi_{sqrk}^{ij}, \upsilon_{sqrk}^{ij}, \nu_{sqrk}^{ij}, \omega_{ij}^{s}, \varphi_{ij}, \sigma_{sqrk}^{ij}, \theta_{sqrk}, \tau_{sqrk}, \varpi_s \mid \hat{X})$

generate initial Benders optimality cut (4.26) and add it to **MP**

while (`runtime` $\leq$ `stoptime` **and** `optgap` $> \epsilon$) **do**

    solve **MP** for Z_{MP} and $\hat{X}$

    if $Z_{MP} > LB$ **then** $LB = Z_{MP}$

    end if

    if `optgap` $< \epsilon$ **or** `runtime` $\geq$ `stoptime` **then** break (return best UB solution)

    end if

    solve **DRSP**$(\psi_{sqrk}^{ij}, \upsilon_{sqrk}^{ij}, \nu_{sqrk}^{ij}, \omega_{ij}^{s}, \varphi_{ij}, \sigma_{sqrk}^{ij}, \theta_{sqrk}, \tau_{sqrk}, \varpi_s \mid \hat{X})$

    if DRSP is bounded **then**

        solve **SP**$(e_i^{sqrk},\ c_{ij}^{sqrk}, y_{ij} \mid \hat{X})$

        if $Z_{SP} + Z_{MP} - \zeta < UB$ **then** $UB = Z_{SP} + Z_{MP} - \zeta$

            if `optgap` $< \epsilon$ **or** `runtime` $\geq$ `stoptime` **then** break (return best UB solution)

            end if

            generate initial Benders optimality cut (4.26) and add it to **MP**

        end if

    else

        generate combinatorial Benders cut (4.28) and add it to **MP**

    end if

end while

The iterative procedure then starts by solving MP for a lower bound and a locations vector $\hat{X}$ (line 9). If none of the stopping criteria are met, we proceed by solving DRSP (line 14). If DRSP is found to be bounded, we proceed by solving SP for a new upper bound (lines 16 - 18), and use the solution of DRSP to generate a Benders cut (line 20). In the case where DRSP is unbounded, we generate a combinatorial Benders cut and add it to **MP** (line 23). The iterative procedure continues until at least one stopping creation is met.

4.6. Computational Study on Algorithmic Performance

To assess the efficiency of the proposed solution algorithm, we conduct a computational experiment to compare the performance of the proposed algorithm to the Branch and Cut method (B&C) as implemented by CPLEX. For this purpose, we randomly generate 6 data sets, each consisting of 10 different networks. Furthermore, to evaluate the effectiveness of the cut strengthening technique and the proposed upper bound heuristic, we solve each test instance using four different algorithmic settings. At first, we use BD as described above but with the exclusion of the upper bound heuristic and the cut strengthening. We denote this setting by $\mathrm{BD_I}$. For the second setting ($\mathrm{BD_{II}}$), we add cut strengthening as described in 4.5.4 to $\mathrm{BD_I}$. The third setting $\mathrm{BD_{III}}$ consists of $\mathrm{BD_I}$ and the upper bound heuristic. Finally, the fourth setting ($\mathrm{BD_{IV}}$) combines $\mathrm{BD_I}$ with cut strengthening and the upper bound heuristic. Experiments are conducted using Java environment with CPLEX and Concert Technology (IBM, Inc.) on a machine with Intel Core i7 3.60 GHz processor and 32.0 GB RAM running 64-bit OS.

4.6.1. Data Generation

For the computational experiments, we generate 6 data sets, each consisting of 10 different randomly generated instances representing different traffic networks. To generate the test instances, we consider 3 sizes of grids including 10×10, 15×15, and 20×20. For each network, we consider 12 different traffic periods, representing peak and off-peak periods. For each traffic period, we consider a set of origin/destination nodes and we generate traffic

demands accordingly. We obtain the UE assignment for each traffic period using the Method of Successive Averages (presented in Appendix A). We summarize the input data in Table 4.12. We denote the number of nodes, the average number of arcs over the 10 instances of a data set, and the number of OD pairs by $|\mathcal{N}|$, $|\bar{\mathcal{A}}|$, and $|\mathcal{Q}|$, respectively. The test instances full data including networks topology and traffic assignments can be found online at http://lyle.smu.edu/INETS/TestInstances/EV-wireless-charging-network-data2.htm.

The wireless charging system associated parameters are provided in Table 4.13. We further consider 3 different classes of EVs and we provide the associated data in Table 4.14. We assume that all vehicles in the networks are EVs with wireless charging capabilities and that each EV class represents one-third of the vehicles in each network.

Table 4.12: Data classes and the associated sizes

Data set	c1	c2	c3	c4	c5	c6
$\|\mathcal{N}\|$	100	225	400	100	225	400
$\|\bar{\mathcal{A}}\|$	325	732	1315	325	732	1315
$\|\mathcal{Q}\|$	500	500	500	750	750	750

Table 4.13: Wireless charging system parameters

Parameter	fc	vc	cc	tr	p_{cap}	ϱ	m_{cap}	ξ	η
Value	\$800,000	\$11,000	\$0.15	7,200	20	200	5,000	0.33	80%

Table 4.14: EV classes data

	γ	ie	ee
EV class A	40	U[30,35]	U[5,10]
EV class B	40	U[35,40]	U[15,20]
EV class C	40	U[20,25]	U[0,5]

4.6.2. Numerical Results

Table 4.15 provides the numerical results of the computational experiments described above. For each data set, we provide the runtimes and optimality gaps obtained using B&C and using each algorithmic setting of our proposed BD algorithm. The results indicate that all four settings of the proposed BD outperform B&C since the latter could not provide bounds for any of the test instances before reaching the stopping time limit.

The results also show that for the data sets containing the smallest test instances (i.e., data sets c1 and c2), the algorithmic setting BD_{I} is found to be the preferred setting as it outperforms the rest of the settings in terms of algorithmic convergence. That is, performing cut strengthening and adding the UBH did not help the convergence when applied to the test instances in data sets c1 and c2.

In the case of data set c3, the algorithmic setting BD_{I} provided the fastest average runtime, while the setting BD_{II} provided a slightly longer average runtime but, on average, slightly better optimality gaps.

The results of data set c4 is similar to the results obtained for data sets c1 and c2. That is, for these 10 X 10 test instances, BD_{I} outperformed the other settings in convergence.

The case is different when considering the two data sets c5 and c6 that contain the largest test instances. Specifically, the results show that the algorithmic settings BD_{III} and BD_{IV} dramatically outperformed the other two settings. That is, implementing the UBH is very essential for the effectiveness of the algorithm to solve the large test instances in these data sets. This is because BD_{I} and BD_{II} could not always generate feasible solutions to the problems before reaching the stopping time limit. On the other hand, the UBH implemented in BD_{III} and BD_{IV} guarantees obtaining a feasible solution at an early stage of the algorithm. Finally, we observe that combining UBH and cut strengthening, while not helpful in the case of data set c5, was useful in obtaining better bounds at shorter runtimes when applied to data set c6 corresponding to the largest test instances.

Table 4.15: Numerical results

		Data set	c1	c2	c3	c4	c5	c6
		Size	10 x 10	15 x 15	20 x 20	10 x 10	15 x 15	20 x 20
B&C	Runtime	avg	1800	1800	1800	1800	1800	1800
		max	1800	1800	1800	1800	1800	1800
		min	1800	1800	1800	1800	1800	1800
	Opt. Gap%	avg	N.B.	N.B.	N.B.	N.B.	N.B.	N.B.
		max	N.B.	N.B.	N.B.	N.B.	N.B.	N.B.
		min	N.B.	N.B.	N.B.	N.B.	N.B.	N.B.
BD_{I}	Runtime	avg	226	190	934	312	1041	1432
		max	932	226	1800	1800	1800	1800
		min	91	170	334	128	260	555
	Opt. Gap%	avg	1.48	1.64	2.21	1.48	21.60	22.06
		max	1.94	1.98	3.95	2.09	N.B.	N.B.
		min	0.66	1.19	0.61	0.95	0.57	1.82
BD_{II}	Runtime	avg	331	190	937	317	1041	1433
		max	1358	211	1800	1800	1800	1800
		min	89	171	336	130	259	565
	Opt. Gap%	avg	1.48	1.64	2.02	1.49	21.60	22.06
		max	1.94	1.98	3.90	2.22	N.B.	N.B.
		min	0.66	1.19	0.19	0.95	0.57	1.82
BD_{III}	Runtime	avg	376	315	1080	543	1154	1428
		max	1160	414	1800	1800	1800	1800
		min	153	285	528	215	265	538
	Opt. Gap%	avg	1.51	1.60	2.10	1.44	2.20	2.81
		max	1.95	1.92	4.39	2.22	3.58	7.02
		min	0.66	1.12	0.19	0.90	1.14	1.55
BD_{IV}	Runtime	avg	538	326	1085	609	1167	1381
		max	1722	368	1800	1800	1800	1800
		min	170	299	565	240	291	606
	Opt. Gap%	avg	1.51	1.66	2.06	1.44	2.20	2.78
		max	1.95	1.98	4.14	2.22	3.45	7.02
		min	0.66	1.20	0.19	0.90	1.14	1.55

4.7. A Case Study: U.S. 75 Corridor Network

To demonstrate the applicability of the robust WCS network design and the capability of the proposed algorithm, we conduct a case study based on the U.S. 75 corridor network in north Texas. The network consists of 1378 nodes, 3148 arcs, and 9410 origin-destination pairs. Twelve different UE assignments (representing 12 different daily traffic periods) are considered in the optimization. The network's daily traffic pattern representing the 12 traffic periods is depicted in figure 4.6. The network data along with the UE assignments data can be found online at http://lyle.smu.edu/INETS/TestInstances/EV-wireless-charging-network-data2.htm.

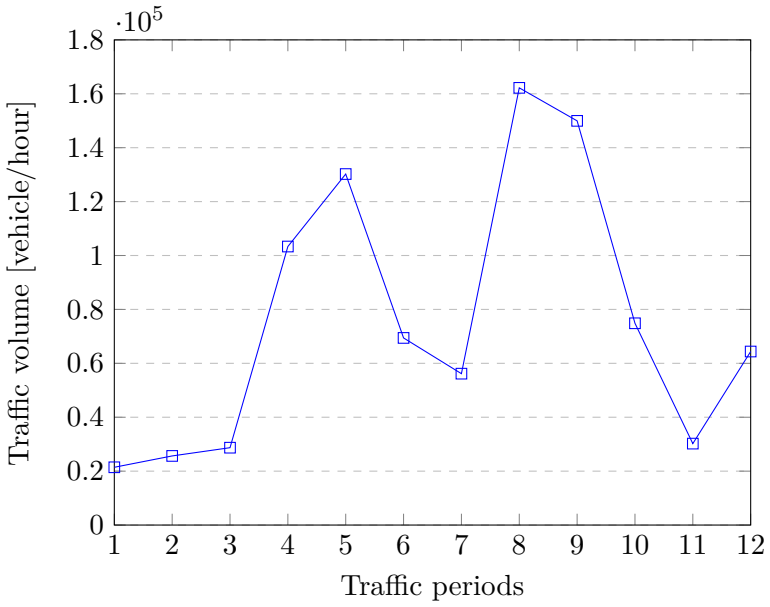

Figure 4.6: U.S. 75 corridor daily traffic pattern

All vehicles traveling in the network are assumed to be EVs with wireless charging capabilities. We further assume that there are three different classes of EVs in the network, where each class represents one-third of the total traffic volume. The initial and ending energy data for each class are given in Table 4.16. For this case study, we use the wireless charging system parameters that are given in Table 4.13.

Table 4.16: EV classes data

	γ	ie	ee
EV class D	40	40	35
EV class E	40	30	25
EV class F	40	25	15

To observe the differences between the robust solution and the single-period solutions obtained when considering each traffic period individually, we first solve a single period problem for each traffic period (s_1 to s_{12}) individually. Then we solve the robust model considering all 12 traffic periods together. The optimization results are provided in Table 4.17 and depicted in Figures 4.7, 4.8 and 4.9. Specifically, Table 4.17 and the two figures 4.8 and 4.9 show, for each component of the total cost, a comparison between the robust solution and the individual single-period solutions. The results show that the cost of the robust solution is \$M43.21 (%38.32) higher than the optimal cost under the morning peak period (s5). As illustrated in Figure 4.8, the biggest portion of this difference (\$M34.61) is associated with the charging cost, while the construction cost and the power installation cost account for \$M2.98 and \$M5.62 of the difference, respectively.

Comparing the robust solution to the solution of the evening peak period (s8) tells a different story. The difference here is only \$M3.61 (%3.2). Figure 4.8 shows that this difference is mainly due to the construction cost and the power installations cost.

To better recognize the differences between the robust solution and the individual single-period solutions, we repeat the optimization while considering a new value for parameter ϱ. Specifically, we consider $\varrho = 50$. The new results are provided in Table 4.18 and depicted in Figure 4.10 and Figure 4.11. The results show that under the new value of parameter ϱ, the relative differences between the cost of the robust solution and the costs of the two peak periods solutions are significantly higher than the first case. Specifically, the total cost of the robust solution is %40.51 and %11.67 higher than the costs associated with the individual single-period solutions under the morning peak period and the evening peak

Table 4.17: Costs comparison

	Construction cost ($M)	Power cost ($M)	Charging cost over project lifetime ($M)	Total cost ($M)	Number of deployed WCSs	Number of installed charging units
Robust	7.75	11.62	93.41	112.77	22	1056
s1	4.95	0.64	6.69	12.28	10	58
s2	4.90	0.21	2.64	7.75	10	19
s3	4.95	0.34	3.79	9.08	8	31
s4	5.11	4.98	49.10	59.19	14	453
s5	4.77	6.00	58.80	69.56	13	545
s6	4.93	5.03	49.42	59.38	10	457
s7	5.06	3.17	32.04	40.27	9	288
s8	6.77	9.54	92.85	109.16	23	867
s9	5.65	8.18	84.79	98.62	29	744
s10	5.42	3.23	31.83	40.49	12	294
s11	5.24	1.09	11.38	17.70	8	99
s12	5.12	1.66	16.43	23.22	9	151

period, respectively (Figure 4.10).

4.8. Concluding Remarks

In this study, we propose a robust approach to address the network design of wireless charging stations in traffic networks. The proposed approach takes into consideration the dynamic nature of the traffic condition in effort to generate WCS network designs that are feasible and cost-effective for all considered traffic periods. We illustrate, via two of examples, that the WCS network design problem of interest needs to be tackled via a robust approach. Specifically, we show that solving this problem when considering the peak traffic period does not guarantee the feasibility of the solution under other off-peak traffic periods. For this purpose, we propose a robust model that can handle multiple traffic periods represented by multiple UE assignments as model input. We further propose a BD solution algorithm to solve the large instances of the robust model and we straighten it using several techniques

Table 4.18: Costs comparison

	Construction cost ($M)	Power cost ($M)	Charging cost over project lifetime ($M)	Total cost ($M)	Number of deployed WCSs	Number of installed charging units
Robust	29.42	11.65	93.42	134.48	49	1059
s1	18.51	0.67	6.70	25.89	22	61
s2	18.54	0.29	2.59	21.42	24	26
s3	18.50	0.39	3.78	22.67	24	35
s4	17.90	5.16	49.14	72.21	27	469
s5	15.85	6.27	58.81	80.93	27	570
s6	18.02	5.14	49.47	72.63	24	467
s7	19.74	3.31	32.09	55.15	26	301
s8	15.67	9.91	93.21	118.79	30	901
s9	16.18	8.80	84.94	109.92	49	800
s10	20.03	3.34	31.80	55.17	26	304
s11	20.05	1.14	11.38	32.58	27	104
s12	19.79	1.68	16.40	37.87	27	153

including surrogate constraints, cut strengthening, and an upper bound heuristic. We provide an extensive computational experiment illustrating the effectiveness of each strengthening technique individually. Finally, we illustrate the applicability of the robust approach by conducting a case study on real traffic network from Dallas, TX where we compare the robust optimal solution to the single-period optimal solutions obtained individually for each traffic period. We further analyze the difference in the total system implementation cost between the robust optimal solution and the single-period optimal solutions, and we explain how the different components of the total cost differ between the two cases.

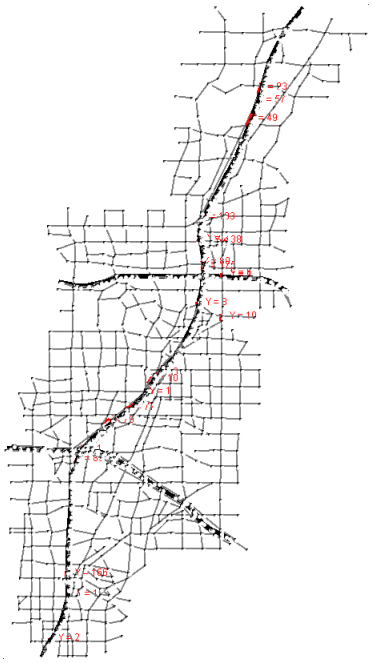

(a) Optimal robust solution

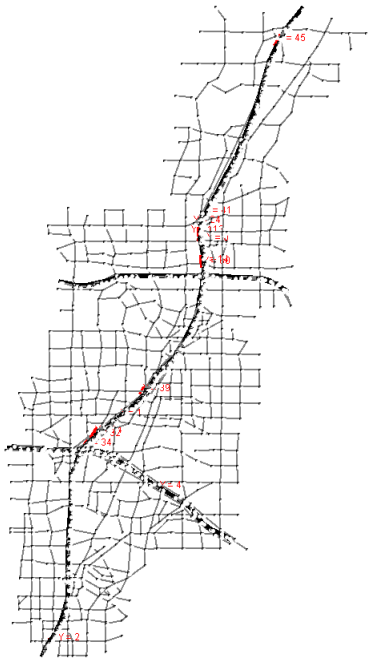

(b) Single-period optimal solution for the morning peak period

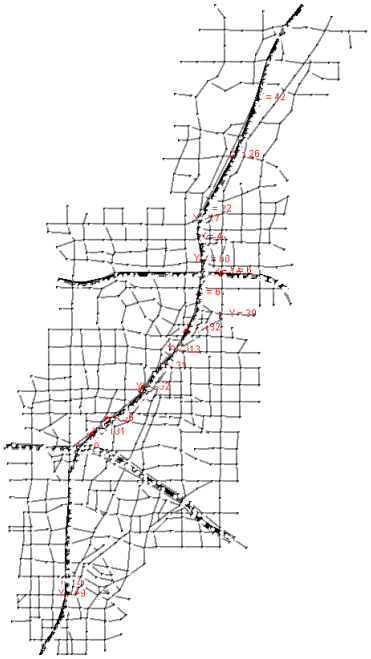

(c) Single-period optimal solution for the evening peak period

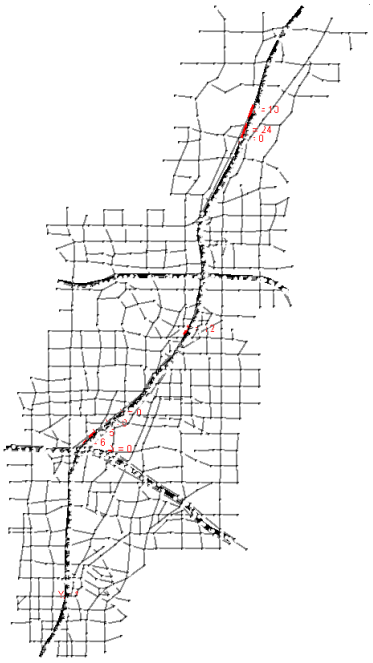

(d) Single-period optimal solution for the off-peak period 1

Figure 4.7: U.S. 75 corridor network

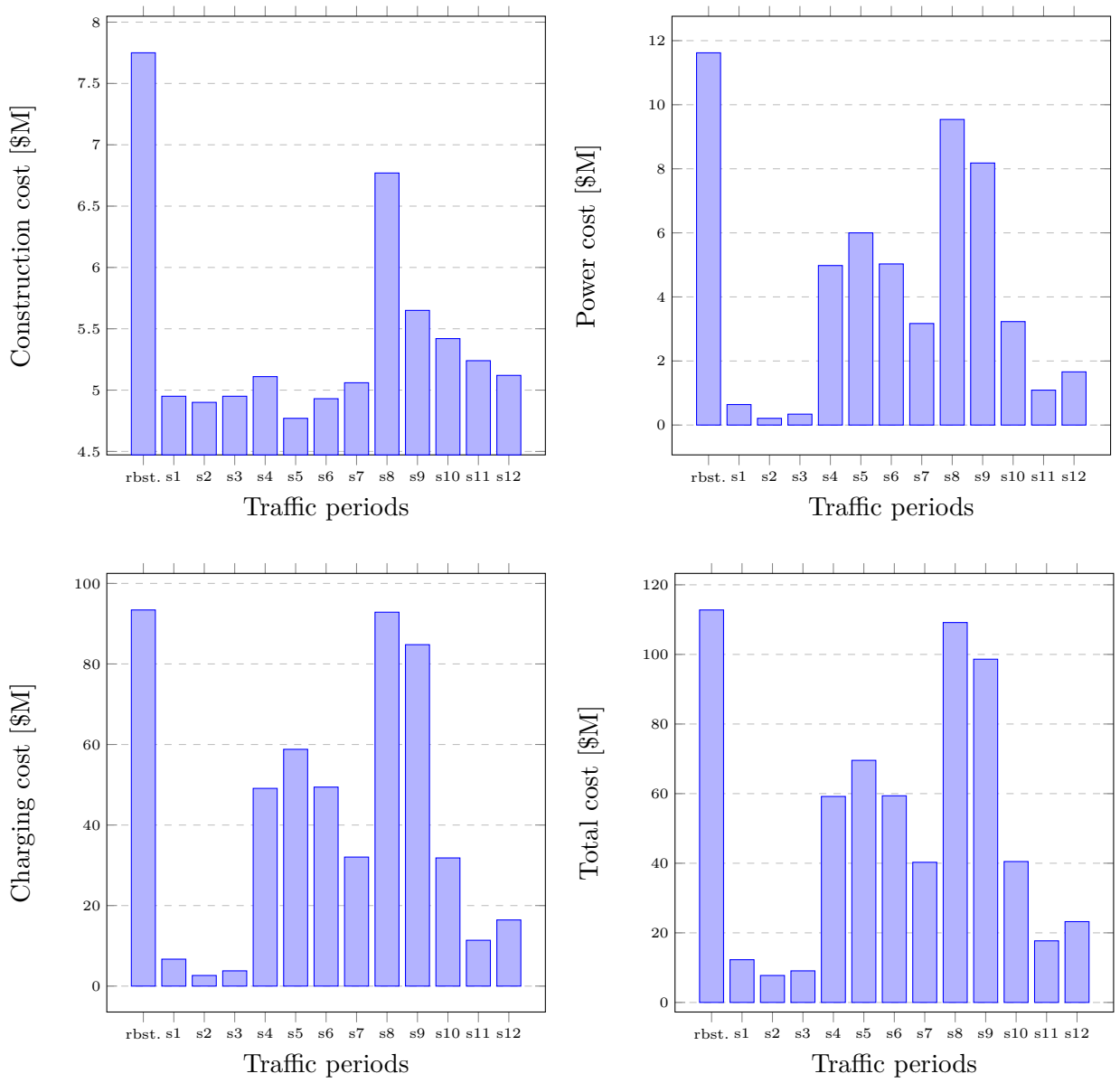

Figure 4.8: Cost comparison between the robust solution and the individual solutions under each traffic period

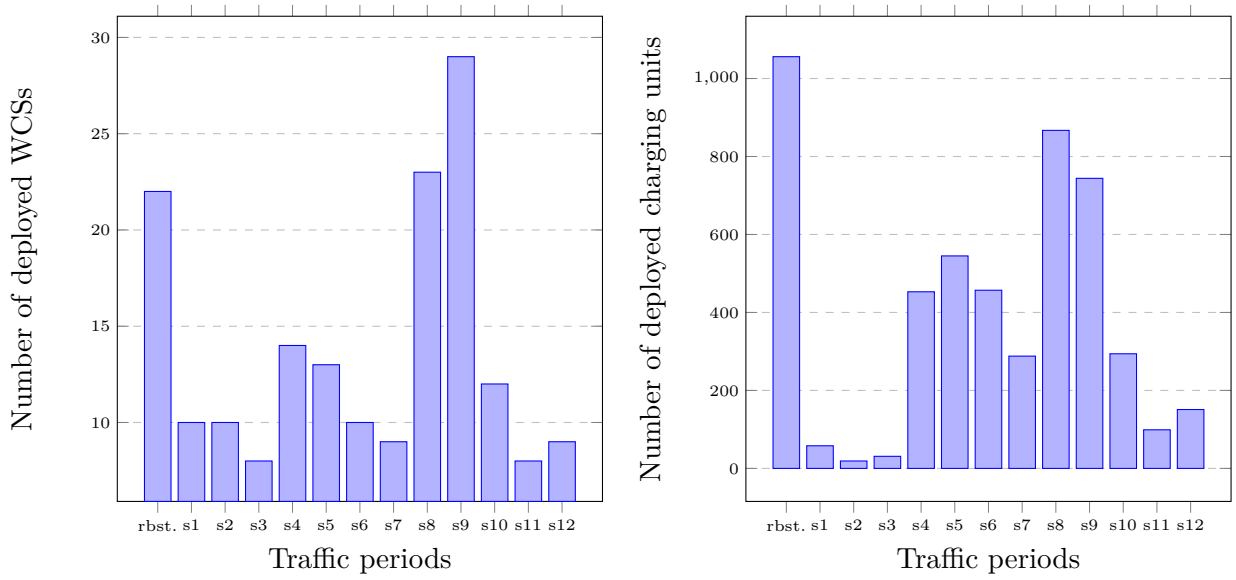

Figure 4.9: Number of deployed WCSs and deployed charging units in the robust solution vs. the individual solutions under each traffic period

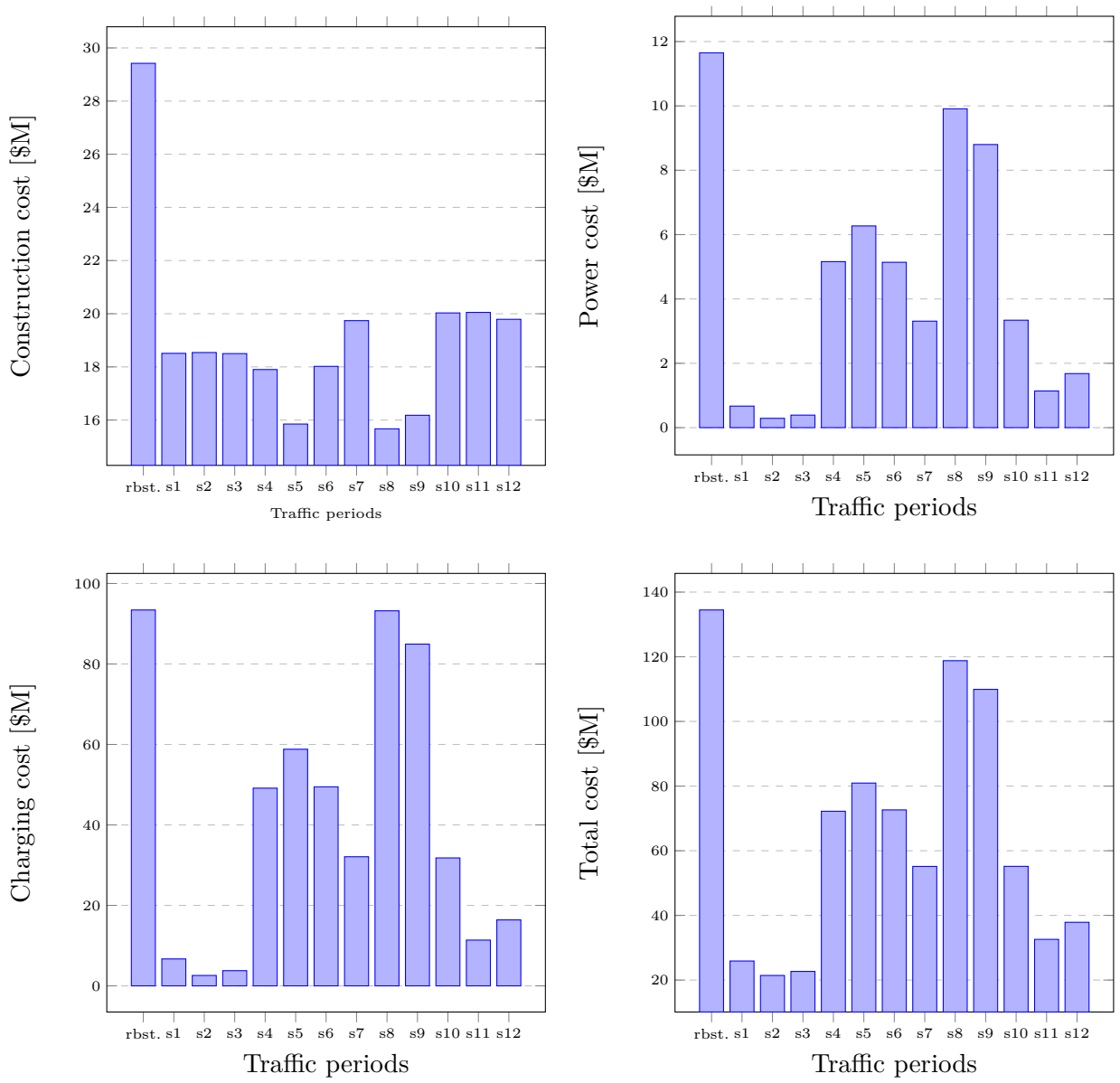

Figure 4.10: Cost comparison between the robust solution and the individual solutions under each traffic period

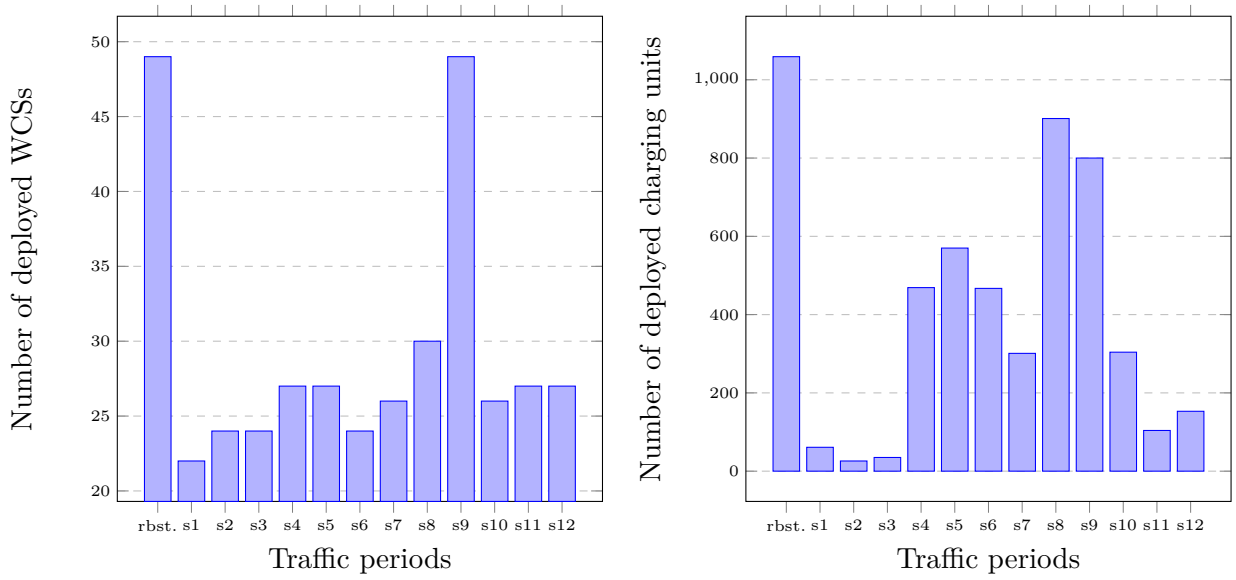

Figure 4.11: Number of deployed WCSs and deployed charging units in the robust solution vs. the individual solutions under each traffic period

Chapter 5

UTILIZING WIRELESS CHARGING OF ELECTRIC VEHICLES TO IMPROVE TRAFFIC ASSIGNMENTS IN CONGESTED NETWORKS

5.1. Introduction

Traffic congestion remains to be a serious threat to economic prosperity and quality of life in urban areas. A recent study estimated the cost of congestion across 25 major cities in the U.S. to reach $480 billion over the next decade [51]. Lost time and wasted fuel are major components of this cost. From a transportation planning point of view, congestion can be reduced via an efficient utilization of the road network which can only be achieved if travelers cooperate with one another. However, acting on self-interests, travelers select their routes in a way that minimizes their individual travel times under the traffic condition. According to Wardrop's first principle, this behavior leads the road network into a state of user equilibrium (UE) where travel times on all used routes between a certain origin-destination pair are equal [63]. Nevertheless, from a system perspective, UE does not necessarily represent the most efficient utilization of the road network. That is, the traffic assignment that minimizes the total travel time in the system usually differs from UE, and is referred to as the system optimal (SO) traffic assignment. In that sense, UE is considered to be a "selfish" optimal assignment, while SO is the socially optimal one. The difference between the two traffic assignments (UE and SO) is best illustrated in the well known Braess Paradox [7] [8].

To shift traffic flows from UE toward SO, traffic planners may encourage traffic redistribution by imposing tolls on certain road segments. The imposed tolls disturb the existing UE assignment as they motivate a portion of users to change their routes. The principle of toll pricing dictates that an optimal tolling policy is designed such that the tolled UE traffic assignment is an un-tolled system optimal [3]. Alternatively, traffic planners can encourage a

portion of travelers to change their routing behavior by offering incentives as "negative tolls." These incentives can include cash, store credit, or HOV (high-occupancy vehicle) passes [38].

For EV drivers, an opportunity to recharge while traveling could be viewed as a great incentive as it helps them reduce their range anxiety. Therefore, a route that offers wireless charging might seem more attractive than another route with a similar (or even shorter) travel time but does not offer the same service. This "attractiveness" of electrified road segments could be viewed as a negative toll and can be utilized to influence the traffic flows in congested networks. Motivated by this idea, we propose the concept of utilizing wireless charging stations (WCS) as a traffic redistribution tool to influence the travel behavior of EV drivers in an effort to achieve system optimality. Specifically, in contrast to our approach in the previous chapters, which maintains the UE traffic assignment, in this chapter, we study a deployment plan of WCSs that does disturb UE and induce the traffic flows to shift toward SO. To that end, in what follows we propose a mathematical model to optimize the deployment plan of WCSs with the objective of minimizing the total travel time in the traffic network.

The rest of this chapter is organized as follows: In Section 5.2, we present the formulations of the traffic assignment models including the multiclass UE and SO. In Section 5.3, we provide the definition and formulation of the problem of interest. In Section 5.4 we illustrate the applicability of the proposed approach on the famous Braess Network. In Section 5.5 we provide another example to illustrate our approach by testing the proposed model on Nguyen-Dupuis network.

5.2. Definitions and Background

To set the stage for our problem definition, we start by presenting the formulations of two traffic assignment models including UE and SO. We consider a directed graph $\mathcal{G}(\mathcal{N}, \mathcal{A})$ representing a traffic network with $\mathcal{N}$ representing the set of nodes and $\mathcal{A}$ representing the set of arcs. For a better representation of the real life application, we consider two classes of vehicles traveling in a traffic network: conventional vehicles (CVs), and electric vehicles

(EVs). We now introduce the following notations.

Sets:

$\mathcal{A}$ set of arcs, $a \in \mathcal{A}$

$\mathcal{Q}$ set of all OD-pairs within the network, $q \in \mathcal{Q}$

$\mathcal{R}_q$ set of routes connecting a certain OD-pair q, $r \in \mathcal{R}_q$

$\mathcal{K}$ set of vehicle classes, $k \in \mathcal{K}$

Parameters:

d_q^k travel demands of class $k \in \mathcal{K}$ between OD pair $q \in \mathcal{Q}$

δ_a^r an indicator with value of one if arc a is part of route r, 0 otherwise, $a \in \mathcal{A}$, $r \in \mathcal{R}_q$, $q \in \mathcal{Q}$

Decision Variables:

v_a^k traffic flow of class $k \in \mathcal{K}$ on arc $a \in \mathcal{A}$

v_a traffic flow on arc $a \in \mathcal{A}$

t_a travel time on arc $a \in \mathcal{A}$

u_a^k disutility of on arc a for a vehicle of class k, $a \in \mathcal{A}$, $k \in \mathcal{K}$

f_r^k traffic flow of class $k \in \mathcal{K}$ on route $r \in \mathcal{R}_q$, $q \in \mathcal{Q}$

u_r^k disutility of route r for a vehicle of class k, $r \in \mathcal{R}_q$, $q \in \mathcal{Q}$, $k \in \mathcal{K}$

5.2.1. User Equilibrium (UE)

According to Wardrop [63], if drivers are completely aware of the current traffic condition, they will act on their self interest and select a route that will minimize their individual travel disutility. Such behavior leads the traffic network into a steady-state of UE where no driver

can improve her travel disutility by changing her route. Wardrop [63] describes this steady-state, between each OD-pair in the network, in his first principle which reads:

> The journey times on all routes actually used are equal, and less than those which would be experienced by a single vehicle on any unused route.

Let travel times define travel disutilities on arcs. To handle the two classes of vehicles (CVs and EVs), we consider a multiclass UE formulation as introduced by [46]. Given the above notations, the time-dependent multiclass user equilibrium formulation is given as

$$\sum_{r \in \mathcal{R}_q} f_r^k = d_q^k \qquad \forall\, q \in \mathcal{Q},\ k \in \mathcal{K} \tag{5.1}$$

$$v_a^k = \sum_{q \in \mathcal{Q}} \sum_{r \in \mathcal{R}_q} \delta_a^r\, f_r^k \qquad \forall\, a \in \mathcal{A},\ k \in \mathcal{K} \tag{5.2}$$

$$v_a = \sum_{k \in \mathcal{K}} v_a^k \qquad \forall\, a \in \mathcal{A} \tag{5.3}$$

$$t_a = f(v_a) \qquad \forall\, a \in \mathcal{A} \tag{5.4}$$

$$u_r^k = \sum_{a \in \mathcal{A}} \delta_a^r\, t_a \qquad \forall\, r \in \mathcal{R}_q,\ q \in \mathcal{Q},\ k \in \mathcal{K} \tag{5.5}$$

$$u_r^k \begin{cases} = \lambda_r^k & \textbf{if } f_r^k > 0 \\ \leq \lambda_r^k & \textbf{if } f_r^k = 0 \end{cases} \qquad \forall\, r \in \mathcal{R}_q,\ q \in \mathcal{Q},\ k \in \mathcal{K} \tag{5.6}$$

$$v_a^k,\ v_a,\ f_r^k,\ t_a,\ u_r^k \geq 0 \qquad \forall\, a \in \mathcal{A},\ r \in \mathcal{R}_q,\ q \in \mathcal{Q},\ k \in \mathcal{K} \tag{5.7}$$

The first three sets of constraints are flow conservation constraints. Constraints (5.1) indicate that the traffic demands of each class of vehicles between each OD pair is equal to the sum of the flows of that class on all the routes connecting the OD pair. Constraints (5.2) dictate that the traffic flow of each class of vehicles on each arc is equal to the sum of the flows of that class on each route that contains that arc. Constraints (5.3) indicate that the total traffic flow on each arc is equal to the sum of the flows of all classes of vehicles on that arc. Constraints (5.4) represent the travel time function associated with each arc. Constraints (5.5) state that the travel disutility of each route is equal to the summation of the travel

times of all the arcs that form the route. Constraints (5.6) are the multiclass equilibrium constraint following Wardrop's first principle, stating that all used routes between an OD pair have equal and minimal travel disutility. Finally, constraints (5.7) are the non-negativity constraints.

5.2.2. System Optimal (SO)

SO traffic assignment aims to minimize congestion in the traffic network. Therefore, in contrast to UE, SO assignment minimizes the travel time for the whole system rather than the individual travel times for drivers. This traffic assignment is based on Wardrop's second principle which describes SO as the traffic assignment where

> The average journey time is a minimum [63].

Reaching the state of SO can be achieved if drivers cooperate with one another. The mathematical formulation for SO is given as

$$\text{Minimize} \quad \sum_{a \in \mathcal{A}} v_a \, t_a \tag{5.8}$$

$$\text{subject to (5.1) - (5.5), and (5.7)}$$

Note that (5.6) is not a part of the SO formulation since SO is not associated with equilibrium condition.

SO is not behaviorally realistic. However, understanding SO helps traffic planning entities to design the appropriate traffic management tools and regulations that could potentially shift the traffic flows from UE toward SO, and therefore minimize congestion.

5.3. Problem Definition and Formulation

We consider a traffic network, as defined above, with conventional vehicles and electric vehicles, i.e., $\mathcal{K} = \{CV, EV\}$. For simplicity and without loss of generality, all EVs in the network are assumed to be capable of wireless charging. For CVs, we let travel times define

travel disutilities of arcs. By contrast, for EVs, the availability of a WCS on a certain arc lessens the arc's disutility. Therefore, we define a non-positive parameter α_{EV} to represent the attractiveness of a WCS for EVs, measured in time value (TV). Accordingly, we define travel disutility for EVs, on electrified arcs, by the summation of travel time and parameter α_{EV}. Since α_{EV} is non-positive by definition, locating a WCS on a given arc can only decrease the arc's disutility for EVs. On the other hand, travel disutilities of un-electrified arcs are considered to be equal to the travel times of these arcs. Clearly, for CVs, the attractiveness of a WCS, α_{CV}, is equal to zero.

Based on the above definition of travel disutility, the deployment of WCSs in the network will adjust travel disutilities of arcs for EVs. Therefore, motivated by the attractiveness of the deployed infrastructure, EV drivers will select new routes to minimize their adjusted individual travel disutilities. That is, the infrastructure deployment plan could potentially disturb the existing UE and lead to a new UE based on the new disutilities vector[1]. Our objective is to determine the WCSs deployment plan that disturbs the existing UE in such a way that new UE assignment is shifted toward SO. Specifically, we optimize the number and the locations of WCSs in the network in such a way that minimizes the total travel time (system time) associated with the new UE which results as a response to the deployment of the WCSs.

In contrast to the toll pricing problem where the flows vector is fixed (set equal to SO flows vector) and the tolls are optimized to achieve the fixed flows, in this framework we optimize the flow and the locations of WCSs based on presumed values of the attractiveness of WCS (negative toll). To that end, we introduce a binary variable x_a equal to one if a WCS is installed on arc a, zero otherwise. Accordingly, our problem can be formulated as follows:

[1]unless all used routes in the network are served as discussed in the previous two chapters.

$$\text{Minimize} \quad \sum_{a \in \mathcal{A}} v_a \, t_a \tag{5.9}$$

subject to

$$\sum_{r \in \mathcal{R}_q} f_r^k = d_q^k \qquad \forall\, q \in \mathcal{Q},\, k \in \mathcal{K} \tag{5.10}$$

$$v_a^k = \sum_{q \in \mathcal{Q}} \sum_{r \in \mathcal{R}_q} \delta_a^r \, f_r^k \qquad \forall\, a \in \mathcal{A},\, k \in \mathcal{K} \tag{5.11}$$

$$v_a = \sum_{k \in \mathcal{K}} v_a^k \qquad \forall\, a \in \mathcal{A} \tag{5.12}$$

$$t_a = f(v_a) \qquad \forall\, a \in \mathcal{A} \tag{5.13}$$

$$u_a^k = t_a + \alpha_k \, x_a \qquad \forall\, a \in \mathcal{A}\, k \in \mathcal{K} \tag{5.14}$$

$$u_r^k = \sum_{a \in \mathcal{A}} \delta_a^r \, u_a^k \qquad \forall\, r \in \mathcal{R}_q,\, q \in \mathcal{Q},\, k \in \mathcal{K} \tag{5.15}$$

$$u_r^k \begin{cases} = \lambda_r^k & \textbf{if } f_r^k > 0 \\ \leq \lambda_r^k & \textbf{if } f_r^k = 0 \end{cases} \qquad \forall\, r \in \mathcal{R}_q,\, q \in \mathcal{Q},\, k \in \mathcal{K} \tag{5.16}$$

$$v_a^k,\, v_a,\, f_r^k,\, t_a,\, u_a^k \, u_r^k \geq 0,\, x_a \in \{0, 1\} \qquad \forall\, a \in \mathcal{A},\, r \in \mathcal{R}_q,\, q \in \mathcal{Q}, k \in \mathcal{K} \tag{5.17}$$

The objective function (5.9) minimizes the total travel time in the system. Constraints (5.10), (5.11), and (5.12) are the flow conservation constraints as defined in 5.2.1. Constraints (5.13) are the travel time function constraints. Constraints (5.14) are the arc disutility constraints for each class of vehicles. Since α_{EV} is non-positive by definition, triggering the binary variable x_a (installing a WCS on arc a) reduces the disutility of the arc for EVs by α_{EV} units of time. Constraints (5.15) are the route disutility constraint for each class of vehicles. Constraints (5.16) are the multiclass UE condition as defined in 5.2.1. Finally, Constraints (5.17) provide the structural requirements of the model.

The logic of our formulation can be described as follows. The objective of the model is

to regulate the traffic in the network in a way that shifts the traffic assignment form UE toward SO. Because our goal is to get as close as possible to SO, we adopt the objective function associated with SO, i.e., minimizing the total travel time in the system. The flows conservation constraints are required to obtain feasible assignments. The UE constraint is adopted because the traffic will regulate itself, after the WCS deployment, to reach a new UE. The key in our model, is constraint (5.14). Specifically, the model will trigger variables x_a to reduce the disutilities of some arcs for EVs. As a response to the reduction in traffic disutility for EVs, a new UE must emerge in order for the UE constraint (5.16) to hold. And since the disutilities u_a, the volumes v_a, and the travel times t_a are interconnected via constraints (5.13) and (5.14), triggering variables x_{ij} leads to adjustments in variables v_a and variables t_a. Thus, the model uses variables x_{ij} as regulates to adjust the values of variables v_a and variables t_a in order to minimize the value of the objective function.

Note that the model formulation is nonlinear due to the nonlinear objective (5.9), and the UE constraint (5.16). Furthermore, depending on the netowrk under study, the travel time function (5.13) could also be nonlinear as we assume in a later example.

In what follows, we put the model to work and illustrate its applicability vie two examples.

5.4. Illustrating Example - Single OD Network

To illustrate the proposed approach, we apply our model on the well known Braess network (Figure 5.1). The network contains four nodes and five arcs. A hundred travelers are assumed to be traveling from node A to node D. The labels on the arcs represent the assumed travel time functions adopted from [15]. The optimal flows and travel times associated with both UE and SO are presented in Tables 5.1 and 5.2. As shown in the Tables, UE assigns 25 vehicles to route ABD, 50 vehicles to route ABCD, and 25 vehicles to route ACD. As a result of this assignment, the travel time on each route is equal to 3.75 time units. The total travel time in the system is equal to $(75 \times 1.75) + (25 \times 2) + (50 \times 0.25) + (25 \times 2) + (75 \times 1.75) = 375$ time units. By contrast, SO assigns 50 vehicles to route ABD and 50 vehicles to route ACD. No vehicle is assigned to route ABCD. As a result, the

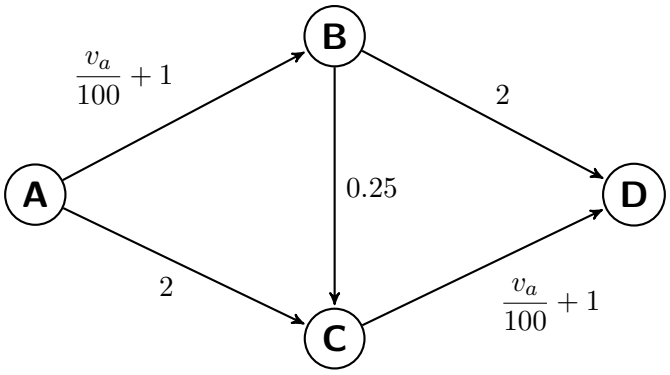

Figure 5.1: Braess network

travel times on the used routes drop to 3.5 time units, and the total travel time in the system drops to $(50 \times 1.5) + (50 \times 2) + (0 \times 0.25) + (50 \times 2) + (50 \times 1.5) = 350$ time units.

Table 5.1: Routes flows and travel times under UE and SO - Braess network

	User Equilibrium		System Optimal	
	f_r	t_r	f_r	t_r
ABD	25	3.75	50	3.5
ABCD	50	3.75	0	3.25
ACD	25	3.75	50	3.5

Table 5.2: Arcs flows and travel times under UE and SO - Braess network

	User Equilibrium		System Optimal	
	v_a	t_a	v_a	t_a
AB	75	1.75	50	1.5
AC	25	2	50	2
BC	50	0.25	0	0.25
BD	25	2	50	2
CD	75	1.75	50	1.5

In this example, we assume an electric vehicle penetration rate (EVPR) of 50%, i.e., $d_{AD}^{EV} = d_{AD}^{CV} = 50$. We further assume that $\alpha_{EV} = -0.25$. We use COUENNE (which is a

solver designed to solve MINLPs with nonlinear objective function) to solve our proposed model considering the network at hand [5]. The solution is depicted in Figure 5.2 where the dashed red arc represents a WCS. The flows, travel times, and disutilities associated with the solution are presented in Tables 5.3 and 5.4.

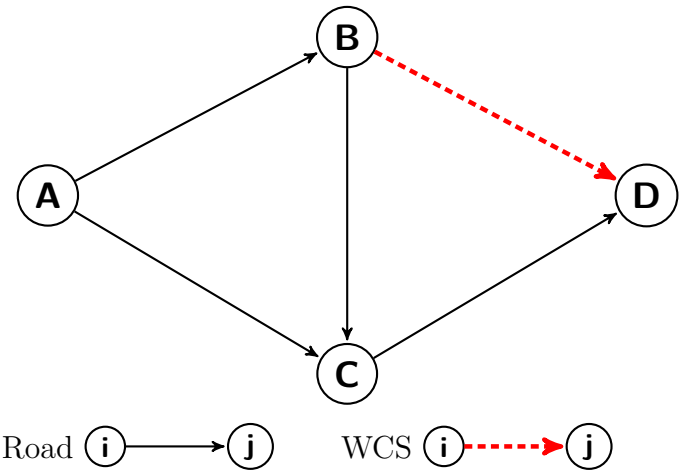

Figure 5.2: WCS deployment plan - Braess network

Table 5.3: Routes flows, travel times, and disutilities under the WCS deployment plan

	f_r^{EV}	f_r^{CV}	f_r	t_r	u_r^{EV}	u_r^{CV}
ABD	50	0	50	3.75	3.5	3.75
ABCD	0	25	25	3.5	3.5	3.5
ACD	0	25	25	3.5	3.5	3.5

Table 5.4: Arcs flows, travel times, and disutilities under the WCS deployment plan

	v_a^{EV}	v_a^{CV}	v_a	ta	u_a^{EV}	u_a^{CV}
AB	50	25	75	1.75	1.75	1.75
AC	0	25	25	2	2	2
BC	0	25	25	0.25	0.25	0.25
BD	50	0	50	2	1.75	2
CD	0	50	50	1.5	1.5	1.5

As shown in the tables, the WCS installed on arc BD attracted the EV population of the network to route ABD. The remaining vehicles split equally between routes ABCD and ACD. Clearly, the UE condition holds for each class of vehicles; for EVs the disutility of the used route ABD is equal to the disutilities of the other two routes, and for CVs the disutilities of the used routes ABCD and ACD are equal to each other, and are less than the disutility of the unused route ABD.

By comparing the routes' flows (and travel times) in Table 5.3 to their counterparts in Table 5.1 we find that the flows (and travel times) associated with the new assignment fall between the flows (and travel times) associated with the original UE (before the deployment of the WCS) and their counterparts associated with SO. The same can be concluded about the arcs' flows and travel times by comparing Table 5.4 and Table 5.2. Furthermore, the system travel time associated with the new assignment is equal to $(75 \times 1.75) + (25 \times 2) + (25 \times 0.25) + (50 \times 2) + (50 \times 1.5) = 362.5$ time units, which is between the system time associated with the original UE the system time associated with SO. Therefore, we conclude that the WCSs deployment plan shifted the traffic assignment from UE toward SO, and improved the system travel time by producing a new UE that could be viewed as a "hybrid assignment" between SO and the original UE.

Since the WCSs deployment plan and the associated UE depend on parameter α_{EV} and on the number of EVs in the traffic network (determined by EVPR), reaching SO can only be achieved if each of these two parameters crosses a certain threshold. To form a better understanding of the effect of these two parameters on the performance of our proposed approach, in the next section, we provide a sensitivity analysis considering different values of α_{EV} and EVPR.

5.4.1. Evaluating the Potential Impact of Optimal WCS Deployment on Traffic Assignment

To better assess the potential impact of the proposed WCS deployment approach on the traffic assignment, it is essential to understand the effects of parameters α_{EV} and EVPR on the new traffic assignment. To that end, we run the proposed model on the above example

network using different values of parameters α_{EV} and EVPR. Specifically, we assume 16 different values for α_{EV} ranging from 0 to -0.375 with decrements of 0.025. We further assume 5 values for EVPR ranging between 20% and 100% with increments of 20%. We then solve the proposed model 80 times considering all combinations of the two parameters. The experiment's results are depicted in Figure 5.3.

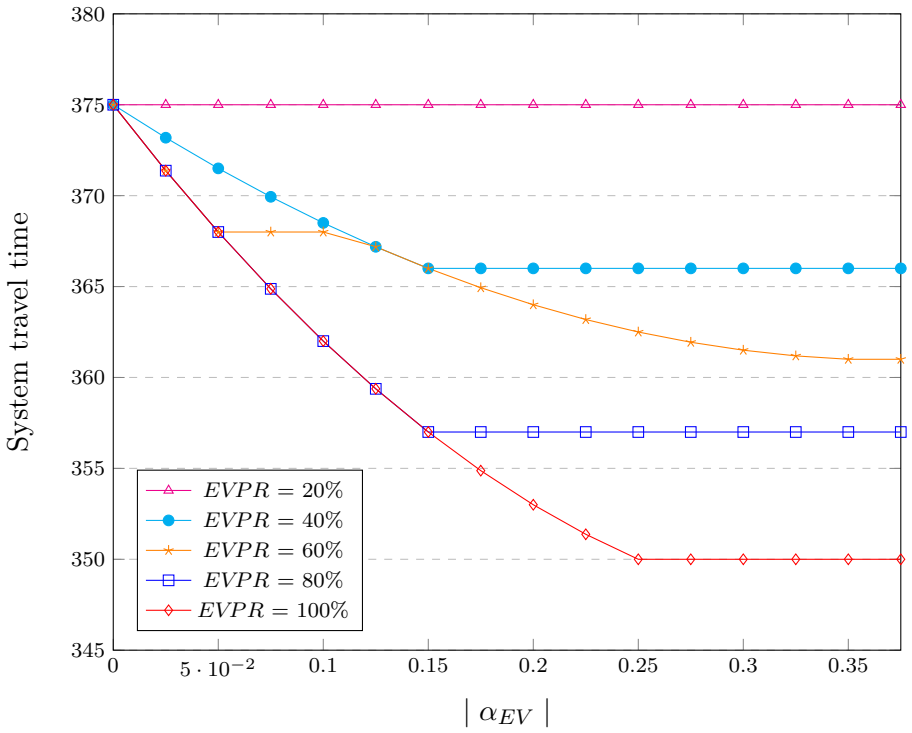

Figure 5.3: Experiment results - Braess network

For each assumed value of EVPR, a curve represents the relationship between the absolute value of parameter α_{EV} and the new system travel time. The results show that when EVPR is 20% (the pink curve), the system travel time remains unchanged no matter what the value of α_{EV} is. This is because at this low EVPR, the EV population in the network is not large enough to affect the UE assignment. For all other values of EVPR, the higher the absolute value of α_{EV} is, the shorter the system travel time.This is because when WCSs are considered more attractive for EV drivers, the deployment of WCSs can cause larger impacts on the traffic assignment which can be further induced toward SO.

Similarly, the results show that the higher EVPR is, the closer the traffic assignment can

get to SO; in this example, when EVPR is 100%, the traffic assignment can be completely shifted to SO and the system travel times can drop to 350.

To summarize, the results show a dependency between the potential impact of WCS deployment on traffic assignment and the two parameters α_{EV} and EVPR; in this example, the more attractive WCSs are considered by EV drivers, and the larger the population of EVs in the network is, the higher the potential impact of WCS deployment on traffic assignment.

5.5. Illustrating Example - Multi-OD Network

To form a deeper understanding of the effect of both α_{EV} and EVPR on the system travel time, we further test our model on the Nguyen-Dupuis network - an extensively used network in the transportation literature (Figure 5.4).

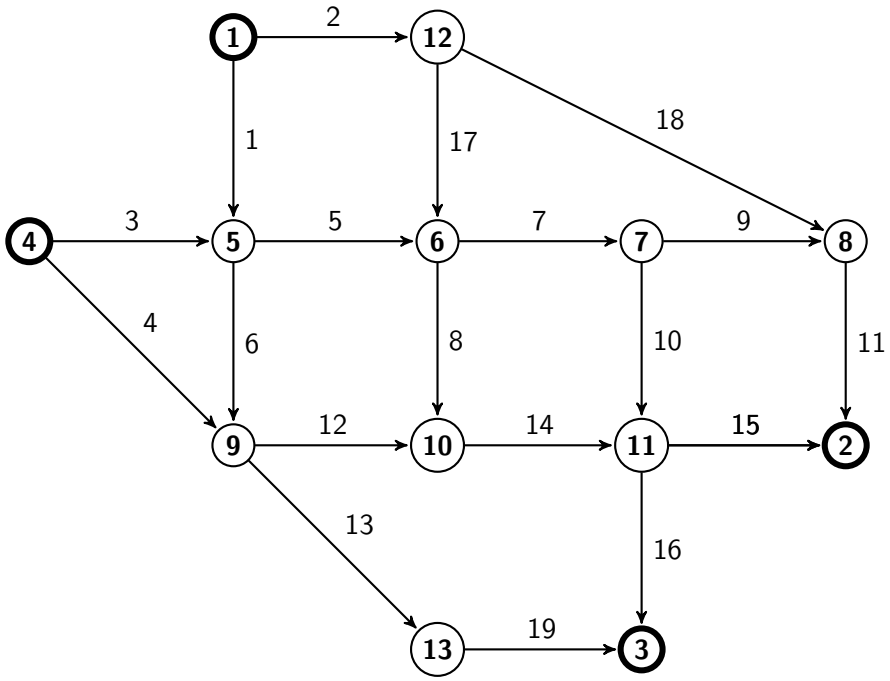

Figure 5.4: Nguyen-Dupuis network

We consider two OD pairs including (1-3) and (4-2). We further consider an asymmetric affine travel time function, adopted from Nguyen and Dupuis [48], of the form: $t_a = c_a\, v_a + b_a$, where c_a and b_a are both input parameters. The values of parameters c_a and b_a are provided in Table 5.5. The travel demands are given in Table 5.6. The optimal flows and travel times

associated with UE and SO are given in Tables 5.7 and 5.8.

Table 5.5: Arcs and their associated parameters - Nguyen-Dupuis network

arc	origin	destination	c_a	b_a
1	1	5	0.0125	7
2	1	12	0.01	9
3	4	5	0.01	9
4	4	9	0.005	12
5	5	6	0.0075	3
6	5	9	0.0075	9
7	6	7	0.0125	5
8	6	10	0.005	13
9	7	8	0.0125	5
10	7	11	0.0125	9
11	8	2	0.0125	9
12	9	10	0.005	10
13	9	13	0.005	9
14	10	11	0.0025	6
15	11	2	0.005	9
16	11	3	0.01	8
17	12	6	0.0025	7
18	12	8	0.01	14
19	13	3	0.01	11

Table 5.6: Travel demands - Nguyen-Dupuis network

OD	travel demands
(1-3)	80
(4-2)	60

We assume 7 different values for parameter α_{EV} ranging from 0 to -1.5 with decrements of 0.25. We further consider 5 values for EVPR ranging between 20% and 100% with increments

Table 5.7: Arcs flows and travel times under UE and SO - Nguyen-Dupuis network

	User Equilibrium		System Optimal	
arc	v_a	t_a	v_a	t_a
1	80.00	8.00	80.00	8.00
2	0.00	9.00	0.00	9.00
3	60.00	9.60	43.42	9.43
4	0.00	12.00	16.58	12.08
5	130.77	3.98	88.52	3.66
6	9.23	9.07	34.90	9.26
7	130.77	6.63	88.52	6.11
8	0.00	13.00	0.00	13.00
9	60.00	5.75	43.42	5.54
10	70.77	9.88	45.10	9.56
11	60.00	9.75	43.42	9.54
12	0.00	10.00	16.58	10.08
13	9.23	9.05	34.90	9.17
14	0.00	6.00	16.58	6.04
15	0.00	9.00	16.58	9.08
16	70.77	8.71	45.10	8.45
17	0.00	7.00	0.00	7.00
18	0.00	14.00	0.00	14.00
19	9.23	11.09	34.90	11.35

Table 5.8: Routes flows and travel times under UE and SO - Nguyen-Dupuis network

		User Equilibrium		System Optimal	
OD pair	route	f_r	t_r	f_r	t_r
1-3	1-12-6-7-11-3	0.00	41.23	0.00	40.12
1-3	1-12-6-10-11-3	0.00	43.71	0.00	43.49
1-3	1-5-6-7-11-3	**70.77**	**37.21**	**45.10**	**35.79**
1-3	1-5-6-10-11-3	0.00	39.69	0.00	39.16
1-3	1-5-9-10-11-3	0.00	41.78	0.00	41.84
1-3	1-5-9-13-3	**9.23**	**37.21**	**34.90**	**37.79**
4-2	4-5-6-7-8-2	**60.00**	**35.72**	**43.42**	**34.29**
4-2	4-5-6-7-11-2	0.00	39.10	0.00	37.85
4-2	4-5-6-10-11-2	0.00	41.58	0.00	41.22
4-2	4-5-9-10-11-2	0.00	43.67	0.00	43.90
4-2	4-9-10-11-2	0.00	37.00	**16.58**	**37.29**

of 20%. We solve the model while considering all combinations of the two parameters.

The results are illustrated by the curves in Figure 5.5, where each curve represents the relationship between α_{EV} and the system travel time under a specific value of EVPR. The results indicate that the optimal WCS deployments are effective in shifting the traffic assignment from UE toward SO, therefore reducing the system travel time, even under a relatively small EVPR value (i.e., EVPR = 20%).

However, unlike the previous single-OD example where the system travel time curves were always non-increasing, in this case, an increase in the absolute value of α_{EV}, or in the value of EVPR, above certain points could lead to a slight fluctuation in the system travel time. An example of this could be found by examining the behavior of the system travel time curve under the EVPR value of 100% (i.e., the red solid curve in Figure 5.5). Specifically, this curve shows that the system travel time decreases (as the traffic responds to the WCS deployment) by the increase of the absolute value of α_{EV} until reaching SO at $\mid \alpha_{EV} \mid = 1$. After that point, an increase in the value of $\mid \alpha_{EV} \mid$ to 1.25 causes an increase in the system travel time. We observe similar behaviors of the system travel time curves under other values

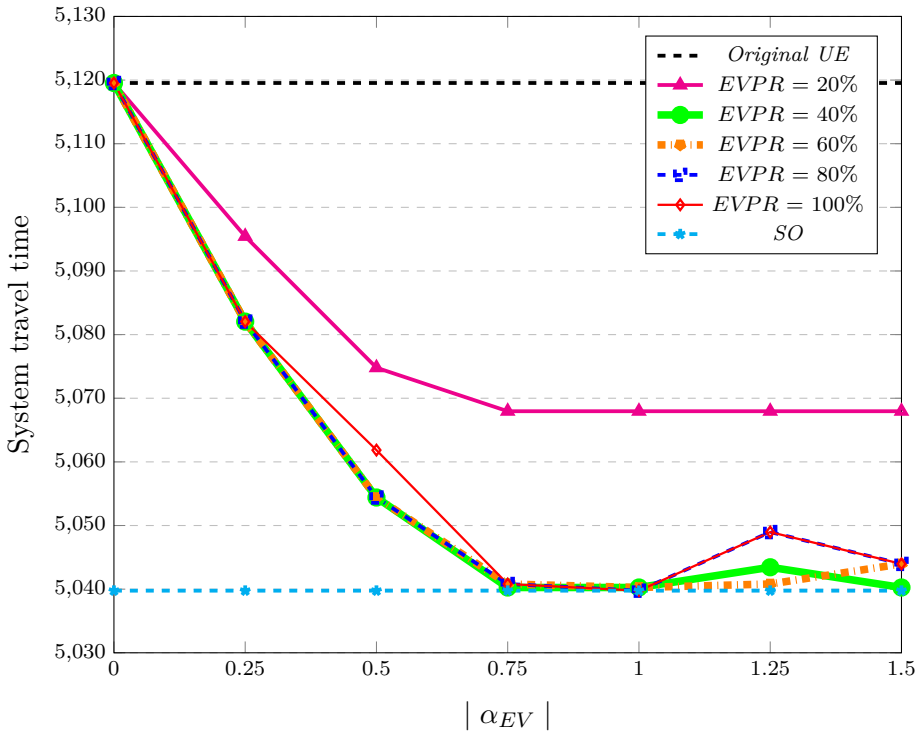

Figure 5.5: Experiment results - Nguyen-Dupuis network

of EVPR including 80% and 40%. We describe this phenomenon in what follows.

Consider the optimal WCS deployment plan given in Figure 5.6 which is obtained by solving the proposed model using the values of $\alpha_{EV} = -1$ and EVPR = 100%.

This WCS deployment adjusts the travel disutilities in the network causing, as a response to this adjustment, 25.67 EVs to change route from 1-5-6-7-11-3 to 1-5-9-13-3, and another 16.58 EVs to switch route from 4-5-6-7-8-2 to 4-9-10-11-2. As a result, the flows in the network reach a new equilibrium as described in Tables 5.9 and 5.10.

By examining the new UE flows in Table 5.10 we find them identical to the SO flows presented in Table 5.7. That is, as a response to the optimal WCS deployment, the traffic assignment shifted completely from UE to SO, and the new system travel time associated with the optimal WCS deployment is 5039.76.

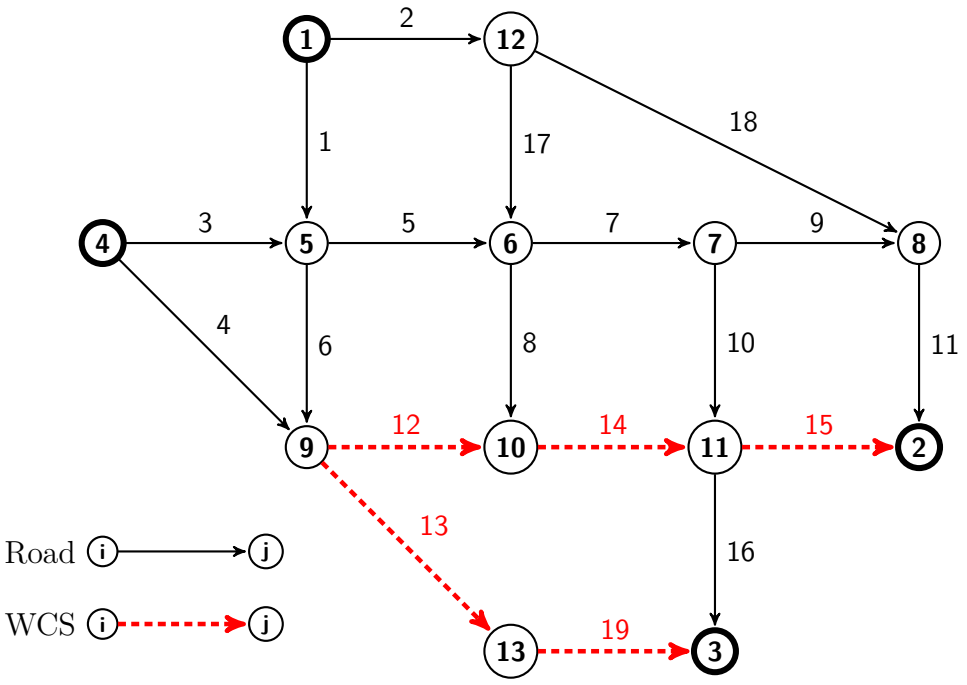

Figure 5.6: Optimal WCS deployment plan - Nguyen-Dupuis network

Table 5.9: Routes flows, travel times, and disutilities under the new UE which emerges as a response to the optimal WCS deployment under EVPR = 100% and $\alpha_{EV} = -1$

		User Equilibrium		
OD pair	route	f_r	t_r	u_r^{EV}
1-3	1-12-6-7-11-3	0.00	40.12	40.12
1-3	1-12-6-10-11-3	0.00	43.49	42.49
1-3	1-5-6-7-11-3	**45.10**	**35.79**	**35.79**
1-3	1-5-6-10-11-3	0.00	39.16	38.16
1-3	1-5-9-10-11-3	0.00	41.84	39.84
1-3	1-5-9-13-3	**34.90**	**37.79**	**35.79**
4-2	4-5-6-7-8-2	**43.42**	**34.29**	**34.29**
4-2	4-5-6-7-11-2	0.00	37.85	36.85
4-2	4-5-6-10-11-2	0.00	41.22	39.22
4-2	4-5-9-10-11-2	0.00	43.90	40.90
4-2	4-9-10-11-2	**16.58**	**37.29**	**34.29**

Table 5.10: Arcs flows, travel times, and disutilities under the new UE which emerges as a response to the optimal WCS deployment under EVPR = 100% and $\alpha_{EV} = -1$

	User Equilibrium		
arc	v_a	t_a	u_a
1	80.00	8.00	8.00
2	0.00	9.00	9.00
3	43.42	9.43	9.43
4	16.58	12.08	12.08
5	88.52	3.66	3.66
6	34.90	9.26	9.26
7	88.52	6.11	6.11
8	0.00	13.00	13.00
9	43.42	5.54	5.54
10	45.10	9.56	9.56
11	43.42	9.54	9.54
12	16.58	10.08	9.08
13	34.90	9.17	8.17
14	16.58	6.04	5.04
15	16.58	9.08	8.08
16	45.10	8.45	8.45
17	0.00	7.00	7.00
18	0.00	14.00	14.00
19	34.90	11.35	10.35

Now consider solving the model again under $\alpha_{EV} = -1.25$. In this case, the optimal deployment plan is found to be identical to the one obtained under $\alpha_{EV} = -1$ (i.e., the deployment plan depicted in Figure 5.6). Tables 5.11 and 5.12 provide the flows, travel times, and disutilities associated with the new UE which emerges as a response to the optimal deployment plan under $\alpha_{EV} = -1.25$.

Since $\mid \alpha_{EV} \mid$ is higher in this case (i.e., WCS is more attractive for EVs), each WCS attracts more EVs than the case where $\alpha_{EV} = -1$. Specifically, 4.93 *additional* EVs change

route from 1-5-6-7-11-3 to 1-5-9-13-3, and another 8.99 EVs switch route from 4-5-6-7-8-2 to 4-9-10-11-2. This behavior creates congestion on the WCS hosting arcs, and therefore, drives the traffic assignment away from SO which is reached under $\alpha_{EV} = -1$. In this case, the new system travel time associated with the optimal WCS deployment is 5048.97 - slightly higher than the system travel time associated with SO (5039.76), but still, considerably lower then the system travel time associated with the original UE (5119.54).

Table 5.11: Arcs flows, travel times, and disutilities under the new UE which emerges as a response to the optimal WCS deployment under EVPR = 100% and $\alpha_{EV} = -1.25$

	User Equilibrium		
arc	v_a	t_a	u_a
1	80.00	8.00	8.00
2	0.00	9.00	9.00
3	34.43	9.34	9.34
4	25.57	12.13	12.13
5	74.61	3.56	3.56
6	39.83	9.30	9.30
7	74.61	5.93	5.93
8	0.00	13.00	13.00
9	34.43	5.43	5.43
10	40.17	9.50	9.50
11	34.43	9.43	9.43
12	25.57	10.13	8.88
13	39.83	9.20	7.95
14	25.57	6.06	4.81
15	25.57	9.13	7.88
16	40.17	8.40	8.40
17	0.00	7.00	7.00
18	0.00	14.00	14.00
19	39.83	11.40	10.15

Table 5.12: Routes flows, travel times, and disutilities under the new UE which emerges as a response to the optimal WCS deployment under EVPR = 100% and $\alpha_{EV} = -1.25$

		User Equilibrium		
OD pair	route	f_r	t_r	u_r^{EV}
1-3	1-12-6-7-11-3	0.00	39.84	39.84
1-3	1-12-6-10-11-3	0.00	43.47	42.22
1-3	1-5-6-7-11-3	**40.17**	**35.40**	**35.40**
1-3	1-5-6-10-11-3	0.00	39.03	37.78
1-3	1-5-9-10-11-3	0.00	41.89	39.39
1-3	1-5-9-13-3	**39.83**	**37.90**	**35.40**
4-2	4-5-6-7-8-2	**34.43**	**33.70**	**33.70**
4-2	4-5-6-7-11-2	0.00	37.47	36.22
4-2	4-5-6-10-11-2	0.00	41.10	38.60
4-2	4-5-9-10-11-2	0.00	43.96	40.21
4-2	4-9-10-11-2	**25.57**	**37.50**	**33.70**

It is important to note that regardless of the values of the input parameters, the new traffic assignment, that emerges as a response to the optimal WCS deployment, cannot be worse than the original UE. That is, the system travel time associated with the original UE is an upper bound to the problem at hand. This is because the proposed model does not impose any requirements for minimum WCS installation. Therefore, in the case where the WCS deployment can only disturb the traffic assignment in a way that would worsen the system travel time, then the model will not deploy any WCS in the network.

In summary, the results confirm the effectiveness of the opposed framework in shifting the traffic assignment from UE toward SO. The results also show that the attractiveness of WCS for EVs, and the EVPR in the network under study, should have significant values in order to achieve significant shifts in the traffic assignment. Furthermore, the results indicate that an increase in the absolute value of the attractiveness of WCS for EVs, until a certain point, helps in decreasing the system travel time. After a certain point, the system travel time could slightly fluctuate near the system travel time value associated with SO.

5.6. Concluding Remarks

This chapter introduces a new approach to plan the deployment of WCSs in traffic networks. The goal of this approach is to take advantage of the attractiveness of WCSs for EV drivers to influence their routing choices in an effort to reach system optimal traffic assignment.

For this purpose, a new mathematical model is proposed. The model locates WCSs in the network with the objective of minimizing the system time associated with the UE traffic assignment which emerges as a response to the WCSs deployment.

The applicability of the proposed model is first illustrated on the well known Braess network, and a sensitivity analysis is conducted. The results show that the optimal deployment plan produced by the model can potentially shift the traffic assignment in the network from UE toward SO. As a response to the optimal deployment plan, the traffic redistributes, causing a new UE to emerge. The new UE can be viewed as a "hybrid assignment" between the original UE and SO.

The results also show that the emerged hybrid assignment gets closer to SO when the EV population in the network is high and when WCSs are considered more attractive by EV drivers. We further found that reaching SO can only be achieved when the EV population in the network and the attractiveness of WCSs for EV drivers, each crosses a certain threshold.

The model is then tested on the multi-ODs Nguyen-Dupuis network, and a new sensitivity analysis is conducted. The results confirm the effectiveness of the proposed approach in shifting the traffic assignment from UE toward SO.

The results also provide a deeper understanding of the relationship between the attractiveness of WCS for EVs and the system travel time. Specifically, we find that an increase in the absolute value of the attractiveness of WCS for EVs is helpful, in improving the system travel time, until a certain point after which the system travel time begins to slightly fluctuate.

Chapter 6

CONCLUSIONS AND FUTURE DIRECTIONS

In this dissertation, we present three studies, each proposing a different framework to address the deployment of wireless charging stations in urban traffic networks.

In Chapter 3, we propose a single-period network design model to optimize the locations and power capacities of the wireless charging stations in effort to promote EV adoption. The objective of the proposed model is to minimize the deployment cost of the infrastructure and the usage cost for EV drivers while producing a network design that does not disturb the current traffic condition in the read network. To solve the large scale instances of this problem, we propose a Benders decomposition framework where we employ a combination of classical Benders cuts and combinatorial Benders cuts for improved algorithmic effectiveness. We further strengthen the proposed solution algorithm via utilizing different sets of surrogate constraints and an upper bound heuristic. The efficiency of the proposed algorithm is tested via an extensive computational experiment. We further conduct a case study using read network data from Chicago, IL, and we perform a sensitivity analysis to investigate the relationships between key technical parameters of the wireless charging system and the implementation cost of the wireless charging infrastructure.

In Chapter 4, we build on the study presented in Chapter 3 to propose a robust framework for the network design of wireless charging stations. The robust approach considers the variability of the traffic condition and aims to produce network designs that are feasible and cost-effective across the traffic conditions of all possible traffic periods. We provide examples illustrating the need for a robust solution and we show that the peak traffic periods can not be considered as bottlenecks when solving the problem of interest. We present a new robust formulation that handles multiple traffic periods, and we propose a straightened BD algorithm to solve the proposed model. We further propose four different algorithmic settings

for the proposed solution algorithm and we provide an extensive computational experiment to evaluate the effectiveness of each strengthening technique individually. We conduct a case study on real network data from Dallas, TX, illustrating the applicability of the robust approach in solving the problem of interest.

Finally, in Chapter 5 we present a new framework for the deployment of wireless charging stations with the aim of improving the traffic conditions in congested networks by taking advantage of the attractiveness of wireless charging for EV drivers. In effort to shift the traffic assignment from the selfish-optimal UE to the socially-optimal SO, we propose a new mathematical formulation that deploys wireless charging stations in a way that influences the routing choices of EV drivers in effort to improve the traffic condition. We illustrate the applicability of the proposed model on the well-known Braess network and we conduct a sensitivity analysis to determine the conditions that would shift the traffic completely from UE to SO.

The first two studies in this dissertation can be extended to incorporate static charging facilities along with the in-motion wireless charging stations. The formulations can also be extended to account for uncertainty in initial and ending states-of-charge at different origins and destinations of the network.

Moreover, these studies set the stage for further studies on the integration of the operational aspects in design, the interaction between pricing and routing decisions in the network design, and integration of design decisions regarding the cost-effective expansion of electrical networks to support EV charging.

Extending the third study can be done by providing a quantifying method to measure the attractiveness of wireless charging for EV drivers. Specifically, while we assumed constant values for this parameter, it is essential to determine the different factors that contribute to the value of this parameter on different road segments. Another possible extension is to consider the uncertainty in the attractiveness of wireless charging stations for EV drivers as well as the uncertainty in the EVPR and the effect of these uncertainties on the infrastructure deployment plan and the associated traffic assignment. Furthermore, a the third study can

be tackled with a robust approach (similar to our approach in the second study) to account for the variability in the traffic pattern.

Appendix A

The Method of Successive Averages (MSA)

In this appendix, we present the Method of Successive Averages (MSA), which is used to solve the UE traffic assignment problem [54]. We employ this method to obtain the UE traffic assignments for our test instances, examples, and case studies presented in Chapter 3 and Chapter 4. The algorithm is widely used to solve the UE problem whose mathematical formulation is provided in 5.2.1. In what follows we present the procedure of the Method of Successive Averages. We first introduce the following notations.

Notations:

$\mathcal{A}$	set of arcs, $a \in \mathcal{A}$
$\mathcal{Q}$	set of OD-pairs in the network, $q \in \mathcal{Q}$
$\mathcal{R}$	set of all used routes in the network, $\mathcal{R}$
i	iteration number
t_a^i	travel time of arc $a \in \mathcal{A}$ at iteration i.
f_q	traffic flow between OD pair $q \in \mathcal{Q}$.
f_{qr}^i	traffic assignment between OD pair $q \in \mathcal{Q}$ on route $r \in \mathcal{R}$ at iteration i.
y_{qr}^i	auxiliary traffic assignment between OD pair $q \in \mathcal{Q}$ on route $r \in \mathcal{R}$.
x_a	traffic flow on arc $a \in \mathcal{A}$
ϵ	marginal contribution of successive iterations
Ω	convergence tolerance

The Method of Successive Averages:

1. Set $i = 0$ and determine an initial set of feasible routes $\mathcal{R}$. For this purpose find the shortest path between each origin-destination pair $q \in \mathcal{Q}$ based on the arcs free-flow travel times t_a^0.

2. For each OD pair $q \in \mathcal{Q}$, assign all the OD demands f_q to the shortest path $r \in \mathcal{R}$. This gives the route assignments f_{qr}^i for each OD pair $q \in \mathcal{Q}$ and route $r \in \mathcal{R}$.

3. Calculate the traffic flows on arcs based on f_{qr} as follows:

$$x_a = \sum_q \sum_r f_{qr}$$

4. Update the travel times on arcs using the calculated arcs flows.

5. Update the set of feasible routes by finding the new shortest path between each OD pair $q \in \mathcal{Q}$ based on the updated travel times.

6. For each OD pair $q \in \mathcal{Q}$, assign all the OD demands f_q to the shortest path $r \in \mathcal{R}$. This generates new route assignments y_{qr}^i for each OD pair $q \in \mathcal{Q}$ and route $r \in \mathcal{R}$.

7. Determine the routes assignments of the next iteration f_{qr}^{i+1} as follows:

$$f_{qr}^{i+1} = \frac{1}{i+1} y_{qr}^i + (1 - \frac{1}{i+1}) f_{qr}^i$$

8. Compare the routes assignments of the next iteration f_{qr}^{i+1} with the current routes assignments f_{qr}^i. Record the number of cases N where the absolute difference is greater than ϵ, i.e.,

$$\mid f_{qr}^{i+1} - f_{qr}^i \mid \leq \epsilon$$

9. If $N \geq \Omega$, the convergence criterion is not met. Thus, update $i = i + 1$ and go to step 2 with the current routes assignments f_{qr}^{i+1}.

To update the travel times on arcs (step 4 of the MSA procedure) we use the Bureau of Public Roads (BRP) arc performance function [55] given as

$$t_{ij} = t_{ij}^{min}\left(1 + \alpha(\frac{v_{ij}}{tc_{ij}})^{\beta}\right) \tag{A.1}$$

where

t_{ij}	is the travel time on arc (i, j)
t_{ij}^{min}	is the free-flow travel time on arc (i, j)
v_{ij}	is the traffic volume on arc (i, j)
tc_{ij}	is the traffic capacity of arc (i, j) measured in vehicles/hour
α and β	are deterministic permeates associated with the type of the road.

We adopt the following values for α and β:

Table A.1: BRP function parameters. Source: Horowitz [26]

	Freeways			Multilane		
Speed (mph)	70	60	50	70	60	50
α	0.88	0.83	0.56	1	0.83	0.71
β	9.8	5.5	3.6	5.4	2.7	2.1

Bibliography

[1] Y. Arai and S. Satake. Method and unit for computing charging efficiency and charged electrical quantity of battery, February 24 2004. US Patent 6,696,818.

[2] Argonne National Labs. Light duty electric drive vehicles monthly sales updates, 2018. URL http://www.anl.gov/energy-systems/project/light-duty-electric-drive-vehicles-monthly-sales-updates.

[3] R. Arnott and K. Small. The economics of traffic congestion. *American scientist*, 82 (5):446–455, 1994.

[4] H. Bar-Gera. Transportation test problems, 2016. URL https://github.com/bstabler/TransportationNetworks.

[5] P. Belotti. Couenne: a user's manual. Technical report, Technical report, Lehigh University, 2009.

[6] J. F. Benders. Partitioning procedures for solving mixed-variables programming problems. *Numerische Mathematik*, 4:238–252, 1962.

[7] D. Braess. Über ein paradoxon aus der verkehrsplanung. *Unternehmensforschung*, 12 (1):258–268, 1968.

[8] D. Braess, A. Nagurney, and T. Wakolbinger. On a paradox of traffic planning. *Transportation science*, 39(4):446–450, 2005.

[9] Z. Chen, F. He, and Y. Yin. Optimal deployment of charging lanes for electric vehicles in transportation networks. *Transportation Research Part B: Methodological*, 91:344–365, 2016.

[10] Z. Chen, W. Liu, and Y. Yin. Deployment of stationary and dynamic charging infrastructure for electric vehicles along traffic corridors. *Transportation Research Part C: Emerging Technologies*, 77:185–206, 2017.

[11] Swagat Chopra and Pavol Bauer. Driving range extension of ev with on-road contactless power transfer-a case study. *IEEE transactions on industrial electronics*, 60(1):329–338, 2013.

[12] Cleantechnica.com. 200 kW Wireless EV Charging? Momentum Dynamics Says So, 2016. URL https://cleantechnica.com/2016/04/20/200-kw-wireless-ev-charging-momentum-dynamics-says/.

[13] CNN. These roads will charge cars as they drive, 2015. URL http://www.money.cnn.com/2015/08/18/technology/uk-electric-cars-roads.

[14] G. Codato and M. Fischetti. Combinatorial benders' cuts for mixed-integer linear programming. *Operations Research*, 54(4):756–766, 2006.

[15] S. Çolak, A. Lima, and Ma. C. González. Understanding congested travel in urban areas. *Nature communications*, 7:10793, 2016.

[16] J. F. Cordeau, G. Stojković, F. Soumis, and J. Desrosiers. Benders decomposition for simultaneous aircraft routing and crew scheduling. *Transportation Science*, 35(4): 375–388, 2001.

[17] Grant Anthony Covic and John Talbot Boys. Modern trends in inductive power transfer for transportation applications. *IEEE Journal of Emerging and Selected topics in power electronics*, 1(1):28–41, 2013.

[18] Federal Highway Administration. Traffic analysis toolbox volume xiv: Guidebook on the utilization of dynamic traffic assignment in modeling, 2017. URL https://ops.fhwa.dot.gov/publications/fhwahop13015/sec6.htm.

[19] T. M. Fisher, K. B. Farley, Y. Gao, H. Bai, Z. Tse, and H. Tsz. Electric vehicle wireless charging technology: a state-of-the-art review of magnetic coupling systems. *Wireless Power Transfer*, 1(02):87–96, 2014.

[20] fleetcarma.com. How soon is wireless electric vehicle charging coming?, 2018. URL https://www.fleetcarma.com/soon-wireless-electric-vehicle-charging-coming/.

[21] M. Fuller. Wireless charging in california: Range, recharge, and vehicle electrification. *Transportation Research Part C: Emerging Technologies*, 67:343–356, 2016.

[22] Carlos A García-Vázquez, Francisco Llorens-Iborra, Luis M Fernández-Ramírez, Higinio Sánchez-Sainz, and Francisco Jurado. Comparative study of dynamic wireless charging of electric vehicles in motorway, highway and urban stretches. *Energy*, 137:42–57, 2017.

[23] greentechmedia.com. Wireless charging: Coming soon to an electric vehicle near you, 2016. URL https://www.greentechmedia.com/articles/read/wireless-charging-coming-to-an-electric-vehicle-near-you.

[24] G. Haddadian, M. Khodayar, and M. Shahidehpour. Accelerating the global adoption of electric vehicles: Barriers and drivers. *The Electricity Journal*, 28(10):53–68, 2015.

[25] M. J. Hodgson. A flow-capturing location-allocation model. *Geographical Analysis*, 22 (3):270–279, 1990.

[26] A. J. Horowitz. *Delay-volume relations for travel forecasting: based on the 1985 Highway Capacity Manual*. US Department of Transportation, Federal Highway Administration, 1991.

[27] Illhoe Hwang, Young Jae Jang, Young Dae Ko, and Min Seok Lee. System optimization for dynamic wireless charging electric vehicles operating in a multiple-route environment. *IEEE Transactions on Intelligent Transportation Systems*, 2017.

[28] insideevs.com. Dynamic ev charging at up to 60 mph, 2017. URL https://insideevs.com/dynamic-ev-charging/.

[29] Y. J. Jang. Survey of the operation and system study on wireless charging electric vehicle systems. *Transportation Research Part C: Emerging Technologies*, 2018.

[30] Y. J. Jang, Y. D. Ko, and S. Jeong. Optimal design of the wireless charging electric vehicle. In *Electric Vehicle Conference (IEVC)*, pages 1–5. IEEE, 2012.

[31] Young Jae Jang, Seungmin Jeong, and Young Dae Ko. System optimization of the on-line electric vehicle operating in a closed environment. *Computers & Industrial Engineering*, 80:222–235, 2015.

[32] Seungmin Jeong, Young Jae Jang, and Dongsuk Kum. Economic analysis of the dynamic charging electric vehicle. *IEEE Transactions on Power Electronics*, 30(11):6368–6377, 2015.

[33] M. E. Khodayar, L. Wu, and M. Shahidehpour. Hourly coordination of electric vehicle operation and volatile wind power generation in scuc. *IEEE Transactions on Smart Grid*, 3(3):1271–1279, 2012.

[34] Y. D. Ko and Y. J. Jang. The optimal system design of the online electric vehicle utilizing wireless power transmission technology. *Intelligent Transportation Systems, IEEE Transactions on*, 14(3):1255–1265, 2013.

[35] P. Kouvelis and G. Yu. Approaches for handling uncertainty in decision making. In *Robust Discrete Optimization and Its Applications*, pages 1–25. Springer, 1997.

[36] M. Kuby and S. Lim. The flow-refueling location problem for alternative-fuel vehicles. *Socio-Economic Planning Sciences*, 39(2):125–145, 2005.

[37] M. Kuby and S. Lim. Location of alternative-fuel stations using the flow-refueling location model and dispersion of candidate sites on arcs. *Networks and Spatial Economics*, 7(2):129–152, 2007.

[38] R. Leblanc and J. L. Walker. Which is the biggest carrot? comparing nontraditional incentives for demand management. In *Proceedings of the Transportation Research Board 92nd Annual Meeting*, number 13-5039, 2013.

[39] S. Li and C. C. Mi. Wireless power transfer for electric vehicle applications. *IEEE Journal of Emerging and Selected Topics in Power Electronics*, 3(1):4–17, 2015.

[40] Zhaocai Liu and Ziqi Song. Robust planning of dynamic wireless charging infrastructure for battery electric buses. *Transportation Research Part C: Emerging Technologies*, 83: 77–103, 2017.

[41] S. Lukic and Z. Pantic. Cutting the cord: Static and dynamic inductive wireless charging of electric vehicles. *IEEE Electrification Magazine*, 1(1):57–64, 2013.

[42] T. L. Magnanti and R. T. Wong. Accelerating benders decomposition: Algorithmic enhancement and model selection criteria. *Operations research*, 29(3):464–484, 1981.

[43] H. S. Mahmassani. Development and testing of dynamic traffic assignment and simulation procedures for ATIS / ATMS applications. Technical Report DTFH6 1-90-R-00074-FG, Center for Transportation Research, The University of Texas at Austin, 1994.

[44] J. M. Miller, O. C. Onar, and M. Chinthavali. Primary-side power flow control of wireless power transfer for electric vehicle charging. *IEEE Journal of Emerging and Selected Topics in Power Electronics*, 3(1):147–162, 2015.

[45] S. MirHassani and R. Ebrazi. A flexible reformulation of the refueling station location problem. *Transportation Science*, 47(4):617–628, 2012.

[46] A. Nagurney. A multiclass, multicriteria traffic network equilibrium model. *Mathematical and Computer Modelling: An International Journal*, 32(3-4):393–411, 2000.

[47] J. Naoum-Sawaya and S. Elhedhli. A nested benders decomposition approach for telecommunication network planning. *Naval Research Logistics (NRL)*, 57(6):519–539, 2010.

[48] S. Nguyen and C. Dupuis. An efficient method for computing traffic equilibria in networks with asymmetric transportation costs. *Transportation Science*, 18(2):185–202, 1984.

[49] O. C. Onar, J. M. Miller, S. L. Campbell, C. Coomer, C. White, L. E. Seiber, et al. A novel wireless power transfer for in-motion EV/PHEV charging. In *Applied Power Electronics Conference and Exposition (APEC), Twenty-Eighth Annual IEEE*, pages 3073–3080, 2013.

[50] Courtney P. Goodbye range anxiety, 2017. URL https://rac.com.au/car-motoring/info/future_charging-roads.

[51] B. Pishue. Us traffic hot spots: Measuring the impact of congestion in the united states. 2017.

[52] R. Riemann, D. Z. Wang, and F. Busch. Optimal location of wireless charging facilities for electric vehicles: flow-capturing location model with stochastic user equilibrium. *Transportation Research Part C: Emerging Technologies*, 58:1–12, 2015.

[53] P. Rubin. Benders decomposition with integer subproblems, 2013. URL http://orinanobworld.blogspot.com/2013/07/benders-decomposition-with-integer.html.

[54] Y. Sheffi. *Urban transportation networks*, volume 6. Prentice-Hall, Englewood Cliffs, NJ, 1985.

[55] P. A. Steenbrink. *Optimization of transport networks*. John Wiley & Sons, 1974.

[56] T. Trigg, P. Telleen, et al. Global EV outlook: Understanding the electric vehicle landscape to 2020. *Int. Energy Agency*, pages 1–40, 2013.

[57] trustedreviews.com. Smart roads could charge your electric car as you drive by 2030, 2017. URL http://www.trustedreviews.com/news/smart-roads-could-charge-your-electric-car-as-you-drive-by-2030-3287692.

[58] C. Upchurch, M. Kuby, and S. Lim. A model for location of capacitated alternative-fuel stations. *Geographical Analysis*, 41(1):85–106, 2009.

[59] U.S. Department of Energy. One million electric vehicles by 2015, 2011. URL https://www.eere.energy.gov/vehiclesandfuels/pdfs/1_million_electric_vehicles_rpt.pdf.

[60] H. Wang, S. Dusmez, and A. Khaligh. Design and analysis of a full-bridge llc-based pev charger optimized for wide battery voltage range. *IEEE Transactions on Vehicular technology*, 63(4):1603–1613, 2014.

[61] Y. W. Wang and C. C. Lin. Locating road-vehicle refueling stations. *Transportation Research Part E: Logistics and Transportation Review*, 45(5):821–829, 2009.

[62] Y. W. Wang and C. C. Lin. Locating multiple types of recharging stations for battery-powered electric vehicle transport. *Transportation Research Part E: Logistics and Transportation Review*, 58:76–87, 2013.

[63] J. G. Wardrop. Some theoretical aspects of road traffic research. *Proceedings of the Institution of Civil Engineers*, 1(3):325–362, 1952.

[64] witricity.com. Hyundai demonstrates wireless charging at 2018 geneva auto show, 2018. URL http://witricity.com/hyundai-demonstrates-wireless-charging-geneva-auto-show.

[65] Yahoo News. GM to test wireless electric car charging, 2016. URL http://sports.yahoo.com/news/gm-test-wireless-electric-car-charging-095554691.html.

[66] M. Yilmaz, V. T. Buyukdegirmenci, and P. T. Krein. General design requirements and analysis of roadbed inductive power transfer system for dynamic electric vehicle charging. In *Transportation Electrification Conference and Expo (ITEC), IEEE*, pages 1–6, 2012.

[67] H. Zheng, X. He, Y. Li, and S. Peeta. Traffic equilibrium and charging facility locations for electric vehicles. In *Transportation Research Board 95th Annual Meeting*, number 16-0715, pages 1–23, 2016.